ISSN 2073-3771
ISSN 2222-5617

МІНІСТЕРСТВО ОСВІТИ І НАУКИ УКРАЇНИ

Вісник Харківського Національного Університету імені В.Н.Каразіна

Серія “Фізика”

Випуск 26

Серія започаткована 1998 р.

Харків 2017

УДК 530.1/539.8

Вісник містить статті, присвячені сучасному стану теоретичних та експериментальних досліджень у галузі фізики Видання призначене для науковців, викладачів, аспірантів та студентів фізичних спеціальностей вищих навчальних закладів та наукових установ.
Видання є фаховим у галузі фіз.-мат. наук (фізика) наказ МОН України №1328 від 21.12.2015.

Затверджено до друку рішенням Вченої ради Харківського національного університету імені В.Н.Каразіна (протокол №1 від 22 вересня 2017 р.)

Адреса редакції:
Україна, 61022, Харків, майдан Свободи, 4, Харківський національний університет імені В.Н. Каразіна, фізичний факультет, 057-707-53-83, ruslan.v.vovk@univer.kharkov.ua
Статті пройшли внутрішнє та зовнішнє рецензування.

Свідоцтво про державну реєстрацію КВ №21573-11473Р від 20.08.2015

UDC 530.1/539.8

Bulletin contains articles on the current state of theoretical and experimental research in the field of physics.
The publication is intended for researchers, teachers and students of physical specialties of higher education and research institutions.
The publication is a professional in the field of physics and mathematics science (Physics) ordered MES of Ukraine #1328 from 12.21.2015.

Approved for publication by the decision of the Academic Council of Kharkiv Karazin National University. (Minutes №1 dated September 22, 2017 p.)

Editorial address:

Svobody Sq. 4, 61022, Kharkiv, Ukraine, V.N. Karazin Kharkiv National University, Department of Physics, 057-707-53-83, ruslan.v.vovk@univer.kharkov.ua

All articles reviewed.

Certificate of registration КВ number 21573-11473P on 20.08.2015

Content

Вісник ХНУ, серія «Фізика», вип. 26, 2017. с. 6-27

PACS
UDC

Mathematical bases of the theory of N-point gravitational lenses. Part 1. Elements of algebraic geometry

S.D. Bronza[1], A.T. Kotvytskiy[2]

Ukrainian State University of Railway Transport[1,2]
V.N. Karazin Kharkov National University[2]
bronza_semen@mail.ua[1] kotvytskiy@gmail.com[2]

In this paper we consider the theory of N-point gravitational lens from the standpoint of classical algebraic geometry. The first section explains the physical statement of the problem and given the conclusion of the basic equation of the gravitational lens. In the second - a brief discussion of the main objects of study in classical algebraic geometry, and justified its application to the theory of N-point gravitational lenses. Then we give the definition of the central concepts of algebraic geometry - and the resultant theorems related. The fourth section shows, a well-known, Bezout theorem on the number of solutions of polynomial equations of the system and its corollary. In our approach, this theorem is needed to study the solutions of the gravitational lens. In the fifth section, we formulate and prove a criterion of irreducibility of polynomials in several variables over the field of complex numbers. We do not know analogues of this criterion for polynomials in several variables over a field of characteristic zero. The final section provides an overview of the solutions of systems of polynomial equations and formulated a number of challenges and problems the solution of which, in our opinion, it is advisable to apply the presented mathematical apparatus.

Keywords

In this paper we consider the theory of N-point gravitational lens from the standpoint of classical algebraic geometry. The first section explains the physical statement of the problem and given the conclusion of the basic equation of the gravitational lens. In the second - a brief discussion of the main objects of study in classical algebraic geometry, and justified its application to the theory of N-point gravitational lenses. Then we give the definition of the central concepts of algebraic geometry - and the resultant theorems related. The fourth section shows, a well-known, Bezout theorem on the number of solutions of polynomial equations of the system and its corollary. In our approach, this theorem is needed to study the solutions of the gravitational lens. In the fifth section, we formulate and prove a criterion of irreducibility of polynomials in several variables over the field of complex numbers. We do not know analogues of this criterion for polynomials in several variables over a field of characteristic zero. The final section provides an overview of the solutions of systems of polynomial equations and formulated a number of challenges and problems the solution of which, in our opinion, it is advisable to apply the presented mathematical apparatus.

Keywords

In this paper we consider the theory of N-point gravitational lens from the standpoint of classical algebraic geometry. The first section explains the physical statement of the problem and given the conclusion of the basic equation of the gravitational lens. In the second - a brief discussion of the main objects of study in classical algebraic geometry, and justified its application to the theory of N-point gravitational lenses. Then we give the definition of the central concepts of algebraic geometry - and the resultant theorems related. The fourth section shows, a well-known, Bezout theorem on the number of solutions of polynomial equations of the system and its corollary. In our approach, this theorem is needed to study the solutions of the gravitational lens. In the fifth section, we formulate and prove a criterion of irreducibility of polynomials in several variables over the field of complex numbers. We do not know analogues of this criterion for polynomials in several variables over a field of characteristic zero. The final section provides an overview of the solutions of systems of polynomial equations and formulated a number of challenges and problems the solution of which, in our opinion, it is advisable to apply the presented mathematical apparatus.

Keywords

1. Physical formulation of problem

When the light ray propagates near a point massive object (gravitational lens), its trajectory bends. In case when the minimum distance ξ (see fig.1) on which the ray approaches to the attracting body is much more than its gravitational radius r_g, the true light ray trajectory can be replaced by asymptotes to hyperbola. Then the angle between the asymptotes is defined with the following expression [1,2]

$$\alpha = \frac{2r_g}{\xi} = \frac{4GM}{c^2\xi}, \qquad (1.1)$$

where M - mass of point lens, G - gravitation constant, c - speed of light in vacuum.

For the possibility of extension of a one-point gravitational lens to a lens consisting of *N* point masses situated in the lens plane in points with radius vectors $\vec{\xi}_i$ the formula for light-ray deflection angle (1) is written in the vector form

$$\vec{\alpha} = \frac{4GM}{c^2 \xi^2} \vec{\xi}, \qquad (1.2)$$

where the direction of vector $\vec{\alpha}$ coincides with the direction of vector $\vec{\xi}$ (where $|\vec{\alpha}| = \alpha$). As the massive body "attracts" the light ray, it deflects to the body under consideration. Hence, the expression for the deflection is $\vec{\vartheta} = -\vec{\alpha}$.

The formula (2) can be easily written for every M_i mass included in the lens

$$\vec{\alpha}_i = \frac{4GM_i}{c^2 \left|\vec{\xi} - \vec{\xi}_i\right|^2} \left(\vec{\xi} - \vec{\xi}_i\right), \qquad (1.3)$$

where vector $\Delta\xi_i = \vec{\xi} - \vec{\xi}_i$ is directed from the point of arrangement of *i*-th mass into the point of intersection of the light ray with the lens plane (which is defined by vector $\vec{\xi}$). It is obvious that at $\vec{\xi}_i \to 0$ (point mass is situated in the origin of coordinates) the formula (1.3) turns into (1.2). The full deflection angle will be equal to the vector sum of deflection angles from every *i*-th mass

$$\vec{\alpha} = \sum_{i=1}^{N} \vec{\alpha}_i . \qquad (1.4)$$

In case of small deflection angles from fig.1 we have

$$\vec{\eta} + D_{ds}\, \vec{\alpha} = \vec{\eta} + \vec{\varsigma} . \qquad (1.5)$$

On the other hand

$$\vec{\eta} + \vec{\varsigma} = D_s \vec{\beta}, \qquad (1.6)$$

where $\vec{\beta} = \vec{\xi} / D_d$.

Finally, from (5) and (6) we obtain the equation of gravitational lens [3,4]

$$\vec{\eta} = \frac{D_s}{D_d} \vec{\xi} - D_{ds}\, \vec{\alpha} \qquad (1.7)$$

Specifically, for a one-point lens we have the following lens equation

$$\vec{\eta} = \frac{D_s}{D_d} \vec{\xi} - D_{ds}\, \frac{4GM}{c^2 \xi^2} \vec{\xi} . \qquad (1.8)$$

At $\vec{\eta} = 0$, i.e. when the light source is situated on the lens axis, we have equation on $\vec{\xi}$

$$\vec{\xi} \left(\frac{D_s}{D_d} - D_{ds}\, \frac{4GM}{c^2 \xi^2} \right) = 0 . \qquad (1.9)$$

The solution (9) is usually denoted as ξ_0

$$\xi_0 = \sqrt{\frac{4GM \cdot D_{ds} \cdot D_d}{c^2 \cdot D_s}} \qquad (1.10)$$

Thus, if the point source, point lens and observer are situated on the same straight line, the observer will see a circle with radius ξ_0. This radius is usually called Einstein-Chwolson radius [5,6], and the circle itself - Einstein-Chwolson ring. Introducing dimensionless variables

$$\vec{x} \equiv \frac{\vec{\xi}}{\xi_0}, \quad \vec{y} \equiv \frac{D_d}{D_s} \frac{\vec{\eta}}{\xi_0} \qquad (1.11)$$

the equation of one-point gravitational lens (8) becomes

$$\vec{y} = \vec{x} - \frac{\vec{x}}{x^2} . \qquad (1.12)$$

The equation of *N*-point lens (7) can be written as

$$\vec{\eta} = \frac{D_s}{D_d} \vec{\xi} - D_{ds} \sum_{i=1}^{N} \frac{4GM_i}{c^2 \left|\vec{\xi} - \vec{\xi}_i\right|^2} \left(\vec{\xi} - \vec{\xi}_i\right). \qquad (1.13)$$

For writing (1.13) in the dimensionless form we take into account that Einstein-Chwolson radius ξ_0 is determined from the full mass of the gravitational lens $M = \sum_i M_i$ (though there is no Einstein-Chwolson ring in case of *N*-point lens).

Rewrite (1.13) in the form

$$\frac{D_d \vec{\eta}}{D_s \xi_0} = \frac{\vec{\xi}}{\xi_0} - \frac{4G D_d D_{ds} M}{\xi_0 D_s c^2} \sum_{i=1}^{N} \frac{M_i / M}{\left|\vec{\xi} - \vec{\xi}_i\right|^2} \left(\vec{\xi} - \vec{\xi}_i\right). \qquad (1.14)$$

Let us note that in (1.14) there is ξ_0^2 / ξ_0 expression before the summation symbol. Taking into account (1.11) and also introducing $m \equiv M_i / M$ – dimensionless masses we obtain from (14)

$$\vec{y} = \vec{x} - \xi_0 \sum_{i=1}^{N} \frac{m_i}{\left|\vec{\xi} - \vec{\xi}_i\right|^2} \left(\vec{\xi} - \vec{\xi}_i\right) = \vec{x} - \sum_{i=1}^{N} \frac{m_i}{\left|\vec{\xi} / \xi_0 - \vec{\xi}_i / \xi_0\right|^2} \left(\vec{\xi} / \xi_0 - \vec{\xi}_i / \xi_0\right). \quad (1.15)$$

Finally, the equation of *N*-point gravitational lens becomes

$$\vec{y} = \vec{x} - \sum_i m_i \frac{\vec{x} - \vec{l}_i}{\left|\vec{x} - \vec{l}_i\right|^2}, \quad (1.16)$$

where $\vec{l}_i = \vec{\xi}_i / \xi_0$ - dimensionless radius vectors of point masses included into the lens. It is obvious that $\sum_i m_i = 1$.

For the further analysis let us rewrite the set of equations (1.16) in the coordinate form. Taking into account that the vectors have the following components $\vec{x} = (x_1, x_2)$, $\vec{y} = (y_1, y_2)$, $\vec{l}_i = (a_i, b_i)$ we receive the following system

$$\begin{cases} y_1 = x_1 - \sum_{i=1}^{N} m_i \frac{x_1 - a_i}{(x_1 - a_i)^2 + (x_2 - b_i)^2} \\ y_2 = x_2 - \sum_{i=1}^{N} m_i \frac{x_2 - b_i}{(x_1 - a_i)^2 + (x_2 - b_i)^2} \end{cases}. \quad (1.17)$$

One of the main tasks of the theory of gravitational lens is the image construction from the specified source. That is, from the known coordinates of the source (y_1, y_2) to find the images coordinates (x_1, x_2). The problem is that in the general case we do not know a constructive or analytic algorithm for the solution of the system (1.17). The availability of such an algorithm would make it possible to apply methods of symbolic programming. Currently, numerical methods similar to the routing method are applied [7-9]. In this paper we develop an approach based on algebraic geometry. This approach makes it possible to construct quasianalytic and, sometimes, analytic algorithms for the solution of a number of problems. The beginning of this approach is initiated in [10].

2. Basic objects of study in classical algebraic geometry

The main direction of algebraic geometry is the study of the properties of algebraic varieties over an algebraically closed field. Most often consider affine and projective variety over the field of real or complex numbers. Obvious reason that studying the variety and not a vector space. If varieties properties do not depend on the structure of a vector space, we can, the basic elements of space, regarded as points, and not as a vector. To study the affine n-dimensional space, it is fixed in some basis (particularly selected origin of coordinates). Further, each *S* - family of polynomials *K* rings put in correspondence the set points *V*(*S*) whose coordinates satisfy all polynomials of the set *S*. Obviously, the coordinates of a set of points *V*(*S*) are solutions of the system, which is composed of equations belonging to the family *S*.

It is known that the property of being a polynomial function does not depend on the choice of basis. On this basis, we can speak of polynomial functions as a set of common zeros of *V*(*S*) of functions of the family *S*. The sets that can be represented in the form *V*(*S*), called algebraic sets. On the other hand, any algebraic set can be uniquely represented as the union of a finite number of disjoint algebraic varieties.

Thus, the main object of study of classical algebraic geometry, as well as in a broad sense and modern algebraic geometry, are the set of solutions of algebraic systems, in particular polynomial, equations. This fact gives us the opportunity to apply the techniques of algebraic geometry in the theory of *N*-point gravitational lenses.

In the late 1950s, Alexander Grothendieck gave a schema definition that the concept of an algebraic variety see [26]. This event is considered the beginning of modern algebraic geometry and the end of classical see. [27].

In algebraic geometry formed a number of directions. We mention some of them. Complex Algebraic Geometry. In a separate direction is isolated, and the study of the real points of a complex manifold. This area is called, real algebraic geometry. Complex Algebraic Geometry. In a separate area is isolated, and the study of the real points of a complex

manifold. This area is called, real algebraic geometry.

Separate direction of studying features of complex algebraic varieties (including one dimension - Riemann surfaces) and real algebraic varieties. Singularity Theory varieties naturally intersects with algebraic topology.

At the intersection of algebraic geometry and computer algebra we have computational algebraic geometry. Its basic task - creation of algorithms and software for studying the properties of explicit algebraic varieties

The concepts and theorems set forth in this article, mostly apply to sections of algebraic geometry, known as elimination theory and the theory of algebraic curves.

All results are set out in affine coordinates, including those that have been proven by using projective coordinates. We managed to avoid the use of projective coordinates by applying the linear fractional transformations of affine coordinates.

We also paid attention an important concept of modern algebra - basis Gröbner, which can be applied to the study of systems of polynomial equations, in particular, for the construction of an efficient algorithm for answering the question: is finite or infinite number of solutions? We are considering the system contain a small number of equations, that allows you to answer these and similar questions, using other available means, such as a theorem of the resultant and the criterion of irreducible polynomials.

3. The resultant is the central concept of classical algebraic geometry. Fundamental theorems on the resultant

This section contains some well-known, definitions and theorems of classical algebraic geometry. These definitions and theorems presented in a form that meets, in our opinion, the objectives of this article. Theorems are given without proof, but are referenced to the appropriate sources.

The resultant is a central concept of classical algebraic geometry. The current literature [13-15] resultant usually defined as follows:

Definition 3.1 Let K - arbitrary field, $f(x)$ and $g(x)$ - ring of polynomials $K[x]$. The resultant $R(f,g)$ of polynomials $f(x)$ and $g(x)$ is called an element field K, defined by the formula:

$$R(f,g) = a_0^n b_0^m \prod_{i=0}^{i=n} \prod_{j=0}^{j=m} (\alpha_i - \beta_j), \tag{3.1}$$

where α_i, β_j - roots of polynomials $f(x) = \sum_{i=0}^{i=n} a_i x^{n-i}$ and $g(x) = \sum_{j=0}^{j=m} b_j x^{m-j}$, correspondingly with the highest coefficients, a_0, b_0 such that $a_0 \neq 0, b_0 \neq 0$.

Assume us know the roots of polynomials $f(x)$ and $g(x)$, to calculate their resultant, we can use the formula (3.1). Assume that the coefficients of these polynomials only then to calculate the resultant can use the Sylvester matrix for these polynomials. Sylvester matrix is a block matrix of the two blocks. Each unit has a banded matrix. We have a definition of the Sylvester matrix.

Definition 3.2. Matrix Sylvester for polynomials $f(x) = \sum_{i=0}^{i=n} a_i x^{n-i}$ and $g(x) = \sum_{j=0}^{j=m} b_j x^{m-j}$, we call a square matrix $S = S(f,g)$ of order $n+m$ with elements s_{ij} defined by the formula:

$$s_{ij} = \begin{cases} a_{j-i}, & \text{if} \quad 0 \le j-i \le n, \quad i = 1,...,m, \quad j = 1,...,n+m; \\ b_{j-i+m}, & \text{if} \quad 0 \le j-i+m \le n, \quad i = (m+1),...,(n+m) \quad j = 1,...,n+m; \\ 0, & \text{for others } i, j \end{cases} \tag{3.2}$$

i.e.

$$S(f,g) = [s_{ij}] = \begin{matrix} n-lines \\ \\ \\ \\ m-lines \\ \\ \\ \\ \end{matrix} \begin{bmatrix} a_0 & a_1 & a_2 & \cdots & \cdots & \cdots & 0 & 0 \\ 0 & a_0 & a_1 & a_2 & \cdots & \cdots & \cdots & 0 \\ \cdots & \cdots & \cdots & \ddots & \ddots & \ddots & \ddots & \cdots \\ 0 & 0 & 0 & \cdots & \cdots & \cdots & a_{n-1} & a_n \\ b_0 & b_1 & b_2 & \cdots & \cdots & \cdots & 0 & 0 \\ 0 & b_0 & b_1 & b_2 & \cdots & \cdots & \cdots & 0 \\ \cdots & \cdots & \cdots & \ddots & \ddots & \ddots & \ddots & \cdots \\ 0 & 0 & 0 & \cdots & \cdots & \cdots & b_{m-1} & b_m \end{bmatrix} \tag{3.3}$$

Sometimes Sylvester matrix is called the matrix:

$$S(f,g)=\left[s_j\right]=\begin{matrix} \\ n-lines\left\{\right. \\ \\ \\ \\ m-lines\left\{\right. \\ \\ \\ \\ \end{matrix}\begin{bmatrix} a_0 & a_1 & a_2 & \cdots & \cdots & \cdots & 0 & 0 \\ 0 & a_0 & a_1 & a_2 & \cdots & \cdots & \cdots & 0 \\ \cdots & \cdots & \cdots & \ddots & \ddots & \ddots & \ddots & \cdots \\ 0 & 0 & \cdots & \cdots & \cdots & a_{n-2} & a_{n-1} & a_n \\ 0 & 0 & \cdots & \cdots & \cdots & b_{n-2} & b_{m-1} & b_m \\ 0 & 0 & \cdots & \cdots & b_{n-2} & b_{m-1} & b_m & 0 \\ \cdots & \cdots & \cdots & \cdots & \cdots & \cdots & \cdots & \cdots \\ b_0 & b_1 & \cdots & \cdots & \cdots & \cdots & 0 & 0 \end{bmatrix}, \tag{3.4}$$

see. e.g. [12], [19], [24].

Sylvester matrix that defined by (3.3) will be denoted by $Sul(f,g)$, see. e.g., [24], and write $Sul(f,g)=S(f,g)$. Sylvester matrix that defined by (3.4) - denote by the $Sul^{>}(f,g)$, and write $Sul^{>}(f,g)=S(f,g)$. Superscript in the designation of the matrix reflects the location of the bands.

The Presentation matrices of Sylvester in various forms have rationale. Many important results are stated in terms of the minors of these matrices.

The determinant of the matrix $Sul^{>}(f,g)$ is different from the determinant of the matrix $Sul(f,g)$ only sign. We have the following relation:

$$\det Sul^{>}(f,g)=(-1)^{[m/2]}\det Sul(f,g), \tag{3.5}$$

where $\left[m/2\right]$ the integer part of number m.

The resultant $R(f,g)$ and matrix of Sylvester $Sul(f,g)$ associated equation.

Theorem 3.1. The resultant $R(f,g)$ of the polynomials f and g is equal to the determinant of Sylvester matrix these polynomials, i.e.

$$R(f,g)=\det Sul(f,g). \tag{3.6}$$

Proof of Theorem 3.1., see. e.g., [13], [14].

Example 3.1. Calculate the resultant of the polynomials: $f_1=x^2-3x+2$ and $f_2=x^2+1$.

Solution. $R(f_1,f_2)=\det Sul(f_1,f_2)=\begin{vmatrix} 1 & -3 & 2 & 0 \\ 0 & 1 & -3 & 2 \\ 1 & 0 & 1 & 0 \\ 0 & 1 & 0 & 1 \end{vmatrix}=0$

Sometimes resultant $R(f,g)$ determine the determinant of the Sylvester matrix $Sul(f,g)$, and equation (3.1) proves, see. e.g. [13], [14].

Have the following

Theorem 3.2. Polynomials f and g have a common root if and only if

$$R(f,g)=0. \tag{3.7}$$

The proof of Theorem 3.2. See, for example, in [19].

Example 3.2. Do polynomials $f_1=x^3-1$ and $f_2=x^2-1$ common roots?

Solution. $R(f_1,f_2)=\det Sul(f_1,f_2)=\det Sul\left(x^3-1,x^2-1\right)=\begin{vmatrix}1&0&0&-1&0\\0&1&0&0&-1\\1&0&-1&0&0\\0&1&0&-1&0\\0&0&1&0&-1\end{vmatrix}=0$,

Polynomials $f_1=x^3-1$ and $f_2=x^2-1$ have common roots.

You can determine the number of common roots of polynomials f and, if you use some of the concepts related to the resultant $R(f,g)$.

Definition 3.2. Let M be an arbitrary square matrix of order n. Innor M_k, $1\le k\le\left[\frac{n}{2}\right]$ (in brackets is the integer part $\frac{n}{2}$), the matrix M is called the matrix obtained from the matrix M by deleting its elements which are in k first and last rows and k the first and last columns. The matrix M is called the matrix of innor, see. [25].

Matrix of innor M is denoted by M_0

Definition 3.3. Let $S=S(f,g)$ Sylvester matrix of the polynomials f and g, it inures will be denoted by S_k..

Definition 3.4. Determinants $\det S_k$ will be denoted by $R^{(k)}$ and name subresultants resultant $R(f,g)$ polynomials f and g.

Have the following

Theorem 3.3. The polynomials $f(x)$ and $g(x)$ have d common roots if and only if

$$R(f,g)=R^{(1)}(f,g)=...=R^{(d-1)}(f,g)=0,$$

where d such that $1\le d\le\min\left(\deg f(x),\ \deg g(x)\right)$.

Example 3.3. What are the common roots of polynomials, $f_1=x^3-1$ and $f_2=x^2-1$?

Solution. We calculate subrezultantes $R^{(1)}(f_1,f_2)$, $R^{(2)}(f_1,f_2)$:

$$R^{(1)}(f_1,f_2)=\begin{vmatrix}1&0&0\\0&-1&0\\1&0&-1\end{vmatrix}=1\ne0,\quad R^{(2)}(f_1,f_2)=\left|-1\right|\ne0,$$

Polynomials $f_1=x^3-1$ and $f_2=x^2-1$ have a common root, because the $R(f_1,f_2)=0$ and $R^{(1)}(f_1,f_2)=1\ne0$ (In the first row subresultants $R(f_1,f_2)$, $R^{(1)}(f_1,f_2)$, $R^{(2)}(f_1,f_2)$ first subresultant, which is not zero, have number 1).

The greatest common divisor $\deg(GCD(f,g)$ of the polynomials $f(x)$ and $g(x)$ can be computed using Euclid's algorithm, see. [12-14], [16], or by using subresultants, see. [12], [19], [25].

A special case of the resultant polynomial is the discriminant.

Definition 3.5. Let K - arbitrary field, $f=f(x)$ - polynomial in the polynomial ring $K[x]$.

The discriminant $D(f)$ of $f=f(x)$ is called an element of K, defined as follows:

$$D(f)=a_0^{2n-2}\prod_{1\le j<i\le n}(\lambda_i-\lambda_j)^2, \tag{3.8}$$

where $n = \deg f(x)$ - the degree of the polynomial $f(x)$, a_0 - its leading coefficient, $\lambda_1,...,\lambda_n$, its roots, see [13].

Have the following

Theorem 3.4. Let $f = f(x)$ - polynomial in the polynomial ring $K[x]$, f' - its derivative, then for the discriminate $D(f)$ we have the relation:

$$D(f) = (-1)^{\frac{n(n-1)}{2}} \frac{1}{a_0} R(f, f'). \tag{3.9}$$

The proof of Theorem 3.4 is given in [13].

From Theorem 3.2 follows

Theorem 3.5. The polynomial f has a multiple root if and only if, $D(f) = 0$.

The proof is given in [13-14], [24].

Similarly, as the subresultants some authors define subdiscriminant, see. [25]. Using concepts: innor, subresultants, subdiscriminant etc. we can formulate and prove a number of theorems on the distribution of the roots of polynomials, such as the criterion of Routh-Hurwitz, see. [19].

An important theorem is the theorem on the number of solutions of systems of polynomial equations. Bezout Theorem is a theorem of this kind. Bezout Theorem is discussed in Section 4.

Many allegations of algebraic geometry begins with the assumption of irreducibility (or reducible) polynomial. Under the irreducible polynomial f over K understands the impossibility of its representation in the form of a product of two polynomials f_1 and f_2 nonzero degree over the same field, i.e. $f \neq f_1 \cdot f_2$.

Here for example one of them.

Theorem 3.6. Let f and g are polynomials with coefficients from the field K and the polynomial f is reducible, i.e. $f = f_1 \cdot f_2 =$, where f_1 and f_2 are not polynomials of degree zero over the field K. Then, to the resultant $R(f, g)$, equation holds:

$$R(f, g) = R(f_1, g) R(f_2, g). \tag{3.10}$$

Theorem 3.6 allows us to reduce the number of operations in the calculation of the resultant.

Availability of convenient criterion is irreducible is an effective tool for studying systems of polynomial equations. In Section 5, we formulate and prove a criterion for irreducible polynomials of several variables.

4. Bezout theorem on the number of solutions of a polynomial system of equations

This section contains several important theorems. One them - Bezout theorem on the number of solutions of polynomial equations of the system, see for example [11]. From this theorem follows the basic theorem of algebra. The wording of some theorems, we present only for special cases. This allows us to give them simple proofs.

We introduce the necessary notation.

Let $f = f(x, y)$ be a polynomial in two variables over a field K, $n = \deg_x f(x, y)$ - his degree in the variable x, $m = \deg_y f(x, y)$ - the degree of the variable y and $d = \deg f(x, y)$ - the degree of the set of variables.

For our purposes, as the K field, unless otherwise stated, we choose the field of complex numbers C. A $C[x]$ will denote the field of rational functions of x with coefficients in C.

Let $f = f(x, y)$ and $g = g(x, y)$ - polynomials two variables over the field of complex numbers C, and let the polynomials are defined as follows:

$$f = f(x, y) = \sum_{i,j=0}^{i,j=n;\ i+j\le n} a_{ij} x^{i\ \ j}, \tag{4.1}$$

$$g = g(x,y) = \sum_{i,j=0}^{i,j=m;\ i+j\le m} b_{ij}x^{i\ \ j}. \qquad (4.2)$$

If at least one of the senior coefficients, a_{ij}, $i+j=n$, of the polynomial f is not zero, then $\deg f = n$, and if at least one of the senior coefficients, b_{ij}, $i+j=m$, of the polynomial g It is not zero, then $\deg g = m$.

Convenient to describe the theory is notion of eliminate polynomials.

Definition 4.1. Let $f(x,y), g(x,y) \in C[x,y]$ - of two polynomials variables over the field of complex numbers C. The Eliminante of polynomials $f(x,y)$ and $g(x,y)$ is called a polynomial $X(x)$, the variable x, is defined by the equation:

$$X(x) = R_y(f(x,y), g(x,y)), \qquad (4.3)(4.3)$$

where $R_y(f(x,y), g(x,y))$ - resultant polynomial $f(x,y)$ and $g(x,y)$ in the variable y.

Similarly, determined the second eliminante for polynomials of the system $Y(y)$, i.e.:

$$Y(y) = R_x(f(x,y), g(x,y)). \qquad (4.4)$$

Following [19] the sign $(-1)^{\frac{n(n-1)}{2}}$ in determining both eliminates will be ignored.

Also note that eliminantes is polynomials, and are defined up to a multiplicative constant from the field of coefficients.

Have the following

Theorem 4.1. (Bezout) Let the polynomials f and g are defined by (4.1) and (4.2), respectively. Let their coefficients such that $a_{0n} \neq 0$, $a_{no} \neq 0$, $b_{0m} \neq 0$, $b_{m0} \neq 0$. Then eliminante $X(x)$, such that its degree $\deg X(x) = \deg f(x,y) \cdot \deg g(x,y) = nm$.

The proof of the theorem see, e.g., [19].

Similar assertion holds for eliminate $Y(y)$, i.e., $\deg Y(y) = nm$.

In order to state the next theorem we recall the definition of an algebraic curve.

Definition 4.2. An algebraic curve f is the set of points (a coordinate space), the coordinates of which satisfy the equation:

$$f(x,y) = 0. \qquad (4.5)$$

Equation (4.5) is called the equation of the curve f (x, y).

The polynomial in the left side of the equation (4.5) can be considered over the field of real numbers. In this case, the algebraic curve f is, for example, the curve in the affine plane or in a projective space, i.e. the graph of the function f. If the equation (4.5) is considered over the field of complex numbers, the algebraic curve is a one-dimensional complex manifold in the space $\mathbb{C}^2$. This curve also can be regarded as the graph of a function, or as the Riemann surface of an algebraic function given by equation (4.5).

Have the following

Theorem 4.2. (Bezout) Let the curves are determined by the equations $f(x,y) = 0$ and $g(x,y) = 0$. If they have more than $nmnm$ points in common, they have a common component, i.e. $\deg GCD(f(x,y), g(x,y)) \neq 0$.

The proof of Theorem 4.2 is given in [15].

Corollary of Theorem 4.2. From Theorem 4.2 it follows that if the system of equations

$$\begin{cases} f(x,y)=0 \\ g(x,y)=0 \end{cases} \tag{4.6}$$

has more than nm solutions, the polynomials f and g have a common component.

From Theorem 4.2 obviously follows

Theorem 4.3 Let the polynomials ff and gg have no common components i.e. $deg\mathrm{GCD}(f,g)=0$, then the number of solutions of (4.6) does not exceed nm .

In [19] are examples showing that this bound is attained.

Theorem 4.4. The polynomials f and g have a common component h , positive degree, i.e., $\deg GCD(f,g)=deg(h)\neq 0$, if and only if at least one of eliminante $X(x)=R_y(f,g)$ or $Y(y)=R_x(f,g)$, is identically zero, or that, too, $R_x(f,g)^2R_y(f,g)\equiv 0$.

Proof. Necessity. For definiteness, let eliminante $Y(y)\equiv 0$, then the polynomials f and g , such that, $R_x(f,g)\equiv 0$. From equation $R_x(f,g)\equiv 0$ follows: for any fixed $y=y_0$, holds $R\left(f(x,y_0),g(x,y_0)\right)=0$, therefore, the polynomials f and g have common roots. But then it, by virtue of the freedom to choose y , polynomials f and g coincide in an infinite number of points and, according to Theorem 4.2., have a common component.

Sufficiency. Let the polynomials f and g have a common component h , positive degree, i.e. $deg_x(h)\neq 0$, then $f=f_1h$ and $g=g_1h$. Applying Theorem 1.3., we have:

$$R_x(f,g)=R_x(f_1h,g_1h)=R_x(f_1,g_1h)^2R_x(h,g_1h)=$$

$$=R_x(f_1,g_1)^2R_x(f_1,h)^2R_x(h,g_1)^2R_x(h,h).$$

Given the identity $R_x(h,h)\equiv 0$, we have $R_x(f,g)\equiv 0$ and $Y(y)\equiv 0$.

The theorem is proved.

Corollary theorem 4.4. If eliminante $X(x)$ polynomials $f(x,y),g(x,y)$, such that $X(x)\equiv 0$, *then all of its coefficients is zero, i.e. .:*

$$\frac{d^i}{dx^i}X(x)=0,\ i=1,2,\ldots,m. \tag{4.6}$$

where $m=deg\,X(x)$.

As $X(x)=R_y\left(f(x,y),g(x,y)\right)\equiv 0$, we have the following relations:

$$\frac{d^i}{dx^i}R_y\left(F(x,y),f(x,y)\right)=0,\ i=1,2,\ldots,m. \tag{4.7}$$

The criterion of irreducibility

5. The irreducibility criterion for polynomials in several variables

This section is formulated and proved criterion of irreducibility for polynomials of several variables in a weakened form (for polynomials with real or complex coefficients). We are unaware of other criteria for polynomials in several

variables over a field of characteristic 0.

We give the necessary definitions.

Definition 5.1. Polynomial *n*-form (or *n*-form in the polynomial basis) of the variables x_l, $l=1,\dots k$ over a field K is a formal sum $G=\sum_{0\le l_1+l_2+\dots+l_k\le n} g_{l_1 l_2\dots l_k} x_1^{l_1} x_2^{l_2}\dots x_k^{l_k}$, $n\in\mathbb{N}$ i.e. G - a polynomial of degree n in the variables $x_l, l=1,\dots k$ with coefficients $g_{l_1 l_2\dots l_k}$ of field K.

In particular, the *1*-form of variable $x_l, l=1,\dots k$ over a field K is a linear form. *2*-form on - quadratic form. The polynomial $f(x,y)$ in two variables x and y, the degree n, with complex coefficients is the n-shape of the variables x and y over the field of complex numbers $\mathbb{C}$. The expression "function will be sought in the form of n-form" is generally understood as a procedure for determining the undetermined coefficients given *n*-form

In the proof of the following criteria will be used

Theorem 5.1. Polynomial in several variables over a field K is identically equal to zero, if and only if all its coefficients are zero**,** see. [20].

Occurs

Theorem 5.2. Let $F=F(x,y)$ a polynomial in the variables x and y over the field of complex numbers $\mathbb{C}$ and $d=\deg F(x,y)$ - its extent, let $n=\left[\frac{d}{2}\right]$ (in brackets is the integer part the number of $\frac{d}{2}$), and let G - *n* -form in the variables x and y over the field of complex numbers $\mathbb{C}$, i.e.

$$G(x,y)=\sum_{i,j=0}^{0\le i+j\le n} g_{ij}x^i y^j$$

The polynomial F is decomposable the variable of x, if and only if, the system equations

$$\begin{cases} R_x\left(F(x,y),G(x,y)\right)\big|_{y=0}=0 \\ \dfrac{d^i}{dy^i}R_x\left(F(x,y),G(x,y)\right)\big|_{y=0}=0 \end{cases}, \quad i=1,2,\dots,m; \text{ where } m=degR_x(F,G), \tag{5.1}$$

(The system (5.1) is solved with respect to indeterminate coefficients g_{ij} *n*-form G, as a relatively unknowns) have not zero solution.

Proof. Necessity. Let the polynomial F is decomposable the variable x.

Then F can be expressed as $F=f_1{}^2 f_2$, were $f_1=f_1(x,y)$ and $f_2=f_2(x,y)$ such that $deg_y f_1\neq 0$, $deg_y f_1\neq 0$, and $deg_y f_1+deg_y f_2=deg_y F$. From the condition of $degF=d$ implies that $min(degf_1,degf_2)\le\left[\frac{d}{2}\right]$. Let $degf_1\le degf_2$, then $degf_1\le\left[\frac{d}{2}\right]=n$. Let $degf_1=m_1$, then f_1 polynomial can be written as

$$f_1=f_1(x,y)=\sum_{i,j=0}^{0\le i+j\le m_1} c_{ij}x^i y^j,$$

where not all c_{ij} for $1\le i+j\le m_1$ are equal zero.

We denote by

$$b_{ij} = \begin{cases} c_{ij}, & 0 \le i + j \le m_1 \\ 0, & m_1 < i + j \le n \end{cases}, \qquad (5.2)$$

and we show that

$$g_{ij} = b_{ij}, \qquad (5.3)$$

the non-zero solution of system (5.1).

Let $G \equiv f_1$. The polynomials F and f_1 , as follows from condition of the theorem, have a common component f_1 and, according to Theorem 4.4 of the resultant $R_x(F, f_1) \equiv 0$. Consequently, the resultant $R_x(F,\ G) \equiv 0$, and then, in accordance with Theorem 5.1, all the coefficients are zero simultaneously. Consequently, there is a system of equations for c_{ij} , and, consequently, relatively, b_{ij} . Thus, the ratio (5.3) is a solution of (5.1).

The resulting solution is not zero, as b_{ij} , that certain system of equations (5.2), are not all zero. The necessity is proved.

Sufficiency. We prove first that (5.1) has a zero solution. Indeed, G is not only the form of n-variables x and y , but also linear form for its coefficients. Consequently, we can write: $G(x,y) = G(x,y,g_{ij})$. Because relation holds: $G(x,y,tg_{ij}) = tG(x,y,g_{ij})$, *n*-form *G* is a homogeneous function of its coefficients g_{ij} , and the resultant

$$R_x\left(F(x,y), G(x,y)\right) = R_x\left(F(x,y), G(x,y,g_{ij})\right),$$

is a homogeneous function of the variables $g_{ij}g_{ij}$ degree $d = degFd = degF$. Indeed:

$$R_x\left(F(x,y), G(x,y,tg_{ij})\right) = t^d R_x\left(F(x,y), G(x,y,g_{ij})\right).$$

But then, all the coefficients of resultant, as the polynomial of variable yy, also are homogeneous functions of the variables g_{ij} degree d , and $d \neq 0$. Thus, all of the system (5.3) are homogeneous functions of the variables g_{ij} nonzero of degree d . Homogeneous function nonzero of degree d in the variables g_{ij} is zero, if everyone $g_{ij} = 0$. Consequently, the system (5.1) has a zero solution.

Let the system (5.1), except for the zero solution is still nonzero. Each a nonzero solution of system (5.1) completely determine the undetermined coefficients g_{ij} *n*-form G . Because solution is a nonzero, not all the coefficients g_{ij} zero. Let us denote G_1 n-form G with coefficients g_{ij} , as defined, to some, a non-zero solution of the system (5.1).

We will prove that the resultant $R_x(F, G_1) \equiv 0$. Indeed, the resultant $R_x(F, G_1)$ is a polynomial in the variable y . All coefficients of this polynomial is zero, since, by assumption, we have the system of equations (5.1). Consequently, polynomial, he same resultant $R_x(F, G_1)$ is identically zero. From the identical vanishing of the resultant, follows that the polynomials, F, and G_1 , in accordance with Theorem 4.4, have a general component for the variable x . Consequently, the polynomial F a decomposable to the variable x.

The theorem is proved.

From Theorem 5.2 follows

Theorem 5.3 (The reducibility criterion). Let $F = F(x,y)$ polynomial in the variables x and y over the field of complex numbers $\mathbb{C}$ and $d = \deg F(x,y)$ - its degree, let $n = \left[\frac{d}{2}\right]$ and G is an n-form in the variables x and

y over the field of complex numbers $\mathbb{C}$, i.e.

$$G(x,y)=\sum_{i,j=0}^{0\le i+j\le n} g_{ij}x^i y^j$$

The Polynomial, F is reducible if and only if at least one of the systems of equations

$$\begin{cases} R_x\left(F(x,y),G(x,y)\right)_{|_{y=0}}=0 \\ \dfrac{d^i}{dy^i}R_x\left(F(x,y),G(x,y)\right)_{|_{y=0}}=0 \end{cases},\quad i=1,2,\ldots,m; \tag{5.4}$$

where $m=degR_x(F,G)$,

$$\begin{cases} R_y\left(F(x,y),G(x,y)\right)_{|_{x=0}}=0 \\ \dfrac{d^i}{dx^i}R_y\left(F(x,y),G(x,y)\right)_{|_{x=0}}=0 \end{cases},\quad i=1,2,\ldots,h; \tag{5.5}$$

where $h=degR_x(F,G)$.

(System is considered relatively of indeterminate coefficients g_{ij} *n*-form G, as a relatively unknowns) has a nonzero solution.

It has the assertion, converse to the opposite assertion of the previous theorem

Theorem 5.4 (The irreducibility criterion). Let $F=F(x,y)$ polynomial in the variables x and y over the field of complex numbers $\mathbb{C}$ and $d=\deg F(x,y)$ - its degree, let $n=\left[\dfrac{d}{2}\right]$ and G is an n-form in the variables x and y over the field of complex numbers $\mathbb{C}$, i.e.

$$G(x,y)=\sum_{i,j=0}^{0\le i+j\le n} g_{ij}x^i y^j$$

The Polynomial, F is reducible if and only if for each of the two variables x_l, $l=1,2$, the systems of equations

$$\left\{\frac{d^i}{dx_l^i}R_{x_l}\left(F(x,y),G(x,y)\right)=0\right.,\quad i=1,2,\ldots,m; \tag{5.6}$$

where $m=degR_{x_l}(F,G)$, (systems is considered relatively of indeterminate coefficients g_{ij} *n*-form G, as a relatively unknowns, and in equations of systems, the variables with index is not equal *l*, we equated to zero) have only the zero solution.

Corollary of Theorem 5.4. To determine the irreducibility of polynomials in two variables it is sufficiently rational operations over a field of its coefficients. If a polynomial in two variables, over the field of complex numbers $\mathbb{C}$ reducible, then to determine it's of the irreducible components, of the rational operations, generally speaking, is not enough. To determine its irreducible components is enough to add a method for calculating of the roots for polynomials of degree n in one variable.

From the theorems proved above follows:

Theorem 5.5 (The irreducibility criterion for polynomials in several variables).

Let KK - the field of real or complex numbers, $F=F(x_1,x_2,\ldots,x_k)=F(\overline{x})$ - polynomial in k variables $x_1,x_2,\ldots,x_k$, with coefficients from K and $d=\deg F(\overline{x})$ - its degree, let $n=\left[\dfrac{d}{2}\right]$ ((in brackets is the integer part the number of $\dfrac{d}{2}$) and let G - *n*-form in k variables $x_1,x_2,\ldots,x_k$, i.e.

$$G = G(\overline{x}) = \sum_{0 \le l_1 + l_2 + \ldots + l_k \le n} g_{l_1 l_2 \ldots l_k} x_1^{l_1} x_2^{l_2} \ldots x_k^{l_k} \ , \ n \in \mathbb{N} \ .$$

Let

$$R_t = \sum_{0 \le r_1 + r_2 + \ldots + r_k \le m_t} r_{r_1 r_2, \ldots, r_k} x_1^{r_1} x_2^{r_2}, \ldots x_k^{r_k} \ , \ n \in \mathbb{N},$$

Lexical-graphical representation in increasing powers of the resultant $R_{x_t}\left(F(\overline{x}), G(\overline{x})\right) = R_t$, in the alphabet of variables $x_1, x_2, \ldots, x_{t-1}, x_{t+1}, \ldots, x_k$, and let $m_t = degR_t$ - its degree.

The Polynomial, F is irreducible (in the expansion of $K\left[x_1, x_2, \ldots, x_k\right]$ field coefficients), if, and only if, for any of the variables x_t, $t = 1, \ldots, k$ system of equations

$$\left\{ r_{r_1 r_2, \ldots, r_k} = 0 \ , \quad i = 1, 2, \ldots, m_t; \quad 1 \le r_1 + r_2 + \ldots + r_k \le m_t, \right. \qquad (5.7)$$

where $m_t = degR_t$ (system is being considered relatively undetermined coefficients $g_{l_1 l_2 \ldots l_k}$ n-form G , as unknowns) has only the zero solution.

In the statement of the theorem, we consider that $k = 2, 3, \ldots$ for $k = 1$ the question of the reducibility of polynomials is solved in accordance with the fundamental theorem of algebra and its consequences.

Corollary of Theorem 5.5. To determine the irreducible polynomial in several variables it is sufficiently rational operations over a field of its coefficients.

The following examples illustrate the criteria.

In the examples, polynomial n - form G is denoted by $\hat{O}(x, y)$.

Example 5.1. Prove irreducible polynomial $F(x, y) = x^2 + y^2 - 1$.

Solution. The degree of the polynomial $F(x, y)$, $deg\left(F(x, y)\right) = deg(x^2 + y^2 - 1) = 2$, the degree of the polynomial $\hat{O}(x, y)$, $\hat{O}deg\left(\ y(\ \ ,\ \ )\right) = \left[\dfrac{\deg\left(F(x, y)\right)}{2}\right] = \left[\dfrac{2}{2}\right] = 1$. Dividers polynomial $F(x, y)$ we will be sought in the form of a 1-form $\hat{O}(x, y) = ax + by + c$. We calculate the resultant $\hat{R}_x = R_x\left(F(x, y), \ \ (\ \ ,\ \ )\right)$:

$$\hat{R}_x = R_x\left(F(x, y), \ \ (y\ ,\ \ )\right) = R_x\left(y^2 + \ ^2 - 1, \ \ + \ \ + \ \right) =$$

$$= \det\begin{bmatrix} 1 & 0 & y^2 - 1 \\ a & by + c & 0 \\ 0 & a & by + c \end{bmatrix} = (by + c)^2 + a^2\left(y^2 - 1\right) = \left(a^2 + b^2\right) y^2 + 2bcy - a^2 + \ ^2 \ .$$

From the assumption the decomposition of the polynomial $F(x, y)$ according to Theorem 5.4, we have:

$R_x \equiv 0$, and

$$\left(a^2 + b^2\right) y^2 + 2bcy - a^2 + \ ^2 \equiv 0 \ . \qquad (5.8)$$

According to Theorem 5.1, all the coefficients of the polynomial on the left side of the equation (5.8) are equal to

zero. We have a system of equations:

$$\begin{cases} -\tilde{a}^2 + {}^2 = 0 \\ 2bc = 0 \\ a^2 + b^2 = 0 \end{cases}. \tag{5.9}$$

The system (5.9) decomposes into two systems:

$$\begin{cases} -\tilde{a}^2 + {}^2 = 0 \\ b = 0 \\ a^2 + b^2 = 0 \end{cases}, \qquad a\begin{cases} -\tilde{n}^2 + {}^2 = 0 \\ c = 0 \\ a^2 + b^2 = 0 \end{cases}.$$

Each of the systems has a unique solution: $a = 0, b = 0, c = 0$, and this solution is zero.

Thus, the system (5.9) has only the zero solution. Consequently, according to Theorem 5.2, the polynomial $x^2 + y^2 - 1$ irreducible variable x .

Because of the symmetry of variables in the polynomial $x^2 + y^2 - 1,$ if in the resultant $R_x R_x$ replaced variable, the resultant R_y , the result, obviously, does not change. Is therefore, the polynomial $x^2 + y^2 - 1$ irreducible and other variable and, therefore non-trivial irreducible.

Example 5.2. Prove: the polynomial $F(x, y) = y^3 - 3yx - 2x^2$ is irreducible to the variable y .

Solution. The degree of the polynomial $F(x, y)$, $deg\left(F(x, y)\right) = deg(y^3 - 3yx - 2x^2) = 3$, the degree of the polynomial $\Phi(x,y)\Phi(x,y),$ $\deg\left(y(\ ,\ )\right) = \left[\dfrac{\deg\left(F(x, y)\right)}{2}\right] = \left[\dfrac{3}{2}\right] = 1$. Dividers polynomial $F(x, y)$ $F(x, y)$ we will be sought in the form $\hat{O}(x, y) = ax + by + c$.

We calculate $\hat{R}_y = R_y\left(F(x, y),\ (\ ,\ )\right)$, and have:

$$= \begin{vmatrix} 1 & 0 & R_y = 3x(y^3 - 3yx - 2x^2, \alpha x + \beta y + \gamma) = 3x & 2x^2 \\ \alpha & \beta x + \gamma & 0 & 0 \\ 0 & \alpha & \beta x + \gamma & 0 \\ 0 & 0 & \alpha & \beta x + \gamma \end{vmatrix} = \begin{vmatrix} 0 & \beta x + \gamma & 3x\alpha & -2x^2\alpha \\ 0 & \alpha & \beta x + \gamma & 0 \\ 0 & 0 & \alpha & \beta x + \gamma \end{vmatrix} =$$

$$= (\beta x + \gamma)^3 - 2x^2\alpha^3 - 3x\alpha^2(\beta x + \gamma) =$$

$$= \beta^3 x^3 + \left(3\beta^2\gamma - 2\alpha^3 - 3\alpha^2\beta\right)x^2 + \left(3\beta^2\gamma - 3\alpha^2\gamma\right) + \gamma^3 ,$$

and then we have:

$$\beta^3 x^3 + \left(3\beta^2\gamma - 2\alpha^3 - 3\alpha^2\beta\right)x^2 + \left(3\beta^2\gamma - 3\alpha^2\gamma\right) + \gamma^3 \equiv 0 . \tag{5.10}$$

Equating the coefficients of equation (5.10) to zero, we have a system of equations to determine the α , β , γ .

$$\begin{cases} \beta^3 = 0 \\ 3\beta^2\gamma - 2\alpha^3 - 3\alpha^2\beta = 0 \\ 3\beta^2\gamma - 3\alpha^2\gamma = 0 \\ \gamma^3 = 0 \end{cases} \Rightarrow \begin{cases} \alpha = 0 \\ \beta = 0 \\ \gamma = 0 \end{cases} \tag{5.11}$$

Thus, the system (5.11) has only the zero solution, and therefore a polynomial $y^3 - 3yx - 2x^2$ is irreducible to the variable y .

Example 5.3. Explore: will be whether the polynomial irreducible?

$$F(x,y) = x^3 - x^2 + (y^2 - 1)x - y^2 + 1.$$

Solution. The degree of the polynomial $F(x,y)$,

$$deg\left(F(x,y)\right) = deg\left(x^3 - x^2 + (y^2 - 1)x - y^2 + 1\right) = 3 ,$$

the degree of the polynomial $\hat{O}(x,y)$, $deg\left(\hat{O}(x,y)\right) = \left[\frac{\deg\left(F(x,y)\right)}{2}\right] = \left[\frac{3}{2}\right] = 1$. Dividers polynomial $F(x,y)$ we will be sought in the form $\hat{O}(x,y) = ax + by + c$.

We calculate the resultant $\hat{R}_x = R_x\left(F(x,y), \hat{O}(x,y)\right)$.

$$\hat{R}_x = R_x\left(F(x,y), \hat{O}(x,y)\right) = R_x\left(x^3 - x^2 + (y^2 - 1)x - y^2 + 1, ax + by + c\right) =$$

$$= det\begin{bmatrix} 1 & -1 & y^2 - 1 & -y^2 + 1 \\ a & by + c & 0 & 0 \\ 0 & a & by + c & 0 \\ 0 & 0 & a & by + c \end{bmatrix} =$$

$$= det\begin{bmatrix} by + c & 0 & 0 \\ a & by + c & 0 \\ 0 & a & by + c \end{bmatrix} - a^2 det\begin{bmatrix} -1 & y^2 - 1 & -y^2 + 1 \\ a & by + c & 0 \\ 0 & a & by + c \end{bmatrix} =$$

$$= (by + c)^3 + a\left((by + c)^2 + a^2(y^2 - 1)\right) + a(by + c)(y^2 - 1)) =$$

$$= y^3\left(a^2 b + b^3\right) + y^2\left(a^3 + a^2 c + ab^2 + 3bc^2\right) + y\left(-a^2 b + 2abc + 3bc^2\right) +$$

$$+\left(-a^3 - a^2 c + ac^2 + c^3\right) .$$

From the assumption reducibility of a polynomial $F(x,y)$ according to Theorem 5.2, we have:

$R_x \equiv 0$, and

$$y^3\left(a^2 b + b^3\right) + y^2\left(a^3 + a^2 c + ab^2 + 3bc^2\right) + y\left(-a^2 b + 2abc + 3bc^2\right) +$$
$$+\left(-a^3 - a^2 c + ac^2 + c^3\right) \equiv 0 \qquad (5.12)$$

According to Theorem 5.1, all the coefficients of the polynomial on the left side of the equation (5.12) equal to zero. We have a system of equations:

$$\begin{cases} -a^3 - a^2 c + ac^2 + c^3 = 0 \\ -a^2 b + 2abc + 3bc^2 = 0 \\ a^3 + a^2 c + ab^2 + 3bc^2 = 0 \\ a^2 b + b^3 = 0 \end{cases}, \qquad (5.13)$$

and transforming the system (5.13), have:

$$\begin{cases} \left(a^2-c^2\right)\left(a+c\right) = 0 \\ b\left(-a^2+2ac+3c^2\right) = 0 \\ a^3+a^2c+ab^2+3bc^2=0 \\ b\left(a^2+b^2\right)=0 \end{cases} = 0 \\ = 0 \\ .$$

The system decomposes into eight sub-systems:

$$\begin{cases} a=c \\ b=0 \\ a^3+a^2c+ab^2+3bc^2=0 \\ b=0 \end{cases}, \quad \begin{cases} a=c \\ b=0 \\ a^3+a^2c+ab^2+3bc^2=0 \\ a^2+b^2=0 \end{cases},$$

$$\begin{cases} a=c \\ -a^2+2ac+3c^2=0 \\ a^3+a^2c+ab^2+3bc^2=0 \\ b=0 \end{cases}, \quad \begin{cases} a=c \\ -a^2+2ac+3c^2=0 \\ a^3+a^2c+ab^2+3bc^2=0 \\ a^2+b^2=0 \end{cases},$$

$$\begin{cases} a=-c \\ b=0 \\ a^3+a^2c+ab^2+3bc^2=0 \\ b=0 \end{cases}, \quad \begin{cases} a=-c \\ b=0 \\ a^3+a^2c+ab^2+3bc^2=0 \\ a^2+b^2=0 \end{cases},$$

$$\begin{cases} a=-c \\ -a^2+2ac+3c^2=0 \\ a^3+a^2c+ab^2+3bc^2=0 \\ b=0 \end{cases}, \quad \begin{cases} a=-c \\ -a^2+2ac+3c^2=0 \\ a^3+a^2c+ab^2+3bc^2=0 \\ a^2+b^2=0 \end{cases},$$

For the first, we have:

$$\begin{cases} a=c \\ a^3+a^2c+ab^2+3bc^2=0 \\ b=0 \end{cases} \Rightarrow \begin{cases} a=c \\ a^3+a^2c=0 \\ b=0 \end{cases} \Rightarrow \begin{cases} a=c \\ a^2\left(a+c\right)=0 \\ b=0 \end{cases} \Rightarrow$$

The system decomposes into two subsystems, deciding that we have:

$$\begin{cases} a=c \\ a^2=0 \\ b=0 \end{cases} \Rightarrow \begin{cases} a=0 \\ b=0 \\ c=0 \end{cases}$$

$$\begin{cases} a=c \\ a+c=0 \\ b=0 \end{cases} \Rightarrow \begin{cases} a=c \\ a=-c \\ b=0 \end{cases} \Rightarrow \begin{cases} a=0 \\ b=0 \\ c=0 \end{cases}$$

System has only the zero solution.

For the system:

$$\begin{cases} a=c \\ -a^2+2ac+3c^2=0 \\ a^3+a^2c+ab^2+3bc^2=0 \\ b=0 \end{cases} \Rightarrow \begin{cases} a=c \\ -a^2+2ac+3c^2=0 \\ a^3+a^2c=0 \\ b=0 \end{cases} \Rightarrow \begin{cases} a=c \\ 4a^2=0 \\ 2a^3=0 \\ b=0 \end{cases} \Rightarrow \begin{cases} a=0 \\ b=0 \\ c=0 \end{cases}.$$

System has only the zero solution.

For the system:

$$\begin{cases} a=-c \\ b=0 \\ a^3+a^2c+ab^2+3bc^2=0 \\ b=0 \end{cases} \Rightarrow \begin{cases} a=-c \\ b=0 \\ a^2(a+c)=0 \end{cases}$$

The system decomposes into two subsystems:

$$\begin{cases} a=-c \\ b=0 \\ a^2=0 \end{cases}; \qquad \begin{cases} a=-c \\ b=0 \\ a+c=0 \end{cases}.$$

System have a solution: $a=-c,\ b=0$.

Solution of the system corresponds to the divisor $\hat{O}(x,y)=a(x-1)$, где $a\neq 0$.

For the system:

$$\begin{cases} a=-c \\ -a^2+2ac+3c^2=0 \\ a^3+a^2c+ab^2+3bc^2=0 \\ b=0 \end{cases} \Rightarrow \begin{cases} a=-c \\ -a^2+2ac+3c^2=0 \\ a^3+a^2c=0 \\ b=0 \end{cases} \Rightarrow \begin{cases} a=-c \\ b=0 \end{cases},$$

we have this same solution.

Similarly, we find solutions to other systems. They have only the trivial solution.

Finally, we have one nonzero solution: $a=-c, b=0$, which determines the divisor $(x-1)$.

Thus polynomial $F(x,y)$ is decomposable:

$x^3-x^2+(y^2-1)x-y^2+1=(x-1)(x^2+y^2-1)$, and $F(x,y)=(x-1)(x^2+y^2-1)$

This example illustrates the case: if the divisor (even trivial) includes a variable, then on it the polynomial is reducible. In this case, by the resultant of the variable produces a system of equations this is non-zero solution.

Example 5.4. Explore: will be whether the polynomial irreducible to the variable y ?

$$F(x,y)=x^3-x^2+(y^2-1)x-y^2+1 .$$

Solution. The degree of the polynomial F (x, y)

$$deg\left(F(x,y)\right)=\deg\left(x^3-x^2+(y^2-1)x-y^2+1\right)=3 ,$$

the degree of the polynomial $\hat{O}(x,y)$, $deg\left(\hat{O}(y)\right)=\left[\frac{\deg\left(F(x,y)\right)}{2}\right]=\left[\frac{3}{2}\right]=1$. Dividers polynomial

$F(x,y)$ we will be sought in the form $\hat{O}(x,y)=ax+by+c$.

We calculate the resultant $\hat{R}_x = R_x\left(F(x,y),\ (\ ,\ )\right)$.

$$\hat{R}_y = R_y\left(F(x,y),\ (y,\ )\right) = {}_y\left((x-1)^2+(ax-1)(y^2-1),\ +\ +\ \right) =$$

$$= det\begin{bmatrix} (x-1) & 0 & (x-1)(x^2-1) \\ b & ax+c & 0 \\ 0 & b & ax+c \end{bmatrix} =$$

$$= (x-1)\left((ax+c)^2+b^2(x^2-1)\right) = (x-1)\left(\left(a^2+b^2\right)x^2+2acx-b^2\right)=0$$

We have: $\left(a^2+b^2\right)x^2+2acx-b^2=0$ where we have a system of equations:

$$\begin{cases} -b^2=0 \\ 2ac=0 \\ a^2+b^2=0 \end{cases} \Rightarrow \begin{cases} b^2=0 \\ 2ac=0 \Rightarrow \\ a^2=0 \end{cases} \begin{cases} a=0 \\ b=0 \\ c=0 \end{cases}.$$

The system has only the zero solution, so the polynomial $F(x,y)$ is irreducible variable y .

Example 5.5. Investigated for an irreducible polynomial

$$F(x,y)=x^2y^2-2x^2-y^2+2$$

with respect to x .

Solution. The degree of the polynomial $F(x,y)$,

$$deg\left(F(x,y)\right)=deg_x\left(F(x,y)\right)=\deg_x\left((y^2-2)x^2-(y^2-2)\right)=2\ ,$$

the degree of the polynomial $\hat{O}(x,y)$, $deg\left(y(\ ,\ )\right)=\left[\dfrac{\deg\left(F(x,y)\right)}{2}\right]=\left[\dfrac{2}{2}\right]=1$. Dividers polynomial $F(x,y)$ we will be sought in the form $\hat{O}(x,y)=ax+by+c$.

We calculate the resultant $\hat{R}_x = R_x\left(F(x,y),\ (\ ,\ )\right)$:

$$\hat{R}_x = R_x\left(F(x,y),\ (x,\ )\right) = {}_x(\ ^2-2)\ ^2-(\ ^2-2)) =$$

$$= (y^2-2)\left(b^2y^2-2bcy+c^2-a^2\right) =$$

$$= b^2y^4-2bcy^3+(c^2-a^2)y^2-2b^2y^2+4by-2c^2+2a^2 =$$

$$b^2y^4-2bcy^3+(c^2-2b^2-a^2)y^2+4by-2c^2+2a^2\equiv 0$$

According to Theorem 5.1, all the coefficients of the polynomial on the left side of the equation equal to zero. We have a system of equations:

$$\begin{cases} b^2=0 \\ -2bc=0 \\ c^2-2b^2-a^2=0 \\ 4b=0 \\ -2c^2+2a^2 \end{cases} \Rightarrow \begin{cases} b=0 \\ bc=0 \\ c^2-2b^2-a^2=0 \\ c^2-a^2=0 \end{cases} \Rightarrow \begin{cases} b=0 \\ c^2-a^2=0 \end{cases} \Rightarrow \begin{cases} b=0 \\ c=\pm a \end{cases}.$$

The system has two non-zero solutions $(a,0,a)$ and $(a,0,-a)$, which correspond to the divisors

$\hat{O}_1(x,y)=ax+a=a(x+1)$ and $\hat{O}_2(x,y)=ax-a=a(x-1)$.

Is therefore, the polynomial F (x, y) reducible with respect to x, and

$$F(x,y)=(x-1)(x+1)(y^2-2).$$

6. General scheme of solution of systems of polynomial equations

When solving systems of polynomial equations (in particular, the equations of N-point gravitational lenses) we believe the best the following algorithm:

1. Check each equation of the system, whether a it is reducible. If it is reducible, the system decomposes into subsystems, each of which we are solving separate.

2. Select one of the equations and one unknown therein. Exclude this unknown of other equations, if possible. If you cannot perform a simple substitution, then eliminate the unknown using the resultant. Exclude selected variable from the other equations, if it is there.

Go to the new system of equations, which will consist of selected equations and calculated resultants, equal to zero. This system of equations is equivalent to the initial one.

However, if the system of two equations with two unknowns to a system of equations of the two resultants is equal to zero, then this transition, generally speaking, is not equivalent. The resulting solution in such a transition cannot be solutions of the original system of equations, see. E.g. [19].

4. The built in system of claim 3, consider a subsystem consisting of resultants, equal to zero. The subsystem will contain at least one equation and one less unknown. None of the resultants cannot be identically zero (except in the case when the equations are the same), because each polynomial is irreducible on the right side of equations. In the case that one of the matching equations remove from the system. The subsystem will contain less at least one equation and one unknown.

To this subsystem apply the process from 1-4.

5. After a finite number of steps we obtain the resultants to be polynomials in one variable. Imagine every one of them as a product of polynomials with multiple roots. Each of these polynomials we associate a polynomial with non-multiple roots, which is equal to the original roots of the polynomial

6. Thus, it remains to find the roots of the polynomial on the condition that they are all different. Note that up to this point, we only had a finite number of rational operations. Therefore, before this stage of the algorithm can be considered as constructive and analytical. Such an algorithm can be implemented using a symbolic programming. We can use the packages of general purpose applications such as REDUCE, MACSYMA, MATHEMATICA, MAPLE, AXIOM, MuPAD, algorithmic basis of which are operations on polynomials and rational functions.

7. The Calculation of the roots of a polynomial in one variable is a standard procedure. It can be performed with any precision. Note that the final procedure of the algorithm is, the computation of roots of polynomials. Therefore, the accuracy of calculation of the roots of one polynomial will not affect the accuracy of calculating the other.

Below are a few examples of solutions of systems of polynomial equations.

Example 6.1. Solve the system of equations

$$\begin{cases} f(x,y)=4x^2-7xy+y^2+13x-2y-3=0 \\ g(x,y)=9x^2-14xy+y^2+28x-4y-5=0 \end{cases}, \tag{6.1}$$

Solution. Compose the elimination $X(x)=R_y(f(x,y),g(x,y))X(x)=R_y(f(x,y),g(x,y))$:

$$f(x,y)=y^2+(-7x-2)y+(4x^2+13x-3)=0\ ,$$
$$g(x,y)=y^2+(-14x-4)+(9x^2+28x-5)=0\ ,$$

$$X(x)=\begin{vmatrix} 1 & -7x-2 & 4x^2+13x-3 & 0 \\ 0 & 1 & -7x-2 & 4x^2+13x-3 \\ 0 & 1 & -14x-4 & 9x^2+28x-5 \\ 1 & -14x-4 & 9x^2+28x-5 & 0 \end{vmatrix} = 24\left(x^4-x^3-4x^2+4x\right).$$

We find eliminante roots $X(x)$. We have: $x_1=0$, $x_2=1$, $x_3=2$, $x_4=-2$.

Each found the root of the substitute in (6.1). For $x_1=0$, we have:

$$\begin{cases} f(x,y)=y^2-2y-3=0 \\ g(x,y)=y^2-4y-5=0 \end{cases} \tag{6.2}$$

The equations (6.2) have a common root $y_1=0$.

Similarly, substituting the other found in the roots of the system (6.1). We have the solution of the system: ($1,2);(2,3);(0,-1);(-2,1).$ By the theorem of Bezout (the number of solutions of polynomial equations) solutions must be four as $degf(x,y)=2$ and $degg(x,y)=2$. Consequently, we find all solutions.

Example 6.2. Solve the system of equations

$$\begin{cases} f(x,y)=x^2-2xy+y^2-1=0 \\ g(x,y)=x^2-y^2+2x+1=0 \end{cases}. \tag{6.3}$$

Solution. Both eliminanty $X(x)\equiv 0$, $Y(y)\equiv 0$, hence the equations system (6.3) have a common component. Really:

$$\begin{cases} x^2-2xy+y^2-1=0 \\ x^2-y^2+2x+1=0 \end{cases} \Rightarrow \begin{cases} (x-y)^2-1=0 \\ (x+1)^2-y^2=0 \end{cases} \Rightarrow \begin{cases} (x-y+1)(x-y-1)=0 \\ (x-y+1)(x+y+1)=0 \end{cases},$$

and the system (6.3) decomposes into four systems::

$$\begin{cases} x-y+1=0 \\ x-y+1=0 \end{cases}, \begin{cases} x-y+1=0 \\ x+y+1=0 \end{cases}, \begin{cases} x-y-1=0 \\ x-y+1=0 \end{cases}, \begin{cases} x-y-1=0 \\ x+y+1=0 \end{cases}.$$

The first system has an infinite number of solutions: $(\alpha,\alpha+1)$ for any $\alpha\in\mathbb{C}$. The second - a unique solution: (-1.0), which satisfies the first system. The third system solution in affine coordinates is not. A fourth system has a unique solution (0, -1).

Note that instead of four systems can be considered one - fourth and one equation $x-y+1=0$. In both cases, the set of solutions (in affine coordinates) obviously coincides.

The geometric meaning of the set of solutions (in affine coordinates) the following: algebraic curves $f(x,y)=0$ and $g(x,y)=0$ have a common branch – direct $y=x+1$ and additionally point (0, -1)

In [19] there is an interesting example in which there is a “false” solution.

Example 6.3 Solve the system of equations:

$$\begin{cases} f(x,y)=xy-1=0 \\ g(x,y)=x^2y+x-2=0 \end{cases}, \tag{6.4}$$

Solution. Each of the system eliminant

$$Y(y)=-2y(y-1)\ ,\ \ Y(x)=2x(x-1)$$

It has “extra” root, the result generated by the “false” solution $(0,0)$.

There is given the following explanation:

«The reason for the effect is the same as in the previous example (in the previous example: In the explanation of the fact of the appearance of "extra" roots eliminants draw attention to the fact that at x = 0 degree polynomials f and g are reduced, and this effect is manifested in the construction eliminant as a determinant of the matrix».

And later in [19] it is proposed: to monitor such cases it is necessary to check the suspicious values of the variables, i.e., those that reduce the extent of the original equations.

From our point of view a simple reason for the emergence of "false" solution is in technology and computing is clear: no system of equations is equivalent to the system eliminant are equal to zero.

To find out of deeper reasons we pay attention to the number of solutions of (6.4). By Theorem Bezout them, counting multiplicities, must be greater than one (the system is not linear), and we have only one $x=1$, $y=1$.

It is natural to ask: where are the other solutions?

Some solutions may not belong to $\mathbb{C}^2$ and should be sought in the space $\overline{\mathbb{C}}^2$. Such decisions are easy to find if we use a fractional-linear transformation of variables, such as the inversion of one of the variables: $y=\frac{1}{t}$. After the system transformation (6.4) we have the system of equations:

$$\begin{cases} x-t=0 \\ x^2+xt-2t=0 \end{cases}.$$

Where we have solutions for Bezout's theorem, there must be two solutions, and these solutions $x=0$, $t=0$ and $x=1$, $t=1$. By making the inverse transformation, we obtain the solution: $x=0, y=\infty$. Similarly, we obtain another solution of the system (6.4): $x=\infty, y=0$. Thus, the system of equations (6.4) has a $\overline{\mathbb{C}}^2$, at least three different solutions.

The solution (0.0) is the solution of system of equations consisting of eliminant equal to zero. Each of eliminant, is a polynomial in one variable. Decision of such a system will have a direct multiplication of sets of their roots. In this set included (0,0), and one zero belongs to the improper initial decision system, and the second the other.

N o t e also that the system of equations (6.3) (. See example 6.2) has another solution $\overline{\mathbb{C}}^2$, namely:

$$x=\infty, y=\infty .$$

Research the solutions of (6.4) and (6.3), can be carried out differently, for example, if you go to the homogeneous coordinates, but the transition to the homogeneous coordinates is beyond the scope of this paper.

7. Stakes and challenges. Solved and set

The above theorems and algorithms allow to solve a number of problems in the theory of N-point gravitational lenses, namely,

- Finding the source of the images in the plane gravitational lens (the problem is reduced to finding the solutions of the lens equation - the variety is an algebraic set), see [10].

- Finding the of extended images in the source plane (the problem is reduced to finding the one-dimensional submanifolds of a manifold is an algebraic set);

- The distribution of images in plane gravitational lens(the problem reduces to the problem of the distribution of the roots of a polynomial in one variable);

- Calculation of critical curves and their research;
- Computation of caustics and their research;
- Calculation of the light curves and their research;

- Study of the lens equation, including the study of its fixed points, multiple points, and other local features;

- The study of harmonic component of the lens equation and its complexification;

-Calculating the type multiplicity lens equations of (the problem is reduced to the special case the solved problem, see [17]);

- Classification of the point of gravitational lenses on the basis of features of the lens equation (arithmetic classification).

References

1. Weinberg S. Gravitation and Cosmology. Massachusetts Institute of Technology, 1972. P 657.
2. Ландау Л.Д., Лифшиц Е.М. Теория поля. М. Наука, 1988. Т.2 С 512.
3. Захаров А.Ф. Гравитационные линзы и микролинзы. М. Янус-К, 1997. С. 328.
4. Schneider P., Ehlers J., Falco E.E. Gravitational lenses. Springer-Verlag Berlin Heidelberg 1999 P. 560.
5. Chwolson O. Über eine mögliche Form fiktiver Doppelsterne // Astr. Nachrichten. – 1924, 221, P. 329 - 330.
6. Einstein A. Lens-like action of a star by the deviation of light in the gravitational field // Science. – 1936, 84, No. 2188, P. 506 – 507.
7. Bannikova E.Yu., Kotvytskiy A.T. // MNRAS, 445:4 (2014), 4435-4442.
8. Котвицкий А.Т., Крючков Д.В. // Вестник ХНУ серия «Физика», 1113:20 (2014), 63-73.
9. Kotvytskiy A. T. // Theoretical and Mathematical Physics, 184(1): 1033-1046 (2015).
10. Kotvytskiy A.T., Bronza S.D. // Odessa Astronomical Publications, vol. 29 (2016),

P.31-33. (DOI: http://dx.doi.org/10.18524/1810-4215.2016.29.84958).
11. Серре И.А. Курс высшей алгебры. М.-СПб.: Вольф, Б.г. (1896?). 574 с.
12. Бохер М. Введение в высшую алгебру. М.-Л.: ГТТИ, 1933. 292 с.
13. Ван-дер-Варден Б.Л. Алгебра. -М. Наука, 1976. 648 с.
14. Van Der Waerden B.L.: 1971, Algebra I, II, P. 456.
15. Lang S. Algebra. Columbia University. New York, 1965.
16. Ленг С. Алнебра. М.: Мир, 1968. -564 с.
17. Уокер.Р. Алгебраические кривые. –М.: ИЛ., 1952. 236 с.
18. Walker R.J.: 1950, Algebraic curves, P. 236.
19. Курош А.Г. Курс высшей алгебры. -М.: Наука, 1975. 432 с.
20. Бронза С.Д. Разветвленность рациональных функций // Харьковский гос. ун-т. - Харьков, 1987. – 16с. – Деп в УкрНИИНТИ 24.03.87, за № 1018 Ук-87 Деп.
21. Бронза С.Д. Критерий неприводимости многочленов от двух переменных над полем комплексних чисел. Збірник наукових праць, Харків, УкрДУЗТ 2016, вип.160 (додаток) с.114-115.
22. Калинина Е.А., Утешев А.Ю. Теория исключения. СПб.: Изд-во НИИ химии СПбГУ, 2002. 72 с.
23. Новоселов С.И. Специальный курс элементарной алгебры.- М.: Советская наука, 1954. 560 с.
24. Гриффитс Ф., Харрис Дж. Принципы алгебраической геометрии. Т.1-2.-М.: Мир, 1982. 864 с.
25. Шафаревич И.Р. Основы алгебраической геометрии.-М.: Наука,1972. 568 с.
26. Батхин А. Б. Устойчивость одной многопараметрической системы гамильтона. Препринт.М.: ИПМ им. М. В. Келдыша РАН, 2011. 29 с.
27. Джури Э. Инноры и устойчивость динамических систем. М.: Наука, 1979. 304 с.
28. Juri E.I. Inners and stability of dynamic systems. Nev York-London-Sydney-Toronto.:John Wiley Sons, 1974. 304 p.
29. Гротендик, А. Урожаи и посевы. Размышления о прошлом математика / А. Гротендик. – Ижевск : Удмуртский университет, 1999. – 288 с.
30. Качалин А.В. История и теория науки в исследовательских подходах отечественных естествоиспытателей в XX веке, Ульяновск,: Качалин А.В.,2015 с.450.
31. Bézout É. Théorie générale des Équations Algébriques. P.-D. Pierres, Paris. 1779.

Вісник ХНУ, серія «Фізика», вип. 26, 2017. с. 28-32

PACS 05.45.Xt, 74.50.+r, 85.25.Cp
УДК: 537.312.62

Coherent emission from a stack of long Josephson junctions based on low-temperature superconductors

Alexander Grib*, Ruslan Vovk*, Volodymyr Shaternik**

*Physics Department, Kharkiv V. N. Karazin National University, Svobody sq. 4, 61022, Kharkiv, Ukraine
**G.V. Kurdyumov Institute for Metal Physics, N.A.S. of Ukraine, 36 Academician Vernadsky Boulevard, UA-03142 Kyiv, Ukraine

The theory of coherent emission of intrinsic Josephson junctions was applied for calculations of IV-characteristics and ac power of emission of a stack of two inductively coupled long junctions with high density of critical currents (10^6 A/m^2) which were based on low-temperature superconductors (MoRe films). Barriers were made of the mixture of Si and W. Barriers had thickness of about 15 nm. Randomly distributed clusters of tungsten in the thick silicon barrier provided weak links between superconducting MoRe films. The critical temperature of the MoRe superconducting films was 9 K. Calculations were made for the system at the temperature 7.7 K. Random spread of critical currents along the junction leaded to the formation of the zero-field step in the IV-curve. The same zero-field step appeared when edges of the homogeneous junction were loaded by the resistance, the capacitance and the inductance. In the stack of two junctions, strong coherent emission appeared at the zero-field step which corresponded to the in-phase mode of oscillations of voltages.

Keywords: Josephson junctions; coherent emission; synchronization; zero-field steps.

Теорію когерентної емісії внутрішніх контактів Джозефсона застосовано до розрахунків вольт - амперних характеристик та потужності емісії пачки з двох індуктивно пов'язаних один з одним довгих контактів з високою густиною критичних струмів (до 10^6 А/м^2) на основі низькотемпературних надпровідників (плівок MoRe). Бар'єри були зроблені з суміші Si та W. Бар'єри мали товщину близько 15 нм. Випадково розподілені кластери вольфраму у товстому бар'єрі кремнію забезпечували слабі зв'язки між надпровідними плівками MoRe. Критична температура надпровідних плівок MoRe була 9 K. Розрахунки були зроблені для системи при температурі 7.7 K. Випадковий розбіг критичних струмів вздовж контакту привів до появи сходинки нульового поля на вольт - амперній характеристиці контакту. Та ж сходинка нульового поля виникає, якщо на краях контакту з однорідним розподілом критичних струмів є навантаження з електричного опору, конденсатора та індуктивності. В пачці з двох контактів сильна когерентна емісія виникла на сходинці нульового поля, яка відповідає синфазній моді осциляцій напруги.

Ключові слова: контакти Джозефсона; когерентна емісія; синхронізація; сходинки нульового поля.

Теория когерентной эмиссии внутренних контактов Джозефсона применена для расчёта вольт - амперных характеристик и мощности эмиссии пачки двух индуктивно взаимодействующих друг с другом длинных контактов с высокой плотностью критического тока (10^6 А/м) на основе низкотемпературных сверхпроводников (плёнок MoRe). Барьеры были сделаны из смеси Si и W. Они имели толщину около 15 нм. Случайно расположенные кластеры вольфрама в толстых барьерах из кремния обеспечивали слабые связи между сверхпроводящими пленками MoRe. Критическая температура сверхпроводящих пленок MoRe была 9 K. Вычисления были сделаны для системы, находящейся при температуре 7.7 K. Случайное распределение критических токов в длинном контакте привело к образованию ступеньки нулевого поля на вольт - амперной характеристике. Та же ступенька возникает, если на краях длинного контакта с однородным распределением критических токов имеется нагрузка из сопротивления, ёмкости и индуктивности. В пачке из двух контактов сильная когерентная эмиссия возникла на ступеньке нулевого поля, которая соответствует синфазной моде осцилляций напряжения.

Ключевые слова: контакты Джозефсона; когерентная эмиссия; синхронизация; ступеньки нулевого поля.

Introduction

The increased attention to mechanisms of synchronization of large number of Josephson junctions is caused by the experimentally found coherent emission from more than six hundred intrinsic Josephson junctions in high-temperature superconductors [1]. The found effect allowed obtaining power of emission up to microwatt in the sub-THz region [2]. Following experimental and theoretical investigations allowed to reveal the new mechanism of synchronization which is supposed to produce in-phase locking of voltage oscillations in stacks of intrinsic junctions in mesa structures of high-temperature superconductors [3-6]. Because in the present paper we will apply this mechanism to another type of superconductors, we describe it in details. The inductive interaction between superconducting layers is possible in the stack of junctions. Due to this interaction, normal

modes of electromagnetic waves appear in the system [7, 8]. For example, in the system of two inductively coupled junctions, there appear the in-phase mode and anti-phase mode which have different velocities of propagation [7]. Normal modes can be revealed due to the so-called zero-field steps in IV-characteristics [5, 6]. These steps are formed without applied external magnetic field. It is well known that due to some longitudinal perturbations the standing wave of electromagnetic field can be formed in the long solitary Josephson junction [9]. This wave produces some distribution of ac voltage over the junction. If the distribution of critical currents along the junction is symmetrical, zero-field steps appear in the IV-characteristic of the junction at voltages of even Fiske steps as a result of the interaction between Josephson generation and the standing wave [9]. These voltages are equal to

$$< V_s >= \frac{\Phi_0 \bar{c} s}{D} , \qquad (1)$$

where the sign <…> means averaging over time that is much longer than the period of Josephson oscillations, D is the length of the junction, Φ_0 is the quantum of magnetic flux, $\bar{c}$ is the velocity of light in the junction and s =1,2... is an integer. In the system of two inductively coupled junctions there are two zero-field steps in the IV-characteristic which correspond to two velocities of the propagation of light for different normal modes. In the system of K inductively coupled junctions there are K normal modes and therefore, there is the bunch of K zero-field steps. Among these steps there is the zero-field step that corresponds to the in-phase mode in which all junctions oscillate coherently (the step at highest voltage in the bunch [7]). Thus, to obtain in-phase synchronization of junctions in the stack it is necessary to induce the standing wave in the stack and to measure the zero-field step at highest voltage in the bunch.

The described above mechanism of synchronization can be applied also to the stack of junctions made of low-temperature superconductors. The application of underdamping junctions with high values of the McCumber parameter is not effective for our aim because the subgap steps in the IV-curve can not be revealed properly in ranges of the current-biased scheme which is usually applied in calculations. We consider here the stack of overdamped long junctions. In the present paper we calculated IV-characteristics and power of ac emission for the separate long Josephson junction and the stack of two Josephson junctions. Parameters of calculations were taken for junctions with high density of critical currents (up to 10^6 A/m^2) made of MoRe films with 45% Re and the barrier made of the mixture of Si and W with the concentration of W up to 10% [10]. Clusters of tungsten provide weak links in the barrier. It was proven that at temperatures near the critical temperature ($T_c \approx 9$ K for the given system) and if the length of the weak link is smaller than the length of coherence, dynamics of the weak link can be described by the resistively-shunted model of the Josephson junction (RSJ-model) [9, 11]. We modeled the mentioned system at 7.7 K in the ranges of RSJ-model taking into account capacitances of junctions. We calculated IV-curves for these systems and ac power of emission into the load and discussed obtained results.

The model

The model of calculations is described in details in Refs. [6, 12 - 15]. Here we give only the brief description of the model. Each of the K=2 wide junctions with the index i = 1,2 is divided into n segments. Segments are numbered by the index j=1…n. It is supposed that the 'elementary junction' is placed in the center of each segment. These 'elementary junctions' are divided by the distance $\zeta = \sqrt{\bar{c}CL}$, where $\bar{c}$ is the velocity of light in the junction, L is the inductance of the segment and C is the capacitance of the segment (we suppose all the capacitances are equal to each other). The system of equations which describes the high-frequency scheme of the stack of junctions includes current conservation conditions for 'elementary junctions' and flux quantization conditions:

$$\frac{\Phi_0 C}{2\pi}\frac{d^2\phi_{i,j}}{dt^2} + \frac{\Phi_0}{2\pi R}\frac{d\phi_{i,j}}{dt} + I_{ci,j}\sin\phi_{i,j} = I_b - I^R_{i,j-1,j} + I^R_{i,j,j+1} , \qquad (2)$$

where $i = 1,2,\ j = 2...n-1$,

$$LI^R_{1,j-1,j} - L_f I^R_{2,j-1,j} + \frac{\Phi_0}{2\pi}\left(\phi_{1,j-1} - \phi_{1,j}\right) = 0 , \qquad (3)$$

where $j = 2...n,$

$$-L_f I^R_{1,j-1,j} + LI^R_{2,j-1,j} + \frac{\Phi_0}{2\pi}\left(\phi_{2,j-1} - \phi_{2,j}\right) = 0 , \qquad (4)$$

where $j = 2...n$, $I^R_{i,j-1,j}$ is the current in the loop between two segments with indices j-1 and j, $I_{ci,j}$ and R are the critical current and the resistance of the segment (we suppose that R = *const*), $\varphi_{i,j}$ is the difference of the phase of the order parameter across the junction which is contained in the segment, L_f is the mutual inductance between two adjacent cells of the 'elementary stack', t is time. Equations (2)-(4) can be solved by means of the method of Runge-Kutta. The result of calculations in this case is the IV-characteristic of the system. We can also attach additional contours containing the resistance, the inductance and the capacitance to the edges of junctions. In this case we can calculate power of ac emission extracted to the load. In the following consideration we will use both the system with loads at edges and the system without

loads. To take into account loads, we mark them as fictive segments with indices j=0 and j=n+1 added to edges of junctions. Kirchhoff rules for these segments are as follows:

$$L_{ej}\frac{d^2q_j}{dt^2}+R_{ej}\frac{dq_j}{dt}+\frac{q_j}{C_{ej}}=\mp\frac{\Phi_0}{2\pi}\sum_{i=1}^{2}\frac{d\phi_{i,j\pm1}}{dt}\ , \quad (5)$$

where $j=0,n+1,$ and q_j is the charge flowing through the inductance L_{ej} , C_{ej} and R_{ej} are the capacitance and the resistance of the additional contour. In the present paper we assume $C_{ej}=C$, $L_{ej}=L$ and $R_{ej}=R$. The value of mutual inductance between 'elementary junctions' in the stack was defined as $L_f=\alpha L$, where α is dimensionless parameter. Eqs. (2)-(5) were solved for different bias currents. IV-characteristics were obtained in calculations. The voltage over the system of two junctions was calculated as

$$\left\langle V_{system}\right\rangle=\frac{\Phi_0}{2\pi n}\left\langle\sum_{i=1}^{2}\sum_{j=1}^{n}\frac{d\phi_{i,j}}{dt}\right\rangle\ . \quad (6)$$

For the comparison of IV-curves for the stack of two junctions and those for one separate junction we will use the value $\langle V\rangle=\left\langle V_{system}\right\rangle/K$, where K is the quantity of long junctions in the system, i.e. K=1 for the separate junction and K=2 for the stack.

The value of emitted ac power at the left end of the system was calculated as follows:

$$P_l=\frac{1}{KR}\left\langle\left\{\sum_{i=1}^{K}\left[\frac{\Phi_0}{2\pi}\left(\frac{d\phi_{i,1}}{dt}-\left\langle\frac{d\phi_{i,1}}{dt}\right\rangle\right)\right]\right\}^2\right\rangle. \quad (7)$$

The same expression with j=n was used for the calculation of emitted power from the right end of the system.

For calculations we used values of parameters for superconducting layers made of MoRe films with 45% Re and the barrier made of the mixture of Si and W with the concentration of W up to 10% [10]. The critical temperature of this system is 9 K. To satisfy conditions of the application of the RSJ model to this system, we calculated parameters for the temperature 7.7 K. At first, we stated values of critical currents at temperatures $T<<T_c$ which we defined from experimental data [10]: $I_c(T<<T_c)\approx$ 10 mA, $V_c(T<<T_c)$ $\approx$ 3 mV and density of critical currents was equal to $J_c=10^6$ A/m^2. Dimensions of long layers were 250x40x0.05 cubic micrometers and the thickness of each of the barrier was 15 nm. Then we divided the long junction to n=30 segments and calculated the critical current of the segment and its resistance R. We supposed that the velocity of light in the junction was $\bar{c}(T<\ T_c)=c/\sqrt{\varepsilon}$ where c is the light velocity in vacuum and $\varepsilon\approx12$ is permittivity of silicon, so $\bar{c}\left(T<<T_c\right)\approx8.87\cdot10^7$ m/s. For the calculation of dependences of parameters on the temperature we used the method developed in Ref. 6. For the determination of the value of the critical current at the given temperature we used the plot of the dependence of critical current on the reduced temperature for the weal link in the dirty limit [9].

For the temperature T = 7.7 K parameters of the long junction were as follows: I_c = 2.5 mA, V_c = 0.75 mV, $\bar{c}\left(T=7.7K\right)=6.14\cdot10^7$ m/s, $\beta_c=10.24$. The Josephson depth of penetration of magnetic field was $\lambda_J=86.2\cdot10^{-6}$ m. After the definition of parameters we calculated IV-curves and ac power of emission for one separate long junction and for the stack of two inductively coupled junctions with $\alpha=0.3$. We would like to note that such parameters of our model as the velocity of the propagation of electromagnetic waves in the long junction and the depth of penetration of magnetic field in the junction and temperature dependences of their values were calculated on the base of plausible assumptions and it is of great interest to investigate them experimentally.

Results and Discussion

We discuss at first the electrical properties of the separate long junction without loads at edges. The IV-characteristic of the separate homogeneous long junction is shown in Fig. 1a. It is the typical hysteretic curve which is characteristic for the junction with the finite value of the McCumber parameter β_C . The switch from the hysteretic branch to the zero-current branch appears at 0.38×I_c that corresponds exactly to the switch in the solitary junction of the negligible size with $\beta_C=10.24$ in the range of the RSJ-model [16]. The IV-curve in Fig. 1a does not contain any particularities connected with geometrical dimensions of the system. Analogous results were obtained in Ref. 15 for intrinsic junctions.

Now we consider the IV-curve of the inhomogeneous long junction without loads at edges (Fig. 1b, crosses). Inhomogeneity is created by spread of critical currents of about 10^{-2}%. There is a step in the IV-curve in the hysteretic region at $\left\langle V'_{s=1}\right\rangle\approx0.43$ mV. After the step there is the jump of voltage to the value 0.55 mV. It is shown in Ref. 15 that this behaviour of the IV-curve is caused by the resonant interaction of Josephson generation with standing wave that appears in the inhomogeneous junction. Due to inhomogeneity of critical currents along the junction, there arise longitudinal excitations [15]. They reflect from edges of the junction (it is the so-called Fulton-Dynes mechanism of reflection [17]). The standing wave appears when the even number of halves of wavelengths of the excitation becomes equal to the length of the junction. Just this condition is written in Eq. (1). The standing wave interacts with Josephson generation the same way as the external periodical signal, so zero-field steps appear in the IV-curve.

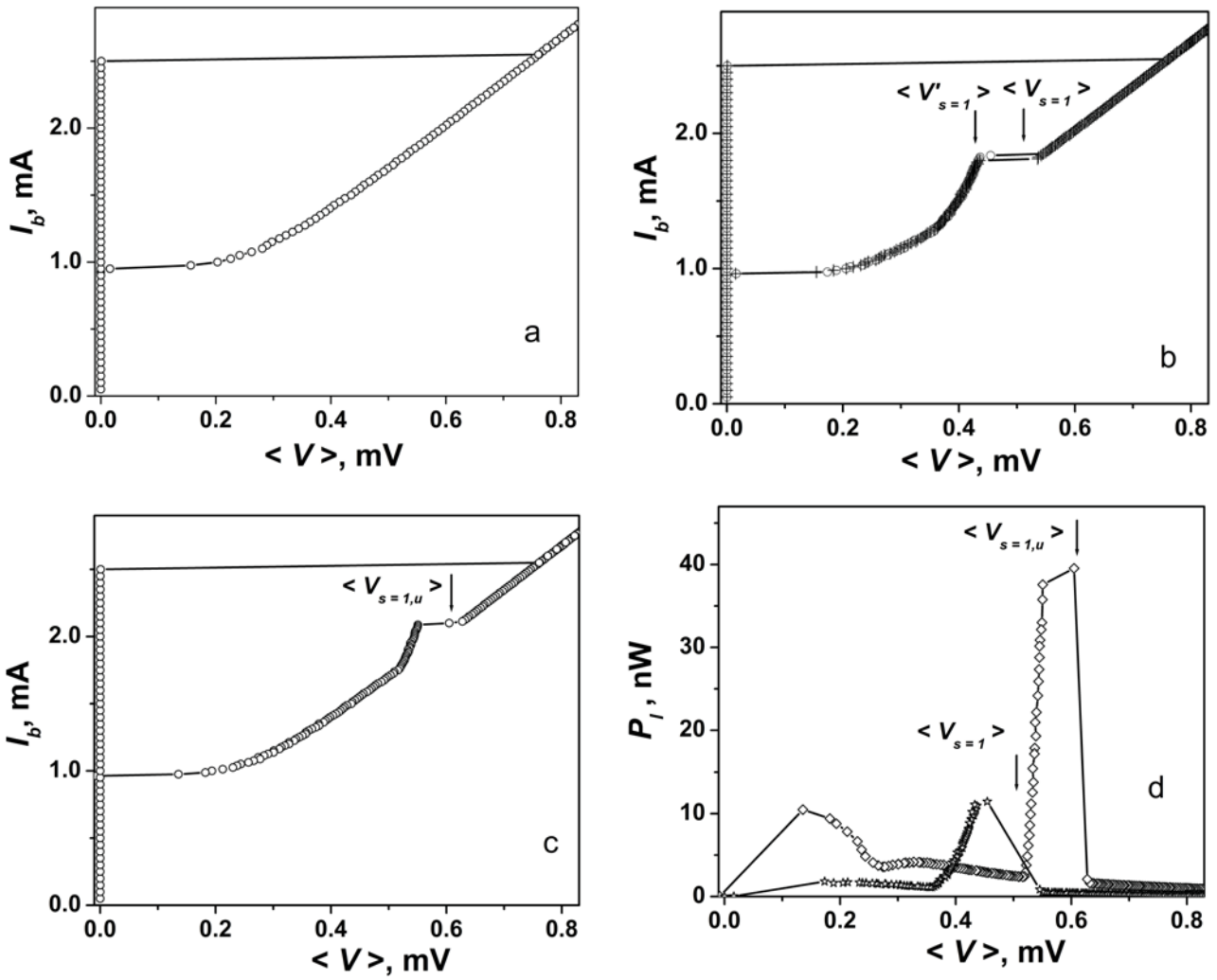

Fig. 1. (a)- the IV-characteristic of one separate long homogeneous junctions without loads at edges. (b)- IV-characteristics of one separate long junction with spread of critical currents 10^{-2}% without loads at edges (crosses) and the same for the homogeneous long junction with loads at edges (circles). Positions of voltages $< V_{s=1} >$ and $< V'_{s=1} >$ are marked by arrows. (c)- the IV-characteristic of the stack of two inductively coupled long junctions with loads at edges. The position of voltage $< V_{s=1,u} >$ is shown by an arrow. (d)- dependences $P_l\left(\langle V \rangle\right)$ for the solitary long junction with the load at edges (stars) and for the stack of two inductively coupled long junctions with loads at edges. Positions of voltages $< V_{s=1} >$ and $< V_{s=1,u} >$ are shown by arrows.

Just this step appears in the IV-curve shown in Fig. 1b. According to Eq. (1), the value of $\langle V_{s=1} \rangle = 0.51$ mV. It is shown by an arrow in Fig. 1b. Due to the ambiguity of the IV-curve in the region of the hysteresis, the full height of the step can not be obtained in the range of the current-biased scheme, so the step is interrupted at the value $\langle V'_{s=1} \rangle \approx 0.43$ mV.

Let us consider now the IV-curve of the fully homogeneous junction with loads at edges (Fig. 1b, circles). It is seen that the zero-field step is reproduced in full despite the junction now is homogeneous. Standing waves in this case are excited due to the influence of the loads at edges. [15]. Loads violate homogeneity of the junction, so perturbations propagate along the junction and at some frequencies produce standing waves.

The IV-characteristic of the stack of two long junctions with loads at edges is shown in Fig. 1c. It is known that due to the inductive coupling of layers the zero-field step is split into two steps at voltages $< V_{s=1,d} > = < V_{s=1} > / \sqrt{1+\alpha}$ and $< V_{s=1,u} > = < V_{s=1} > / \sqrt{1-\alpha}$ [6, 13-15]. However, in Fig. 1c there is only one step near $< V_{s=1,u} > \approx 0.51$ mV. The step at $< V_{s=1,d} > \approx 0.45$ mV is not seen. The split appears due to the formation of normal vibrations in the system of coupled layers. At $< V_{s=1,d} >$ voltages over

junctions in the 'elementary stack' oscillate anti-phase, and at $< V_{s=1,u} >$ there are in-phase oscillations of voltages over junctions in the 'elementary stack'. Just this mode of in-phase oscillations is used for producing of coherent emission from the stack. To prove this we calculated the dependence of averaged over time ac power emitted in the load at the left end of the solitary junction P_l on voltage (Fig. 1d, stars) as well as the dependence $P_l(< V >)$ for the stack (Fig. 1d, diamonds). The dependence $P_l(< V >)$ for the solitary junction has the maximum at the voltage $\langle V'_{s=1} \rangle \approx 0.45$ mV. The dependence $P_l(< V >)$ for the stack has the maximum at the voltage $\langle V'_{s=1,u} \rangle \approx 0.60$ mV. This value corresponds to the in-phase mode of oscillations of voltages over junctions. The maximal value of emitted ac power P_l at $\langle V'_{s=1,u} \rangle$ for the stack of two junctions is equal to 39.54 nW whereas the maximal value of P_l at $\langle V'_{s=1} \rangle$ for the solitary junction is equal to 11.46 nW. The relation of these values is 3.45 that means nearly full phase locking with the constant phase shift (the relation is equal to 4 for the zero phase shift [16]). This result proves that the zero-field step at $\langle V'_{s=1,u} \rangle \approx 0.60$ mV in the stack of two long junctions corresponds to the in-phase normal mode.

Finishing the discussion we note that in the junctions MoRe with the barrier made of silicon and tungsten phase slip phenomena can appear [10]. Zero-field steps appear often in junctions with phase slip processes [9]. Investigations of phase locking including phase slip processes becomes of great interest for the theory of synchronization.

Summary

In the present paper for synchronization of emission from a stack of long Josephson junctions we applied the mechanism of synchronization which was earlier used for the explanation of phase locking of intrinsic junctions in high-temperature superconductors. Parameters of calculations were taken for low-temperature junctions with high density of critical currents (up to 10^6 A/m^2) made of MoRe films with 45% Re and the barrier made of the mixture of Si and W with the concentration of W up to 10%. The layers had dimensions 250x40x0.05 cubic micrometers and the thickness of the barrier was 15 nm. The main advantage of this system is the small McCumber parameter (it is about 10.24 at the given temperature). We calculated IV-curves and emission to the RLC-load for one long junction and for the stack of two inductively coupled long junctions at the temperature 7.7 K that is close to the critical temperature. We showed that standing waves could be excited in such a system if it had the inhomogeneous distribution of critical currents along the junctions or if there were loads attached to edges of the system. We obtained zero-field steps in IV-curves of long junctions with standing waves and showed that these steps were produced by the resonant interaction of standing wave with Josephson generation. We proved that the zero-field step in the IV-curve of the stack was split and obtained strong coherent emission at the upper zero-field step which corresponds to the in-phase mode of oscillations of voltages.

Acknowledgement

This publication is based on the research provided by the grant support of the State Fund for Fundamental Research (project Ф76/36725).

References

1. L. Ozyuzer, A. E. Koshelev, C. Kurter, N. Gopalsami, Q. Li, M. Tachiki, K. Kadowaki, T. Yamamoto, H. Minami, H. Yamaguchi, T. Tachiki, K. E. Gray, W.-K. Kwok, U. Welp. Science, 318, 1291 (2007).
2. K. Kadowaki, H. Yamaguchi, K. Kawamata, T. Yamamoto, H. Minami, I. Kakeya, U. Welp, L. Ozyuzer, A. Koshelev , C. Kurter, K.E. Gray, W.-K. Kwok. Physica, 468C, 634 (2008).
3. B. Gross, S. Guénon, J. Yuan, M. Y. Li, J. Li, A. Ishii, R. G. Mints, T. Hatano, P. H. Wu, D. Koelle, H. B. Wang, and R. Kleiner. Phys. Rev. B 86, 094524 (2012).
4. H. Asai and S. Kawabata, Appl. Phys. Lett. 104 112601 2014).
5. A. E. Koshelev, L. N. Bulaevskii. Phys. Rev. B77, 014530 (2008).
6. Alexander Grib, Paul Seidel and Masayoshi Tonouchi. Supercond. Sci. Technol. 30, 014004 (2017).
7. S. Sakai and P. Bodin, N. F. Pedersen. J. Appl. Phys., 73, 2411 (1993).
8. R. Kleiner, P. Müller, H. Kohlstedt. N. F. Pedersen, S. Sakai. Phys. Rev. B50, 3942 (1994).
9. Antonio Barone and Gianfranco Paternò. Physics and applications of the Josephson effect, A Wiley-Interscience Publication, New York (1982), 529 p.
10. V. E. Shaternik, A. P. Shapovalov, A. Yu. Suvorov, Low Temp. Phys (Fiz. Nizk. Temp.) 43, №7, 1094 (2017).
11. L. G. Aslamazov and A. I. Larkin, JETP Lett. 9, 87 (1969).
12. Alexander Grib. Visnyk Kharkivs'kogo Natsional'nogo Universitetu imeni V. N. Karazina, № 1135, ser. "Fizika", 21, 61 (2014).
13. Alexander Grib. Visnyk Kharkivs'kogo Natsional'nogo Universitetu imeni V. N. Karazina, № 1158, ser. "Fizika", 22, 51 (2015).
14. Alexander Grib and Paul Seidel. IEEE Trans. Appl. Supercond. 26, №3, 1801004 (2016).
15. Alexander Grib and Paul Seidel. IEEE Trans. Appl. Supercond. 27, №4, 1800604 (2017).
16. K. K. Likharev. Dynamics of Josephson junctions and circuits, Gordon and Breach, Philadelphia. (1991), 750 p.
17. T. A. Fulton and R. C. Dynes. Solid State Commun., 12, 57 (1973).

Вісник ХНУ, серія «Фізика», вип. 26, 2017. с. 33-39

PACS
UDK

Multi-fractal analysis of the gravitational waves

Leonid F. Chernogor[1], Oleg V. Lazorenko[2], and Andryi A. Onishchenko[3]

[1]*Space Radio Physics Department V. N. Karazin Kharkiv National University Kharkiv, Ukraine*
Leonid.F.Chernogor@univer.kharkov.ua
[2]*General Physics Department V. N. Karazin Kharkiv National University Kharkiv, Ukraine*
Oleg.V.Lazorenko@karazin.ua
[3]*Physics Department Kharkiv National University of Radioelectronics Kharkiv, Ukraine*
andrey.onishchenko@nure.ua

The fractal and multi-fractal properties of the transient gravitational wave signal generated by a black hole system merging to form a single black and observed on September 14, 2015 at 09:50:45 UTC by the two detectors of the Laser Interferometer Gravitational-Wave Observatory are considered. To investigate these properties, modern method of fractal and multi-fractal analyzes are applied. Using the non-linear paradigm, the results obtained are discussed and explained.
Keywords: gravitational wave signal; fractal analysis; multi-fractal analysis; non-linear paradigm.

The fractal and multi-fractal properties of the transient gravitational wave signal generated by a black hole system merging to form a single black and observed on September 14, 2015 at 09:50:45 UTC by the two detectors of the Laser Interferometer Gravitational-Wave Observatory are considered. To investigate these properties, modern method of fractal and multi-fractal analyzes are applied. Using the non-linear paradigm, the results obtained are discussed and explained.
Keywords: gravitational wave signal; fractal analysis; multi-fractal analysis; non-linear paradigm.

The fractal and multi-fractal properties of the transient gravitational wave signal generated by a black hole system merging to form a single black and observed on September 14, 2015 at 09:50:45 UTC by the two detectors of the Laser Interferometer Gravitational-Wave Observatory are considered. To investigate these properties, modern method of fractal and multi-fractal analyzes are applied. Using the non-linear paradigm, the results obtained are discussed and explained.
Keywords: gravitational wave signal; fractal analysis; multi-fractal analysis; non-linear paradigm.

Introduction

Undoubtedly, one of the biggest discoveries of the XXI century is the gravitational wave detection. On September 14, 2015 at 09:50:45 UTC the two detectors of the Laser Interferometer Gravitational Wave Observatory (LIGO) placed in the United States simultaneously observed a transient gravitational wave signal [1]. A century after the fundamental predictions of Einstein [2, 3] and Schwarzschild [4], the first direct detection of gravitational waves and the first direct observation of a black hole system merging to form a single black hole were reported [1]. In our opinion, by value this discovery can be compared with well-known Hertz's experimental confirmation of the Maxwell's electromagnetic wave existence prediction only. Other hand, the black hole merger discussed is very strong-field and powerful, unique ultra-wideband process [5]. According the so called non-linear paradigm [6], been formulated by one of the authors of this paper in the last 1980th, all processes in open, non-linear, dynamical systems are very complex, non-linear, ultra-wideband, fractal ones. The black hole merger system is one of them. Therefore, it seems to be interesting, actual and useful to check the fractal property existence for the experimental gravitational wave signals, obtained by LIGO [1].

The purpose of the paper is to investigate the fractal and multi-fractal properties of the gravitational wave signals with usage of modern fractal and multi-fractal analysis methods.

Fractal Definition and Fractal Classification

The term 'fractal' (from the Latin 'fractus', meaning 'broken') has been proposed by American mathematician Benoit Mandelbrot in 1975 [7]. Mandelbrot defined a fractal to be a set with Hausdorff dimension strictly greater than its topological dimension [7].

Nevertheless, now there are many different definitions of the fractal introduced in the last forty years by different researchers (see, for example, [8 – 11]), as well as the fractal concept developed rapidly in these years. But on our opinion, the most adequate of them is following one, proposed by K. J. Falconer in 1990 [8]. According to this, when we refer to a set F as a fractal, we will typically have the following in mind.

1. F has a fine structure, i. e. detail on arbitrarily small

scales.

2. F is too irregular to be described in traditional geometrical language, both locally and globally.

3. Often F has some form of self-similarity, perhaps approximate or statistical.

4. Usually, the 'fractal dimension' of F (defined in some way) is greater than its topological dimension D_T.

5. In most cases of interest F is defined in a very simple way, perhaps recursively.

Some later, a self-similarity requirement was generalized and replaced by the self-affinity one [12].

The fractals can be classified in different ways. One hand, all fractals can be separated on mathematical and real, or physical, ones. First of them are a mathematical idealization only, and second of them are really existing natural objects, such as, for example, trees, heaven, mounts et al. The ways of describing of these two fractals types are slightly different [13].

All mathematical fractals can be separated on the deterministic (algebraic and geometric) fractals and stochastic fractals. The properties of self-similarity and self-affinity for the stochastic fractals are considered not in a literal sense, but in a statistical one. It means that fractal properties are shown not by the stochastic object as such, but by its deterministic numerical characteristics [8 – 13].

General difference between mathematical and physical fractals is in following. Strictly speaking, the physical fractals don't satisfy the fractal definition listed above as well as the minimal scale of mathematical fractals vanishes by the definition, but the minimal scale of physical fractal has a finite, non-zero limit. As the result, the self-affine property of physical fractal exists in limited range of scales only [8 – 13]. This is another real difference between the true world (physical fractals) and one of its models (mathematical fractals). Nevertheless, the physical fractals can be divided into deterministic and stochastic ones deter too, as well as their non-stochastic numerical characteristics have namely such properties.

Other hand, there are so called mono-fractals and multi-fractals. To describe a mathematical mono-fractal, it is enough to use the Hausdorff dimension D_H as a fractal dimension D_F [7 – 9]. It is important to point, that only one value of this dimension is able to characterize a mono-fractal as the self-similar (or self-affine) structure. At the same time, to describe a physical mono-fractal, instead of the Hausdorff dimension D_H the Minkowsky dimension D_M is usually applied [14]. All existing algorithms allowing to estimate a fractal dimension D_F of the object investigated, in particular, as a mathematical, as a physical fractal, are included in so called fractal analysis, which can be named more accurately as the mono-fractal analysis too.

Multi-fractal is a fractal, which is not principally allowed to be described with usage of one value of a fractal dimension D_F only. To do this, it is necessary to use a set of fractal dimension values. Such approach is well known as the multi-fractal analysis [15, 16].

Being as natural, as artificial origin, many real signals and processes in nature have fractal properties and, therefore, are the physical fractals [7 – 16]. Using fractal and multi-fractal analyses, these properties having statistical sense can be investigated. The gravitational wave signals listen above are real signals, which require to solve the problem: whether these signals are mono-fractal or multi-fractal or not. If they are, it is necessary to estimate their characteristics. Namely these questions will be answered below.

Fractal Analysis Method

To apply the fractal analysis (more precisely, the mono-fractal analysis) to a real physical signal (or process) investigation, it is necessary [10]:

1) to identify the presence of the self-affinity (or self-similarity) properties of this signal;

2) if they are, to define the scale range (or multiple ranges), in which this happens;

3) using the Minkowski dimension D_M, to estimate the fractal dimension D_F value (or some fractal dimension values, if multiple ranges were found) of the signal investigated.

Oddly enough, but there are many different approximations of the Minkowski dimension D_M, which are usually estimated for the real physical fractal analysis in practice. In particular, there are the cluster dimension D_K [17], the capacity (or box, or fractional) dimension D_C [14], the pointwise dimension D_P and the averaged the pointwise dimension $\left\langle D_P \right\rangle$ [18, 19], the correlation dimension D_G [19], the information dimension D_I [19], the internal (or hidden) dimension D_D [9], the mass dimension D_m [18] and other.

In this paper, we use direct calculation of the capacity dimension D_C and apply another well-known method of the fractal dimension D_F estimation (more precisely, of course, of the Minkowski dimension D_M estimation), which is based on the Hurst exponent H calculation.

Following the Generalized Brownian Motion Model, the Hurst exponent H and fractal dimension D_F are connected with the relation $D_F = 2 - H$ [9].

To estimate the Hurst exponent of the signal $X(t)$, two different ways can be used. Being proposed by H. Hurst in 1951 [20], the first way is the oldest, is known as the Rescaled Range Method or RS-method [9] and is considered as the 'classical' way. The second way is based on the wavelet analysis, namely on the investigation of rate of increasing of mean values of the wavelet coefficient module squares [21].

Then if these dependences obtained in both cases and plotted in the double logarithmic coordinates can be successfully approximated in some scale range with a linear function (for example, with usage of the least square method), the Hurst exponent H in this scale range can obtained. For fractals the Hurst exponent value H should be limited in the range $0 < H < 1.$ Otherwise the signal analyzed is appeared to be not self-affine and, therefore, is not fractal [9]. If the condition $0 < H < 1$ was successfully satisfied, then we can believe that the signal investigated has mono-fractal properties in this range. It is quite possible that for the same signal some different scale ranges with different Hurst exponent values will be obtained [9].

Meanwhile, the real physical processes, special being in open, non-linear, dynamical systems [6], are appeared to be non-stationary ones. Moreover, their fractal properties can vary with time too. So, the Hurst exponent H should be estimated for some limited, slide time window $W(t)$, but not for all signal $X(t)$ at once. In this case, the Hurst exponent becomes a function of the time $H = H(t)$ [22]. In our opinion, it is convenient to connect these Hurst exponent values with corresponding time locations of the center of the slide time window $W(t)$ used. Namely such way is applied in this paper.

Some experienced authors (see, for example, [10, 21]) believe, that fractal analysis is closely connected with wavelet analysis, in particular, with continuous wavelet transform (CWT). Therefore, investigations of CWT spectral density function (SDF) of the signal analyzed and of its skeleton are a part of fractal analysis. In our opinion, this is really appeared to be very important and useful addition to usual fractal analysis tools.

Multi-Fractal Analysis Method

If the process analyzed is appeared to be multi-fractal, the abilities of the mono-fractal analysis will be quite insufficient. Of course, the application of mono-fractal analysis to the multi-fractal signal investigations can not be completely forbidden, but the results, which would be obtained, will relate to the so called multi-fractal support only [16]. The multi-fractal support is considered as a mono-fractal, which makes the greatest contribution in the multi-fractal considered [16]. May be, it seems to be interesting for the researcher too, but to describe the multi-fractal much more complete, another approach named as the multi-fractal analysis must be used.

There are two basic multi-fractal analysis methods, which are usually applied to the signal analysis. First of them is called as the Wavelet Transform Module Maxima (WTMM) method and is based on the CWT [21]. Being the basic informational characteristics of the multi-fractal analysis, the multi-fractal spectrum $f(\alpha)$ of the signal investigated is connected with the CWT SDF of the signal. Traditional shapes of the multi-fractal spectrum $f(\alpha)$ of the signal are shown on the fig. 1, where two experiment registrations of the gravitational waves discussed above were presented. The α value is known as the Holder exponent (see, for example, [15, 16]).

Suddenly, WTMM method has one significant disadvantage. It doesn't allow to consider the non-stationarity of the signal investigated as well as in this method the signal is investigated at once. At the same time, it is reasonable to predict that all multi-fractal characteristics of a non-stationary signal can significantly vary with time.

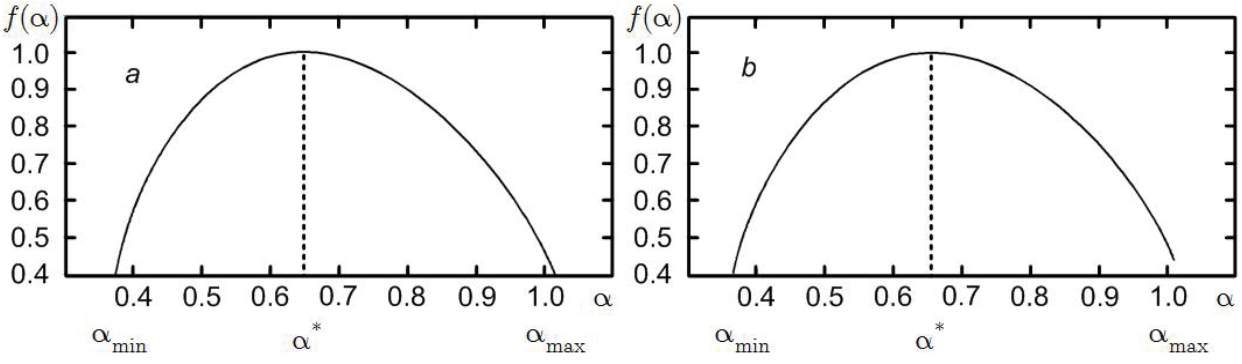

Fig. 1. Multi-fractal spectra $f(\alpha)$ of the gravitational wave signals registered in Hanford (a) and in Livingston (b).

Thus, it is necessary to apply another method, which is free from this disadvantage.

Appearing relatively recently, the second basic multi-fractal analysis method known as the Multi-Fractal Detrended Fluctuation Analysis (MF DFA) is appeared to be convenient to the non-stationary signal investigations in slide time window [23]. As well as the gravitational wave signals are expected to be non-stationary ones, namely MF DFA was chosen in this paper as the main investigation tool.

Let's consider the basic idea of the MF DFA method [23]. Basing on the signal multi-fractal spectrum $F(\alpha)$ analysis (the multi-fractal spectrum of the whole signal was denoted above as $f(\alpha)$) and the slide time window $W(t)$ application, the time dependences of location (minimal $\alpha_{\min}(t)$ and maximal $\alpha_{\max}(t)$ values of α) and of width ($\Delta\alpha(t)$, $\Delta\alpha = \alpha_{\max} - \alpha_{\min}$) of the multi-fractal spectrum can be obtained. Special attention should be paid to the location α^* of the multi-fractal spectrum maximum, given by the requirement $F(\alpha^*) = \max_{\alpha} F(\alpha)$. The α^* value is called as the generalized Hurst exponent as well as for mono-fractal signal we have $\Delta\alpha = 0$ and $\alpha^* = H$. The generalized Hurst exponent α^* describes a multi-fractal support of the signal analyzed. It's fractal dimension is given by relation $D_F = 2 - \alpha^*$ [24].

Analysis Results

Let's start with results of mono-fractal analysis of the gravitational wave signals discussed above. At the fig. 2 these signal registrations obtained in Hanford (fig. 2, a) and in Livingston (fig. 2, c) are shown. One count on the dimensionless time axis corresponds to 21 ms, thus, the whole registration duration is 210 ms. One count on the strain axis is equal to $5 \cdot 10^{-22}$. All calculations described below were performed with usage of the FracLab Toolbox [26] and some original software been developed by authors of this paper.

Capacity dimension D_C of the whole first signal (Hanford) is appeared to be $D_C \approx 1,45 \pm 0,10$ in range of the dimensionless time $t = 0,156 - 5$. The result for second signal (Livingston) is appeared to be $D_C \approx 1,44 \pm 0,10$ in the same range. Corresponding bounds for Hurst exponent H are $H \approx 0,55 \pm 0,10$ and $H \approx 0,56 \pm 0,10$.

Indirect indication on possibility of the fractal property existence for the signals analyzed is given by the CWT skeletons, which have characteristics fork-like looks (fig. 2, b, d) (for CWT SDF calculation the Morlet wavelet was applied). Moreover, on the fig. 2, b, d the fork-like looks of skeletons are excellent seen in the range $T \approx 0,1 - 2$, where T is dimensionless period of the signal, which is used in CWT. This results match well with ones obtained during capacity dimension D_C estimation.

Let's consider the results of the multi-fractal analysis. First, WTMM method application should be described. To obtain the CWT SDF of the signals analyzed, the Daubechie's wavelet of fours order (db4) was used. The

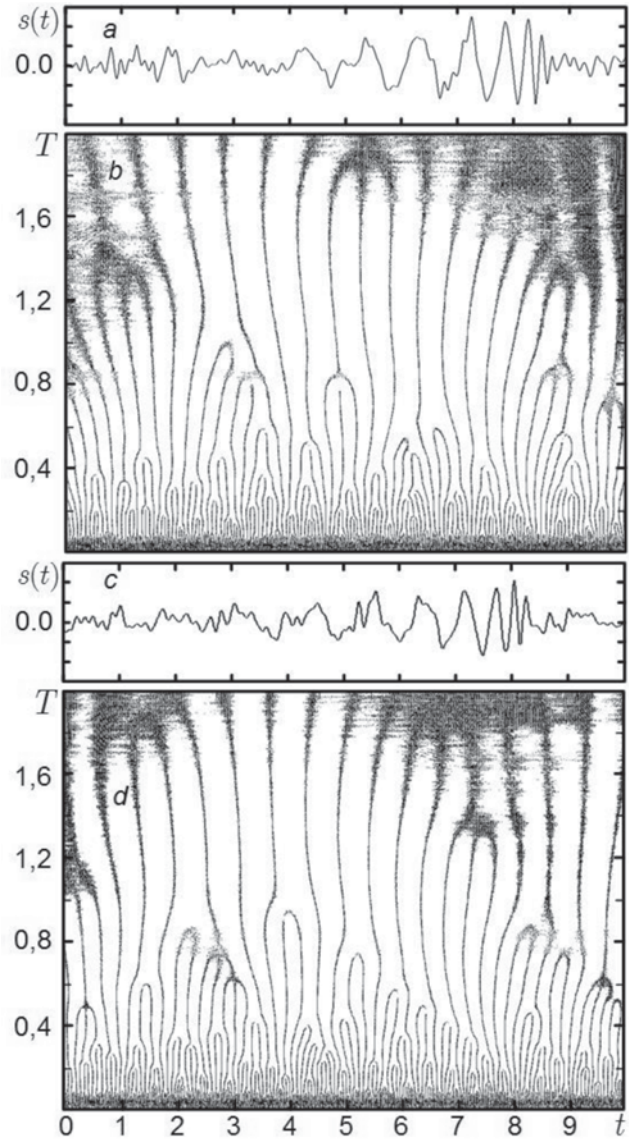

Fig. 2. CWT SDF skeleton analysis results. Signals in time domain: a – Hanford, c – Livingston, CWT skeletons: b – Hanford, d – Livingston.

multi-fractal spectra $f(\alpha)$ of the signal investigated are at the fig. 1. It was found that for the signal registered in Hanford the minimal value of the Holder exponent is $\alpha_{\min} = 0.38$, its maximal value is $\alpha_{\max} = 1.03$, the multi-fractal spectrum width is $\Delta\alpha = 0.65$ and the generalized Hurst exponent is $\alpha^* = 0.65$. For the signal obtained in Livingston we have $\alpha_{\min} = 0.36$, $\alpha_{\max} = 1.01$, $\Delta\alpha = 0.65$ and $\alpha^* = 0.66$ correspondently. These two value sets almost don't differ from each other.

Now let's discuss the results of MF DFA application. All time-dependent values in MF DFA (fig. 3, fig. 4) and additionally the Hurst exponent $H(t)$, which is a part of the fractal analysis method, were calculated with usage of the slide window $W(t)$ with dimensionless width $\Delta t = 3,67$. It is important to point, that each specific value obtained for given window location in time domain was assigned to the position of the window center. The existence of the empty spaces to the right and left of the graphs (fig. 3, b – f, fig. 4, b – f) is explained namely by this reason.

It was found the following. In both cases (as for Hanford, as for Livingston) there are steady tendencies to increase with time for all four multi-fractal functions ($\alpha_{\min}(t)$, $\alpha_{\max}(t)$, $\Delta\alpha(t)$ and $\alpha^*(t)$), which result in a rather sharp decrease. For the Hurst (fig. 3, f, fig. 4, f) exponent there is a weak tendency to increase only. In both cases, the fractality condition for the generalized Hurst exponent ($0 < \alpha^*(t) < 1$) is well satisfied only for $t \le 4,5$. For the Hurst exponent this condition ($0 < H(t) < 1$) is satisfied sometimes in bounds $2 \le t \le 6$.

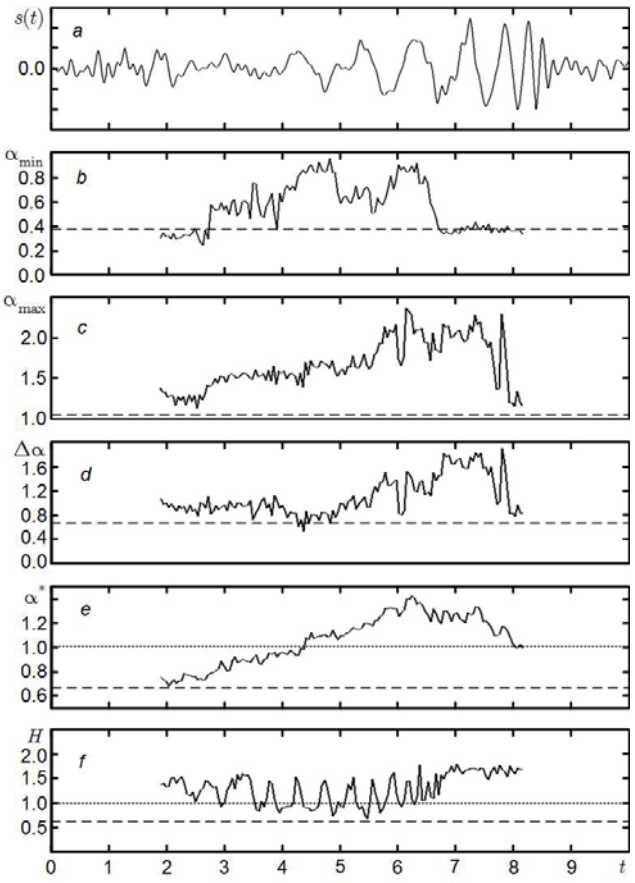

Fig. 3. MF DFA results for gravitational wave signal obtained in Hanford: a – signal in time domain, b – $\alpha_{\min} = \alpha_{\min}(t)$, c – $\alpha_{\max} = \alpha_{\max}(t)$, d – $\Delta\alpha = \Delta\alpha(t)$, e – $\alpha^* = \alpha^*(t)$, f – $H = H(t)$. Dashed lines denote results of the WTMM method, dotted lines indicate upper bound of the value for fractals.

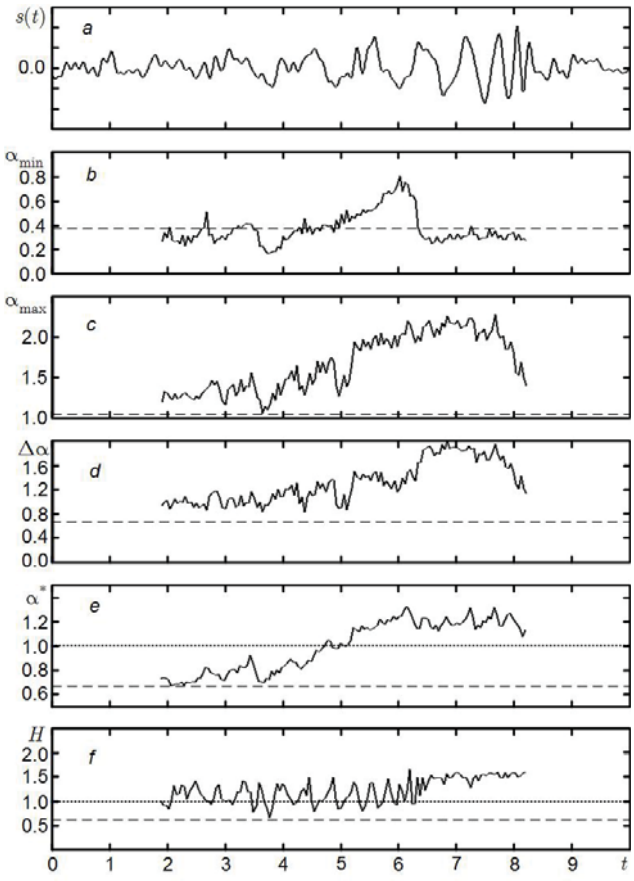

Fig. 4. The same as previous figure for gravitational wave signal registered in Livingston.

Discussion

In one of the previous works of authors [5], it was found that gravitational waves generated by a binary black hole merger were appeared to be a unique natural ultra-wideband (UWB) process with changing mean frequency.

The first gravitational wave registration (Hanford) contains the UWB process with changing mean frequency, which has the duration approximately $\tau \approx 130$ ms, the period band $T \approx 4 - 30$ ms, the dynamic frequency bandwidth changing from 0.4 to 0.9, the signal mean frequency rising with hyperbolic law, and the signal energy distribution with maximum at $T_0 \approx 20$ ms.

The second gravitational wave registration (Livingston) contains the UWB process with changing mean frequency, which has the duration approximately $\tau \approx 120$ ms, the period band $T \approx 4 - 30$ ms, the dynamic frequency bandwidth changing from 0.5 to 0.8, the signal mean frequency rising with hyperbolic law, and the signal energy distribution with maximum at $T_0 \approx 20$ ms.

Taking into account that results and comparing them with present ones, one can assert the following. Both signals analyzed have really fractal structure. This is well confirmed by the results of application as of the mono-fractal analysis, as of the multi-fractal analysis. There is no too significant difference between the results obtained for two signals registered in Hanford and in Livingston. Analyzing the whole both signals, it is important to point, that the value of the generalized Hurst exponent ($\alpha^* \approx 0,65$) is in well agreement with the estimations of the ($H \approx 0,55 \pm 0,10$) obtained with mono-fractal analysis. But the signals analyzed were appeared to be multi-fractal. This is good shown at the fig. 1. Therefore, the values of the Hurst exponent and of the generalized Hurst exponent describe the multi-fractal support only. Based on the estimation of H , one can assume, that multi-fractal support may be partially related to additive white Gaussian noise, which has $H = 0,5$.

But these were the results of whole signal analysis. Meanwhile, as it was pointed above, the signals are appeared to be significantly non-stationary and this fact should be taken into account. The answer was obtained in bounds of the MF DFA application.

Based on the time dependences, it was found that both signals analyzed can be considered as fractal ones approximately in the range of dimensionless time $t \in [0;6]$, where the condition $0 < \alpha^*(t) < 1$ is well satisfied. It is important to point, that on the fig. 4, e, seems, the narrower range $t \in [2;4]$ is observed. But this range should be extended to the one described above, as well as the width of the slide window applied for these calculation is appeared to be no less than $\Delta t = 4$. This limitation is caused by the MF DFA method peculiarities and by the size of the experimental data vectors used by the authors of the paper. In the range $t \in [0;6]$ there is approximately a half of the UWB process with changing mean frequency. Second half of them is appeared to be non-fractal. But whether this fractal component is a part of the gravitational wave signal or is a noise having quite different physical origin, suddenly, this question remains unanswered now.

Thus, the results obtained in the paper is good consistent with non-linear paradigm. Been generated by extremely powerful, open, non-linear, dynamical system, the gravitational waves were appeared to be a unique UWB process with significant complex, non-stationary multi-fractal structure. Suddenly, it remains unknown whether they are a true fractal UWB (FUWB) processes or a UWB processes registered on pretense of the additive multi-fractal noise, which had quite another physical origin. To solve this problem in the future, new observations and investigations are needed.

Conclusions

1. The transient gravitational wave signals generated by a black hole system merging to form a single black and received in Hanford and Livingston were appeared to be multi-fractal ones.

2. Being the unique natural UWB processes with changing mean frequency, they had complex, non-stationary multi-fractal structure.

3. Mono-fractal analysis shows, that capacity dimension D_C of the multi-fractal support of the signals analyzed was appeared to be $D_C \approx 1,45 \pm 0,10$ in range of the dimensionless time $t = 0,156 - 5$ (Hanford) and $D_C \approx 1,44 \pm 0,10$ in the same range (Livingston).

4. Using the classic multi-fractal analysis (WTMM method), it was obtained, that $\alpha_{\min} = 0.36 - 0.38$, $\alpha_{\max} = 1.01 - 1.03$, $\Delta\alpha = 0.65$ and $\alpha^* = 0.65 - 0.66$ for both signals investigated. Therefore, both signals are multi-fractal ones as whole.

5. With MF DFA application, the signals investigated were shown to be strongly non-stationary ones, including

their multi-fractal numerical characteristics. It was found, that in both cases the fractality condition for the generalized Hurst exponent ($0 < \alpha^{*}(t) < 1$) is well satisfied only for $t \leq 4,5$. For the Hurst exponent this condition ($0 < H(t) < 1$) is satisfied sometimes in bounds $2 \leq t \leq 6$.

6. To solve the problem whether the signals investigated are a true FUWB processes or a UWB processes registered on pretense of the additive multi-fractal noise, which had quite another physical origin, the new observations and investigations are needed.

References

1. B. P. Abbott et al. Phys. Rev. Lett., PRL 116, 061 (2016).
2. A. Einstein. Sitzungsber. K. Preuss. Akad. Wiss., 1, 688 (1916).
3. A. Einstein. Sitzungsber. K. Preuss. Akad. Wiss., 1, 154 (1918).
4. K. Schwarzschild. Sitzungsber. K. Preuss. Akad. Wiss., 1, 189 (1916).
5. L. F. Chernogor, O. V. Lazorenko. Proc. 8th UWBUSIS, Ukraine, Odesa (2016), p. 47.
6. L. F. Chernogor. On the Nonlinearity In Nature and Science, V. N. Karazin Kharkiv National University, Kharkiv (2008), 528 p. (In Russian).
7. B. B. Mandelbrot. The Fractal Geometry of Nature, CA-Freeman, San Francisco (1982), 468 p.
8. K. J. Falconer. Fractal Geometry. Mathematical Foundations and Applications, Wiley & Sons, Chichester (1990), 288 p.
9. J. Feder. Fractals, Plenum Press, New York (1988), 305 p.
10. Wavelets and Fractals in Earth System Sciences, ed. by E. Chandrasekhar, V. P. Dimri, V. M. Gadre, CRC Press, Boca Raton (2014), 294 p.
11. D. P. Feldman. Chaos and Fractals. An Elementary Introduction, University Press, Oxford (2012), 431 p.
12. B. B. Mandelbrot. Fractals and Chaos: The Mandelbrot Set and Beyond, Springer (2005), 400 p.
13. A. A. Potapov. Fractals in Radio Physics and Radar, University Book, Moscow (2005), 848 p. (In Russian).
14. R. M. Crownover. Introduction to Fractals and Chaos, Jones and Barlett Publishers, Boston (1995), 300 p.
15. B. B. Mandelbrot. Multifractals and 1/f Noise, Springer (1999), 431 p.
16. D. Harte. Multifractals. Theory and Applications, Chapman and Hall/CRC Press, Boca Raton (2001), 246 p.
17. A. I. Chulichkov. Mathematical Models of the Non-Linear Dynamics, FIZMATLIT, Moscow (2003), 296 p. (In Russian).
18. M. Schroeder. Fractals, Chaos, Power Laws. Minutes from Infinite Paradise, W. H. Freeman and Company, New York (1991), 528 p.
19. F. C. Moon. Chaotic Vibrations. An Introduction for Applied Scientists and Engineers, Wiley and Sons, New York (2004), 310 p.
20. H. E. Hurst. Trans. Amer. Soc. Civ. Eng., 116 (1951), 770.
21. S. Mallat. A Wavelet Tour of Signal Processing, Academic Press, San Diego (1998), 577 p.
22. M. S. Taqqu. Self-similar Processes. Encyclopedia of Statistical Sciences, Wiley, New York (1988), v.8, p. 352.
23. J. W. Kantelhardt, S. A. Zschiegner, E. Konscienly-Bunde, S. Havlin, A. Bunde, and H. E. Stanley. Phys. A, 316, 87 (2002).
24. A. A. Lyubushin. Multivariate Time Series Analysis: A Practical Course, MGRI-RGGRU, Moscow (2010), 113 p. (In Russian).
25. V. V. Yanovskiy. Universitates, 3 (2003) (In Russian).
26. www.project.inria.fr/fraclab/.p

Вісник ХНУ, серія «Фізика», вип. 26, 2017. с. 40-43

UDC 539.3
PACS: 83.50. – v

On role of mass-transfer crowdion mechanism in local relaxation processes

V.G. Kononenko[1], V.V. Bogdanov[1], M.A. Volosyuk[2], A.V. Volosyuk[1]

[1] Karazin Kharkov National University, 4 Svobody Sq., 61022 Kharkiv, Ukraine,
[2]Kharkiv National Automobile and Highway University,
25 Yaroslava Mudrogo Str., 61002 Kharkiv, Ukraine
marina_volosyuk@ukr.net

Character of relaxation processes has been analyzed in crystalline materials near stress local concentrators of various types (a crack in copper under its healing by uniaxial compression; a rigid (corundum) inclusion in a KCl single crystal; a hole in a KCl single crystal due to pulse optical breakdown of the single crystal by ruby laser radiation). It was shown that in the first two cases (crack and rigid inclusion), the main mechanism resulting in relaxation of about 50% stress was the dislocation-diffusion one. According to this mechanism, excess vacancies and interstitials occur at intersections of screw dislocations; as a result, rapid crowdion (interstitial) mass transfer is switched on completing the relaxation process. In the case of laser breakdown, the crowdion mass transfer mechanism is principal. The diffusion-and-dislocation mechanism steps in at the final stage of the process and provides near 5% of the full necessary mass transfer amount.
Keywords: dislocations; crowdions; interstitial atoms; diffusion; concentration of stress; relaxation processes.

Приведен анализ характера релаксационных процессов в кристаллических материалах в окрестности локальных концентраторов напряжений разных типов (трещина в меди при ее залечивании одноосным сжатием; жесткое (корунд) инородное включение в монокристалле KCl; полость в монокристалле KCl, полученная в результате импульсного оптического пробоя монокристалла излучением рубинового лазера). Показано, что в первых двух случаях (трещина, жесткое включение) ведущим механизмом массопереноса, приводящим к снятию до 50 % напряжений, является дислокационно-диффузионный механизм. Согласно этому механизму, на пересечениях винтовых дислокаций появляются избыточные вакансии и межузельные атомы, благодаря чему включается быстрый краудионный (межузельный) массоперенос, завершая релаксационный процесс. В случае лазерного пробоя ведущим является механизм краудионного массопереноса. Диффузионно-дислокационный механизм подключается на заключительной стадии процесса, обеспечивая порядка 5 % полной величины необходимого массопереноса.
Ключевые слова: дислокации; краудионы; межузельные атомы; диффузия; концентрация напряжений; релаксационные процессы.

Приведено аналіз характеру релаксаційних процесів в кристалічних матеріалах навколо локальних концентраторів напружень різних типів (тріщина в міді при її заліковуванні одноосним стисненням; жорстке (корунд) чужорідне включення в монокристалі KCl; порожнина в монокристалі KCl, отримана в результаті імпульсного оптичного пробою монокристала випромінюванням рубінового лазера). Показано, що в перших двох випадках (тріщина, жорстке включення) провідним механізмом масопереносу, що приводить до зняття до 50% напружень, є дислокаційно-дифузійний механізм. Згідно цьому механізму, на перетинах гвинтових дислокацій з'являються надлишкові вакансії і міжвузельні атоми, завдяки чому включається швидкий краудіонний (міжвузельний) масоперенос, завершуючи релаксаційний процес. У разі лазерного пробою ведучим є механізм краудіонного масопереносу. Дифузійно-дислокаційний механізм підключається на завершальній стадії процесу, забезпечуючи порядка 5 % повної величини необхідного масопереносу.
Ключові слова: дислокації; краудіони; міжвузельні атоми; дифузія; концентрація напружень; релаксаційні процеси.

Introduction

Real solid crystalline bodies as physical systems always possess some excess thermodynamic potential in comparison with equilibrium ones due to presence of crystalline lattice defects. These defects as foreign inclusions, pores, grain boundaries, dislocations, vacancies, interstitials (intrinsic and foreign) may be either artificially created with some specific aim (for example, for dispersion strengthening of a material) or production outgoings. Various defects are introduced into material in technologies of diffusion welding, powder metallurgy, dispersion strengthening, etc. [1, 2, 3].

Under analyzing specific situations, one should take into account not only requirements to products under exploitation conditions but also the fact that near any defect being a stress concentrator of external loading, relaxation

processes take place which in one way or another reduce both efficiency and service life of the product. These relaxation processes are necessary to study in order to get a possibility to control them and to estimate real capabilities of specific technologies and quality of materials produced with them.

Experimental Results and Discussion

Based on our previous works [4, 8 – 10] where kinetics of relaxation processes near specific local stress concentrators like cracks, foreign inclusions and pores was considered, we form the intention to accent the main peculiarities of relaxation processes and to specify the transfer mechanisms leading to relieving or damping stress state. Additionally, it is necessary to estimate the role of each of the mechanisms under specific conditions.

In [4] healing of a disc-shaped plane crack with size $2a$ and thickness c was studied. Under uniaxial compression perpendicular to the crack occurrence plane, a dislocation-diffusion mechanism of healing was assumed, i.e. generation of prismatic dislocation loops with their subsequent diffusion dissolution. The kinetic equation [4] for dissolution of dislocation loops contains two components; one of them depends on loading and crack size, and another is defined by the value of lattice supersaturation by interstitials:

$$1-\left(\frac{a}{a_0'}\right)^2=\left(\alpha\gamma+\alpha\beta D_V\Delta C_i\right)\frac{\sigma^3\left(t-t_0\right)}{\sigma_p^2}, \qquad (1)$$

where α, β, γ are experimental constants [4]; a, a_0' are, respectively, current and initial (under loading) radii of the crack; D_V is vacancy diffusion coefficient; $D = D_V C_V^0$, D is self-diffusion coefficient of copper atoms (at T = 873 K $D = 3.1\cdot10^{-17}$ m^2/s); C_V^0 is vacancy equilibrium concentration at a given temperature T; σ is stress created by external loading; t, t_0 are, respectively, current time and the time for formation of a quasi-stationary dislocation assemble in the crack tip after loading (in our case t_0 = 5 minutes); σ_p is Peierls threshold; $\Delta C_i = C_i - C_i^0$ is supersaturation of lattice by interstitials; C_i, C_i^0 are, respectively, real and equilibrium concentrations of interstitials at T temperature.

Naturally, Eq. (1) contains the external load value and Peierls threshold (for details, see [4]). Generally speaking, the level of lattice supersaturation by interstitials is unknown a priori, and we can not take it into account in the process under study without additional considerations. If interstitial atoms are allowed to migrate reliably in crowdion configuration, we can not really evaluate also the contribution of crowdions into cracks healing so far. Let us turn to specific estimations. It has been found that if dislocation loop dissolution flow due to interstitial atoms migration is neglected, i.e. the second summand in parentheses of Eq.(1) is assumed zero, after experimental data treatment we obtain understated Peierls threshold $\sigma_p \approx 0.4\cdot10^5$ N/m^2. On the other hand, using the known from independent sources Peierls threshold we can evaluate the second summand in parentheses of Eq. (1).

If, for example, the typical Peierls threshold $\sigma_p \approx 10^5$ N/m^2 is taken, the second summand in (1) is found to be twice as large as the first one. That means, in this situation under high-temperature healing of cracks in loaded copper, the interstitial (crowdion) mechanism of transfer acts. A specific physical model of such transfer of atoms is in that vacancies occurring within atomic close-packed rows move quickly along the close-packed rows forming crowdion configurations and "take away hollow" from the crack, so the crack is filled by atoms. Such configurations are called anti-crowdion ones in [5]. All theoretical concepts developed in [5] for crowdions are found to be fully applied to anti-crowdions.

A physical model for appearance of lattice supersaturation by interstitials under plastic deformation was proposed by Hirth and Lothe [6]. The supersaturation is related with intersections of screw dislocation loops. Here vacancies and interstitial atoms are generated. But concentration of interstitial atoms is always predominates due to their high mobility [6].

If these considerations are taken, we can believe that experiments done in [4] and results of their treatment prove justifiability of assumption on participation of interstitial migration (crowdions) in the process under study.

Found participation of interstitial (crowdion) mass-transfer for cracks healing in copper samples under uniaxial compression perpendicular to the plane of crack bedding is principal also because this allows correct planning the regimes of technology operations for crack getting out in the production cycle.

Similar situation appears also in other cases like this, for example, during relaxation of stresses near foreign inclusions in the matrix. In literature there are described many different cases on reaction of the system near various inclusions under changing external conditions [7]. Usually, dislocation and diffusion mechanisms of mass-transfer were discussed which were really observed (crowdions did not mentioned practically).

In [8] relaxation processes and transfer mechanisms were studied in a KCl single crystal with immersed into it corundum (Al_2O_3) balls at melting temperature (model experiment). During cooling of the system from melting temperature, as a result of different expansion coefficients of the crystal and the ball, dislocations appear in the KCl single-crystal as in much softer material; some of them are dissolved by diffusion, whereas some new appear again and

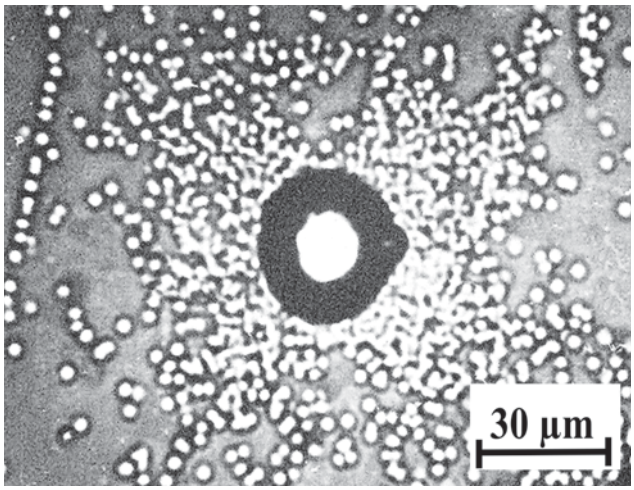

Fig. 1. Typical dislocation structure in KCl single crystal cooled from melting T_m to room T_{room} temperature around a corundum ball of 30 μm diameter (cooling constant $æ = 1.05\times10^{-3}s^{-1}$).

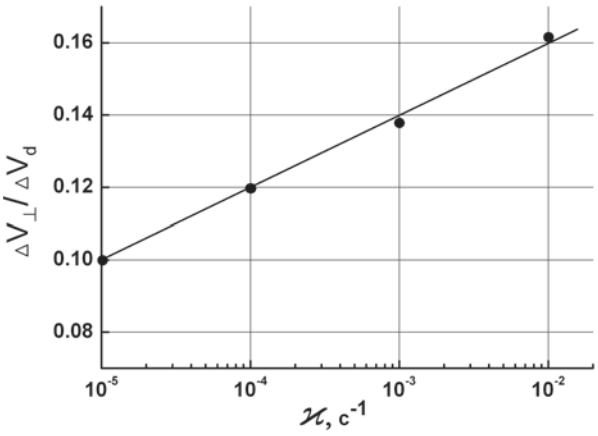

Fig.2. Relative portion of full misfit ($\Delta V_\perp/\Delta V_d$) versus cooling constant æ in KCl single crystals cooled from melting temperature T_m to room value T_{room}.

again due to continuing cooling. As a result, under cooling to room temperature, a certain amount of undissolved dislocations accumulate in the crystal (see Fig. 1). Under cooling, temperature varies by the exponential law ($T = T_m e^{-æ t}$) from melting point T_m to room $T_{room} = 293$ K. In experiments, the cooling constant æ takes the following values: 3.0×10^{-5}s, 1.05×10^{-4}s, 1.05×10^{-3}s, and 1×10^{-2}s.

Quantitative treatment of dislocation structures (like given in Fig.1) obtained at different cooling temperatures near balls of different size was carried out in order to reveal the cooling rate dependence of the relative portion of full volume misfit of dislocation loops ($\Delta V_\perp/\Delta V_d$) remained in the crystal after cooling. The value ΔV_d is the misfit between void and ball volumes at room temperature. According to calculations, the value ($\Delta V_\perp/\Delta V_d$) does not depend on ball size, but depends on cooling rate (Fig.2).

As the cooling rate increases, larger misfit value is "frozen" in dislocation loops as it was expected. But it is important that only (10 – 15) % of the misfit is found to be "frozen" in the remaining dislocation loops. In [8], sufficiently accurate calculations of the misfit value were fulfilled. From these it follows that quantitatively the misfit value in dissolved and unobservable dislocation loops is also rather small, not more (20 – 30) % dependently on the cooling rate.

Thus, in "frozen" and dissolved dislocation loops there is less than a half of substance taken out of the stressed area. Because after cooling the stresses in the crystal near an inclusion were insignificant according to photo-elastic method estimations, we can consider that more than a half of full misfit was taken out from the stressed area by the crowdion (interstitial) transfer.

Another type of stress concentrators was discussed in [9]. These are voids remaining in the ion single crystal after focused laser beam transmission accompanied by so called laser optical breakdown. This phenomenon is being under study for a long time, and a lot of works was devoted to it. Different mechanisms of local optical breakdown (formation of a crystal local destruction) under transmission of laser radiation as well as emission spectra, formation of a plasma clot, kinetics of the breakdown, etc. were considered. In a number of our works, mechanisms of taking out of substance from the breakdown zone and void formation are discussed. The main attention was concentrated at studying the dislocation mechanism as the most rapid for taking out of substance from the breakdown zone.

Quantitative treatment of investigation results and first of all the treatment of dislocation structures around the breakdown zone [9] allowed us to realize that the registered quantity of dislocation loops observed in the cleavage plane intersecting the formed void might explain only about (4 – 5) % of substance taken out of the breakdown zone.

In this connection, we have studied large amount of literature data on this point, analyzed rates of energy losses under transmission of laser radiation through single crystals and developed the mechanism of void pulse formation – the model of a local thermal explosion [10]. According to this model, melting, evaporation and heating of the radiation absorption zone to plasma state take place so rapidly that atoms of the overheated area stay put. Therefore, this process is an explosion with estimated duration less than 10^{-6}s. High pressure occurs and a shock wave forms which, according to explosion theory, initially has the supersonic speed. On the crest of the wave, atoms of overheated substance are taken out with the supersonic speed. This is possible if the atoms form crowdion configurations because only crowdions are able to move with the supersonic speed [11].

According to results of microfilming of the breakdown

zone using nano-second resolution [12], at the initial time, removal of substance and void formation (almost 80% of its size) occur so rapidly that atoms would have the supersonic speed to move to a distance close to observed size of the heated zone. Dislocations and dislocation mass-transfer are observed practically at the final stage after crystallization of the substance.

Conclusions

Thus, analysis of particular but typical cases of relaxation processes by dislocation-diffusion mechanism near stress concentrators in various materials (metals and nonmetals) was proposed. It has been shown that if interstitial atoms and vacancies are generated at dislocation lines intersections, the mass-transfer process is accompanied by joining the crowdion (interstitial) mechanism. In the cases where generation of interstitial atoms is not related with plastic deformation but takes place as a result of local pulse impact onto the crystal (thermal explosion under laser optical breakdown), the crowdion mass-transfer becomes principal.

Under healing of a crack, emptiness – vacancy-by-vacancy – is removed from its volume by generation and movement of vacancy dislocation loops and crowdion configurations of vacancy type.

In the cases of thermo-elastic stress relaxation near a rigid inclusion in the crystal or of a local thermal explosion, atoms are taken out from the defect zone by generation and movement of interstitial prismatic dislocation loops and the flow of interstitial atoms (crowdions).

References

1. V.V. Skorokhod. *Powder Metallurgy*, **9/10**, 42 (2014).
2. I.M. Neklyudov, V.N. Voyevodin, I.N. Laptev, A.A. Parkhomenko. *Problems of Atomic Science and Technology,* **2 (90)**, 21 (2014).
3. R.A. Andrievski. *Phys. Usp*., **57**, 945 (2014).
4. M.A.Volosyuk, A.V. Volosyuk, N.Ya. Rokhmanov. *Functional Materials*, **22**, 51 (2015).
5. J.Hirth, J.Lothe. Theory of dislocations, McGraw-Hill, New York (1968), 600 p.
6. V.D. Natsik, E.I. Nazarenko, *Low Temperature Physics,* **26**, 283 (2000).
7. V.G. Kononenko. *Metallofizika*, **7**, 71 (1985) *[in Russian].*
8. V.G. Kononenko, V.V. Bogdanov, A.N. Turenko, M.A. Volosyuk, A.V. Volosyuk. *Problems of Atomic Science and Technology*, **4 (104)**, 15 (2016).
9. Yu.I. Boyko, M.A. Volosyuk. *Bulletin of Kharkov National University named by V.N. Karazin, ser. «Fizyka»,* **1020**, 42 (2012) *[in Russian].*
10. V.G. Kononenko, M.A. Volosyuk, A.V. Volosyuk. *Problems of Atomic Science and Technology*, **5 (99)**, 15 (2015).
11. A.M. Kosevich, A.S. Kovalev. *Solid State Comm.*, **12**, 763 (1973). A.V. Gorbunov, M.Yu. Maksimuk. *Phys. solid state*, **36** (5), 1416 (1994).

Вісник ХНУ, серія «Фізика», вип. 26, 2017. с. 44-47

PACS: 62.20.F-
UDC 539.4

Thermoelastic stresses and their relaxation at alkali-halide single crystals hardening

O.I.Kovtun[2], D.V.Matsokin[1], I.N.Pakhomova[1]

[1]*V. Karazin Kharkov National University, 4 Svobody sq., 61022, Kharkiv, Ukraine*
matsokin@univer.kharkov.ua
[2]*Physikalisches Institut der Universität Heidelberg, Im Neuenheimer Feld 226, 69120 Heidelberg, Germany*

The origin of internal stresses during hardening of alkali-halide single crystals was investigated. It is shown that the thremoelastic stress relaxation is accompanied by the fragmentation of distinct areas of a single crystal and by the development of new dislocations, which formed a cellular structure. The internal stress distribution is qualitatively analyzed by the photoelasticity method.
Keywords: hardening; thermoelastic stress; dislocation; fragmentation; photoelasticity.

Экспериментально исследовано возникновение внутренних напряжений при закалке щелочногалоидных монокристаллов с решеткой типа NaCl. Показано, что релаксация термоупругих напряжений сопровождается возникновением новых дислокаций, формирующих ячеистые структуры; и фрагментацией отдельных областей монокристалла. Методом фотоупругости качественно проанализировано распределение внутренних напряжений.
Ключевые слова: закалка; термоупругие напряжения; дислокации; фрагментация; фотоупругость.

Експериментально досліджено виникнення внутрішніх напружень при загартуванні лужногалоїдних монокристалів з граткою типа NaCl. Показано, що релаксація термопружних напружень супроводжується виникненням нових дислокацій, які утворюють комірчасті структури, та фрагментацією окремих частин монокристала. Методом фотопружності якісно проаналізовано розподіл внутрішніх напружень.
Ключові слова: гартування; термопружні напруження; дислокації; фрагментація; фотопружність.

Introduction

Thermoelastic stresses (TES) always develop during the growth of dielectric crystals, in particularly alkali-halide. Thermoelastic stress relaxation can significantly change the crystal structure and affect further operating characteristics.

Some experimental observations of structural changes while hardening of alkali-halide single crystals with NaCl-type lattice are presented in this article. The majority of the performed experiments used KBr single crystals, as such crystals are relatively “soft” and do not crack during hardening

Experimental technique

Experiments were performed with alkali halide single crystals of 10x10x10 mm size with initial dislocation density $\rho \sim 10^5\ \text{m}^{-2}$. Crystals were heated on a ceramic substrate at constant rate $W = 6\ \frac{\text{K}}{\text{min}}$ to temperature T, then maintained at this temperature for a particular time t and quickly taken out from the oven (to the room temperature). For the KBr single crystals: $T = 620°\text{C}$, $t = 5\ \text{min}$.

The cooled down crystals were cleaved, the dislocation structure along with the cleavage relief were optically analyzed. By the photoelasticity method the distribution of the internal stresses was studied [1].

Thermoelastic stresses

As well known, cooling begins from the surface. Hence the near-surface layer tends to shrink and thus compresses the internal volume. The situation is similar to the stretching of a metal hoop on a barrel. As a result, in the internal region the compressing stresses appear, while stretching stresses, parallel to the closest crystal side, develop in the near-surface layer. The mean value of these stress can be estimated from a ratio:

$$\sigma \approx \varepsilon E \approx \alpha \Delta T E \qquad (1)$$

where $\varepsilon = \alpha \Delta T$ is the relative crystal strain in the near-surface layer parallel to it’s surface, α is the linear thermal expansion coefficient, $\Delta T = T - T_r$ is the difference between the temperature of the heated crystal and the room temperature T_r, E is Young’s modulus in the direction

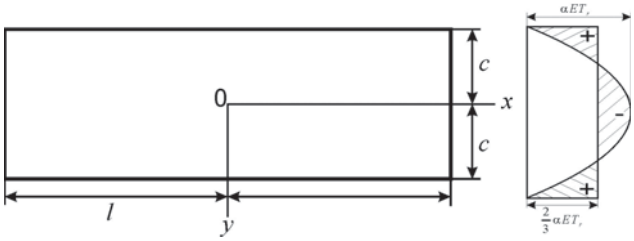

Fig. 1. Thin rectangular plate of constant width 2*c*. Temperature is an even function of *y* and does not depend on *x* and *z*.

parallel to the crystal surface. In our case $\Delta T \approx 600$ K and $\alpha \approx 3 \cdot 10^{-5}$ K^{-1} [2], so after removing of the crystal from the oven the internal stresses reach $\sigma \approx 1.8 \cdot 10^{-2}$ E. This value considerably exceeded the level of stress necessary for dislocation arising in alkali halide crystals.

The TES problem is not solved analytically for isotropic cubic shape bodies [3, 4]. There are solutions for several simple cases of temperature distribution and for rotationally symmetric figures (sphere and cylinder). In particular, for a thin rectangular plate of constant width 2*c* (Fig 1a) in which the temperature is an even function of *y* and does not depend on *x*, namely

$$T = T_r\left(1 - \frac{y^2}{c^2}\right)$$

The solution for TES is [3]

$$\sigma_x = \frac{2}{3}\alpha T_r E - \alpha T_r E\left(1 - \frac{y^2}{c^2}\right) \qquad (2)$$

(see Fig. 1b)

If a sphere of temperature T_0 is dipped into a liquid with temperature T_1 ($T_1 > T_0$) the external part of the sphere will be dilate thus causing the comprehensive uniform radial stretching in the middle. The maximum value of this stress is

$$\sigma_r = 0.771\frac{\alpha E}{2(1-\nu)}(T_1 - T_0) \qquad (3)$$

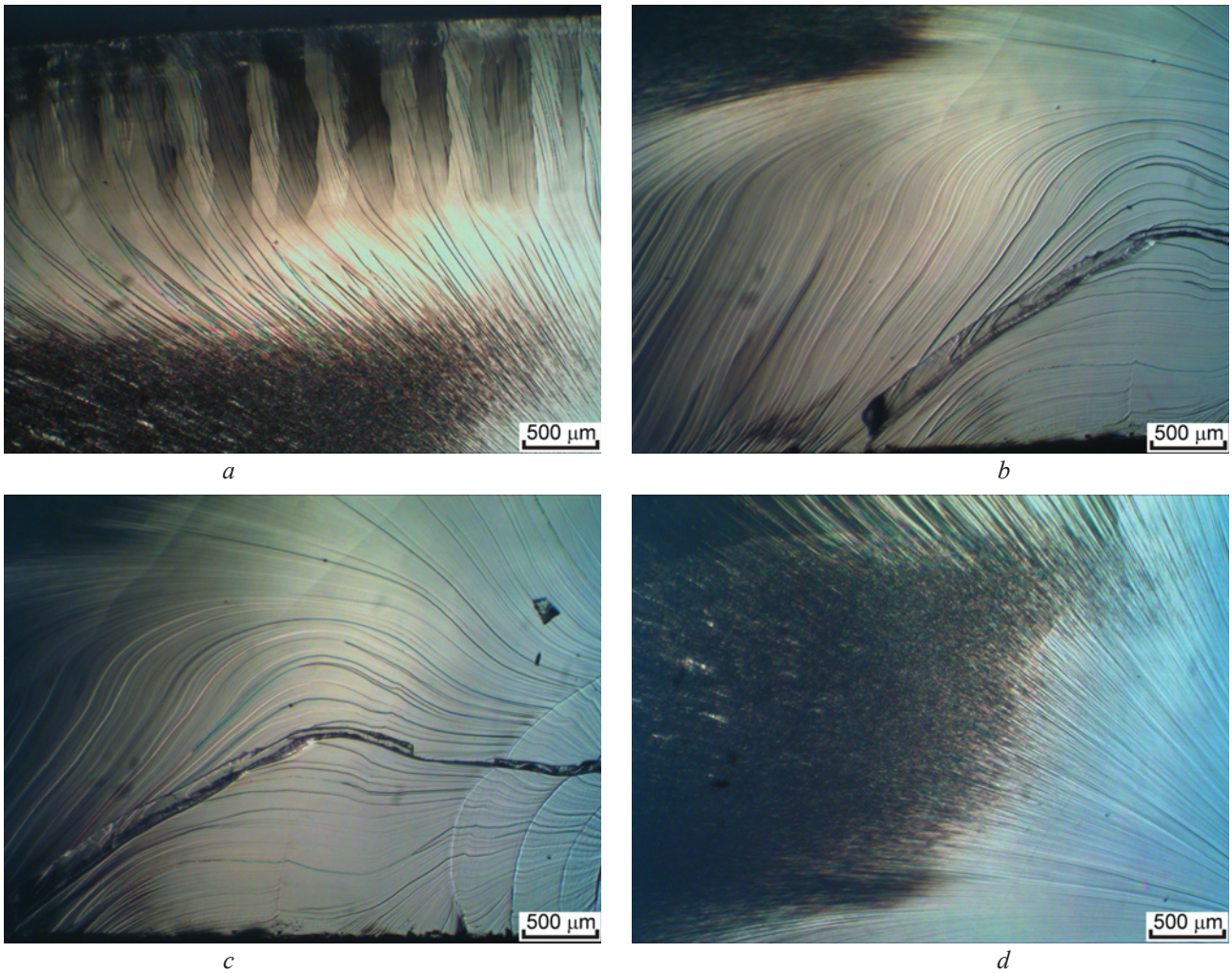

a *b*

c *d*

Fig. 2. The cleavage of hardened KBr single crystal. $T = 620°$C, $t = 5$ min.

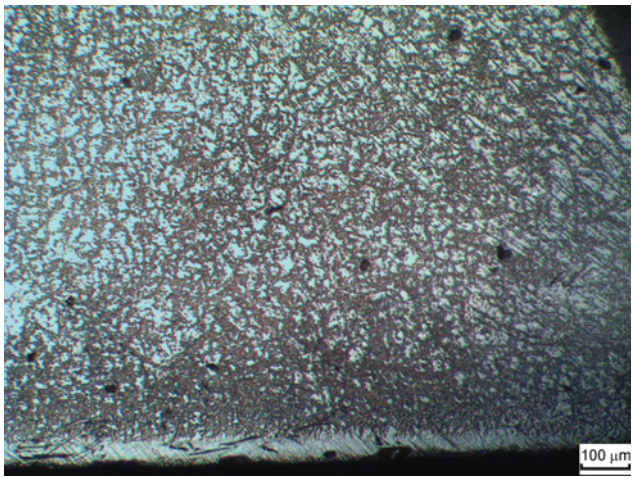

a

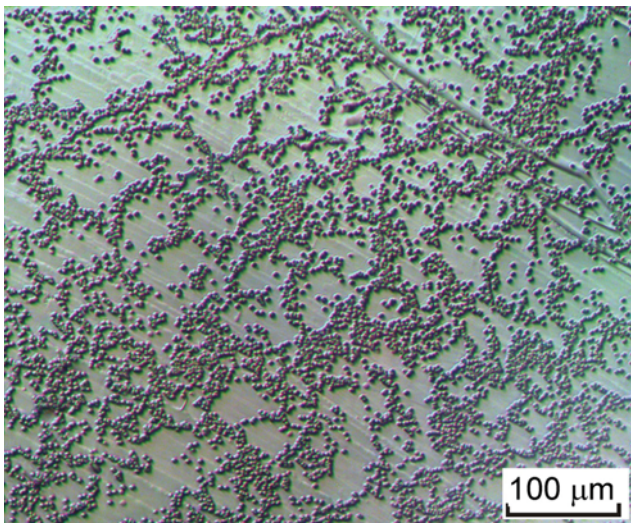

b

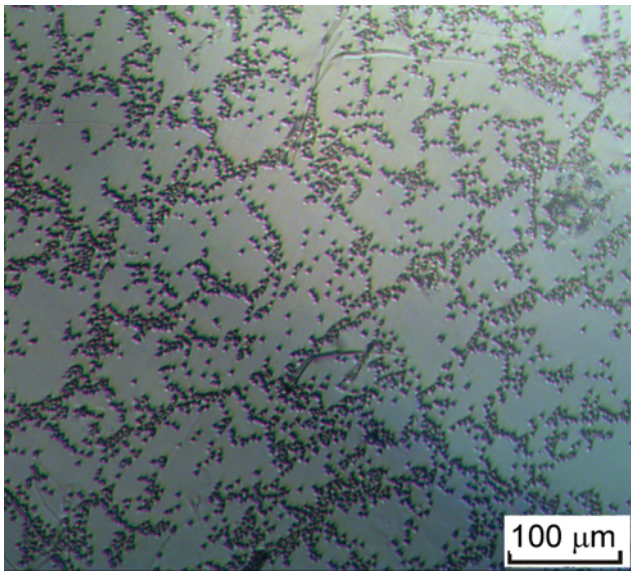

c

Fig. 3. Dislocation structure of a hardened sample: a – near to the surface, b, c – in the middle.

at time

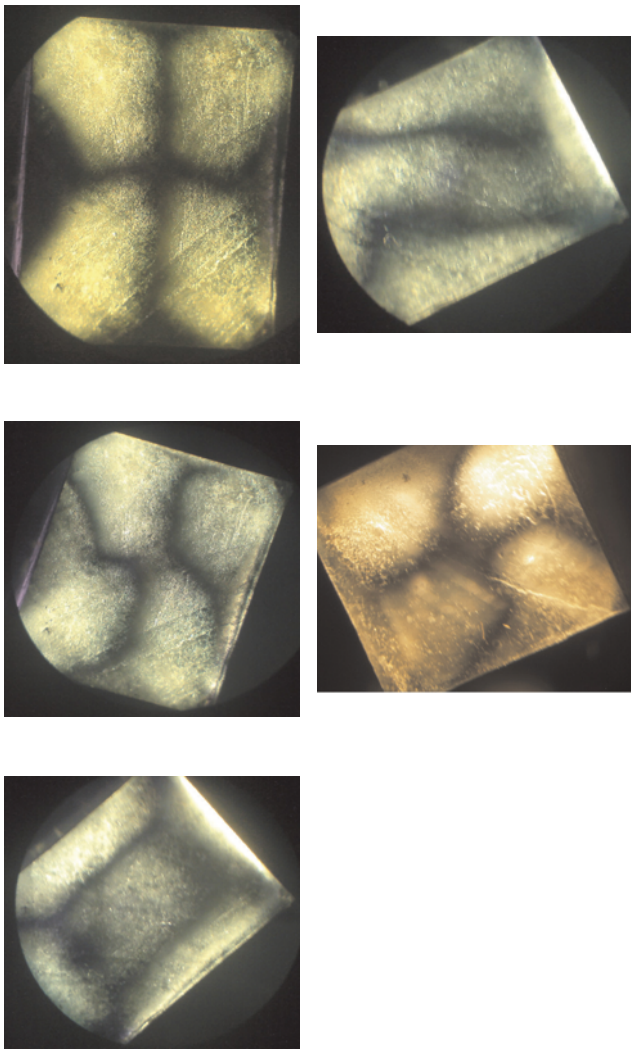

Fig. 4. Photoelastic pictures of KBr single crystals. Isocline parameters: a – 0°, b – 25°, c – 30°, d – 40°, e – 45°.

$$t = 0.0574\frac{R^2 C\rho}{\chi} \qquad (4)$$

In (3) and (4) ν is Poisson's ratio; R – sphere radius; C, ρ, χ – heat capacity, density and heat conductivity.

Results

Surface relief.

1) Periodically located bands of reorientation near to a surface of hardened single crystals.

2) Dense system of cleavage steps; in the outer layer the step orientation becomes normal to the surface (Fig. 2 b, c).

3) The cleavage step density is the greatest in the central part of crystal.

Dislocation structures.

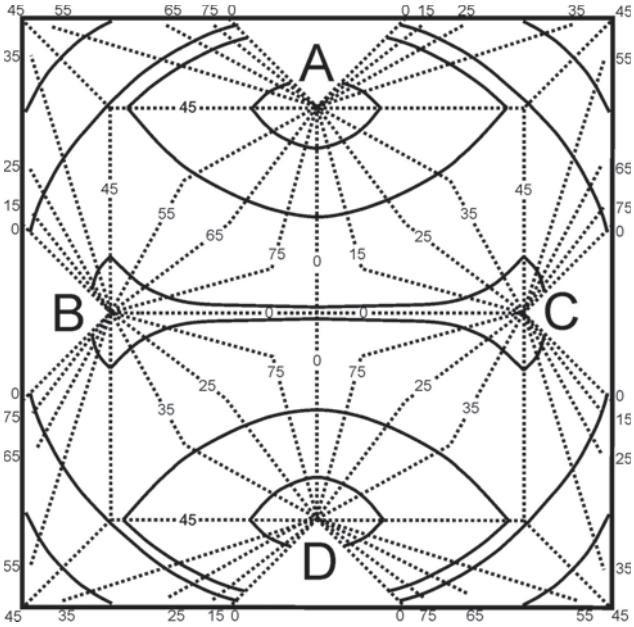

Fig. 5. Image of isoclines (dotted lines) and isostates (solid lines) in a hardened crystal.

The resulting dislocation density is greatest near to the surface. In the central part of the crystal, dislocations form a cellular structure with diffused boundaries (Fig. 3b, c).

The dislocation density is significantly decreased after annealing of the hardened single crystal at $T = 625°\,\mathrm{C}$ for $t = 3\,\mathrm{h}$. This effect can be explained by the annihilation of dislocations with antiparallel Burger's vectors. Cleavage steps became curved and their density decreased.

Photoelastisity.

Observations of the hardened single crystals in polarized light (light source⇒polarizer⇒crystal ⇒analyzer) in the crossed nicols yielded interesting photoelastic images that changed as the crystal was rotated with respect to the light polarization plane (Fig. 4).

Two principal stresses σ_1, σ_2 and the shear stress τ_{12} are presented in each point of plain stressed body. The relation between stresses

$$\tan 2\vartheta_{1,2} = \frac{2\tau_{12}}{\sigma_1 - \sigma_2}.$$

Black lines in Fig. 4 are isoclines along which the angles (ϑ_1, ϑ_2) between principal stresses σ_1, σ_2 and polarization plane [1] are preserved.

The crystal was rotated with respect to the light polarization plane from 0° to 90° in steps of 5°. A schematic isocline pattern is shown in Fig. 5. Each isocline is marked with its parameter. As seen from the figure there are four points of intersection of the isoclines of different parameters (A, B, C, D). So-called "special isotropic points" are where only the hydrostatic pressure is present. Solid lines in Fig. 5 denote isostates; at each point the tangent is consistent with the direction of one of the main stresses.

The difference between principal stresses $\Delta\sigma = \sigma_1 - \sigma_2$ using isochromatic (color) lines could not be determined, as the optomechanical coefficient proportional to $\Delta\sigma$ is small in alkali-halide crystals [1].

The obtained pictures qualitatively obviously show the presence of internal stresses in hardened crystal.

Conclusions

The internal thermoelastic stresses emerge in alkali halide single crystals during hardening. Relaxation of these stresses leads to significant change of the crystal structure up to the transformation of some regions into polycrystal by reorientation and fragmentation.

References

1. Frocht, M.M., Photoelasticity. J. Wiley and Sons, London, 1965.
2. P. D. Pathak, J. M. Trivedi, N. G. Vasavada, Thermal expansion of NaF, KBr and RbBr and temperature variation of the frequency spectrum of NaF, Acta Cryst. (1973). A29, 477-479.
3. Sadd M.H. Elasticity. Theory, Applications, and Numerics. Elsevier. 2005, 473 p.
4. Boley B. A., Weiner J. H. Theory of Thermal Stresses, 1960 (John Wiley, London).

Вісник ХНУ, серія «Фізика», вип. 26, 2017. с. 48-50

PACS: 78.20.Ls, 75.10.Lp, 71.23.An
UDC 537.61; 538.955

Effective renormalization of g - factors anisotropic ferromagnetic narrow-band f –d -metal

E.S. Orel

O.M. Beketov National University of Urban Economy in Kharkiv,Revolyutsii street 12, Kharkov 61002, Ukraine.
Evgeniy.Orel@kname.edu.ua

Conducting anisotropic narrow-band ferromagnetic connections on the basis of f - d - elements attract enhanceable interest, as systems tightly-coupled between electronic, magnon and latticed by subsystems [1-3]. Magnetic resonance is the effective instrument of research of their power spectrum, however the mechanisms of forming of g - factors of magnetic moments in such substances are studied not enough. Methods of theoretical researches of the resonant phenomena, developed for ferromagnetics described within the framework of charts with Heisenberg intersite by an exchange, as in dielectric [4], so in wide-band conducting systems [5], inapplicable for direct description of the connections examined here. In the real work we investigated the spectrums of magnetic excitations in a narrow-band ferromagnetic explorer containing local (f) and quasilocal (d) magnetic moments [6]. These spectrums are formed by the spin correlations generated jointly by interatomic co-operations of d electrons (by an exchange with the electrons of shells and Hubbard pushing away), and them intersite hops, taking into account the spatial chaotization of g - factors d - and f - subsystems [6].
Keywords: magnon; Green function; narrow-band ferromagnetics; g - factors.

Исследованы спектры магнитных возбуждений в узкозонном ферромагнитном проводнике, содержащем локальные (f) и квазилокальные (d) магнитные моменты [6]. Эти спектры формируются спиновыми корреляциями, порождаемыми совместно внутриатомными взаимодействиями d электронов (обменом с электронами f оболочек и хаббардовским отталкиванием), и их межузельными перескоками, с учетом пространственной хаотизации g-факторов d- и f- подсистем [6] и анизотропии параметров «внутриатомного» обмена между локальными и квазилокальными электронами. Полученные выражения для эффективных g-факторов взаимодействующих f - и d – магнитных подсистем в узкозонном ферромагнетике содержат как изотропные поправки к g-факторам невзаимодействующих f - и d - подсистем, так и поправки, зависящие от отношения x,y - и z - компонент тензора локальных обменных параметров, причем знак поправок для f - и d – подсистем различен.
Ключевые слова: магнон; функция Грина; узкозонные ферромагнетики; g-фактор.

Досліджені спектри магнітних збуджень у вузькозонному феромагнітному провіднику, що містить локальні (f) і квазілокальні (d) магнітні моменти [6]. Ці спектри формуються спіновими кореляціями, що породжуються спільно внутрішньоатомними взаємодіями d електронів (обміном з електронами f оболонок і хаббардовским відштовхуванням), і їх міжвузельними перескоками, з урахуванням просторової хаотизації g -факторів d - і f - підсистем [6] і анізотропії параметрів «внутрішньоатомного» обміну між локальними і квазілокальними електронами. Отримані вирази для ефективних g -факторів взаємодіючих f - і d - магнітних підсистем у вузькозонному феромагнетику містять як ізотропні поправки до g -факторів невзаємодіючих f - і d - підсистем, так і поправки, залежні від відношення x, y - і z - компонент тензора локальних обмінних параметрів, причому знак поправок для f - і d - підсистем різний.
Ключові слова: магнон; функція Гріна; вузькозонний феромагнетик; g-фактор.

Model and method

The charts of electronic power spectrum (Fig. 1) and spectrum of elementary excitations (Fig. 2) of the investigated system used in-process are analogical to used in [6].

Electronic descriptions of the investigational system were analogical to considered in [6], except for the parameters of “interatomic” exchange between local and quasilocal electrons, which in this case was anisotropic, -

$$H_{ex} = -2\left[J_{\perp}\left(S^X s^X + S^Y s^Y \right) + JS^Z s^Z \right].$$

Here S and s are backs local *f* - shells and quasilocal *d* -электрона, accordingly, S>>1; $J_{\perp}$ and J is interatomic exchange constants, $0< J_{\perp} \leq J$.

Model Hamiltonian

Hamiltonian of the system in the external magnetic field of H, directed along the co-ordinate axis of Z, looks like

$$H = H_e + H_m ,$$

where

$$H_e = -\frac{W}{2z}\sum_{\ddot{e},\c{c},\acute{o}} c^{+}_{\ddot{e}+\c{c},\acute{o}} c_{\ddot{e},\acute{o}} + \frac{U}{2}\sum_{\ddot{e},\acute{o}} \hat{n}_{\ddot{e},\acute{o}}\hat{n}_{\ddot{e},-\acute{o}} - 2\sum_{\substack{\alpha,\beta \\ \ddot{e},\acute{o},\acute{o}'}} J^{\alpha,\beta}\left(\mathrm{S}^{\alpha}_{\ddot{e}}\mathrm{s}^{\beta}\right)_{\acute{o},\acute{o}'} c^{+}_{\ddot{e},\acute{o}} c_{\ddot{e},\acute{o}'}$$

- electronic Hamiltonian in presentation of numbers of filling, qualificatory energies of both one-particle and collective states, in particular is a magnon spectrum [6]. Element

$$H_m = -\mu_B \mathrm{H}\cdot\sum_{\ddot{e}}\left(g_f S^z_{\ddot{e}} + g_d s^z_{\ddot{e}}\right)$$

describes co-operating of spin subsystem with the external magnetic field of H; $c^{+}_{\ddot{e},\sigma}$, $c_{\ddot{e},\sigma}$ are electronic Fermi operators; λ is a sites of grate, μ_B is the Bohr magneton; $n_{\ddot{e},\sigma} = c^{+}_{\ddot{e},\sigma}c_{\ddot{e},\sigma}$ are electronic numbers of filling; σ is the spin index (the values of this index are represented by the symbols ↑(↓) or +(–)); $s^z_{\ddot{e}} = \frac{1}{2}\left(c^{+}_{\ddot{e}\uparrow}c_{\ddot{e}\uparrow} - c^{+}_{\ddot{e}\downarrow}c_{\ddot{e}\downarrow}\right)$ are operators of electronic spins; J is an interatomic (d - f -) exchange integral, U is the Hubbard interaction constant; W is a width of electronic zone; g_d (g_f) - is the crystal averaged value of the g factor for the d and f electrons; inequalities of $W<<4zJS$ are used, $U/2JS<<1$, $0<W\leq 2zJ$, $U>J$, where z is a co-ordinating number of crystalline grate.

There is a calculation of magnon spectrum in the region of small values of the magnon quasimomenta.

The site magnetic moment of the crystal looks like

$$\mathbf{M}_{\ddot{e}} = \mu_B\left(g_{f\ddot{e}}\mathbf{S}_{\ddot{e}} + g_{d\ddot{e}}\mathbf{s}_{\ddot{e}}\right);$$

his transversal components in circular coordinates are equal

$$\mathrm{M}^{\pm}_{\ddot{e}} = \mathrm{M}^{x}_{\ddot{e}} \pm i\mathrm{M}^{y}_{\ddot{e}}.$$

Transversal dynamic magnetic susceptibility of the system

$$\div^{+-}\left(\mathbf{Q},\mathbf{Q}',\tilde{\omega}\right) = \frac{1}{N}\sum_{\ddot{e},\ddot{e}'}\left\langle \div^{+-}_{\ddot{e},\ddot{e}'}\left(\tilde{\omega}\right)\right\rangle_{c}\cdot \mathrm{e}^{-i(\mathbf{Q}\ddot{e}+\mathbf{Q}'\ddot{e}')}$$

can be expressed through Fourier transforms of twotemporal late temperature of the Green's function

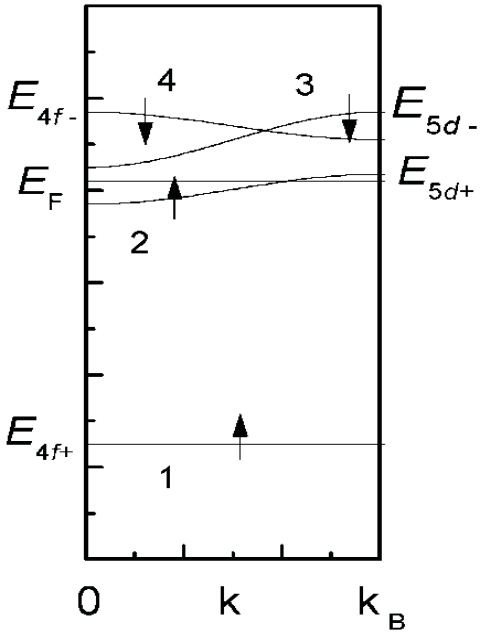

Fig. 1. Scheme of the electron energy spectrum of the model: 1 – partially filled magnetically active 4 f level (E_{4f+}), 2 – partially filled 5d band, 3 – band of unfilled 5d states, 4 – band of unfilled 4 f states, E_F – the Fermi energy, E_{d+} , E_{d-} , and E_{4f-} – maximum energies in the corresponding bands, k_B is the Brillouin quasimomentum; the arrows represent the spin indices of the electron states.

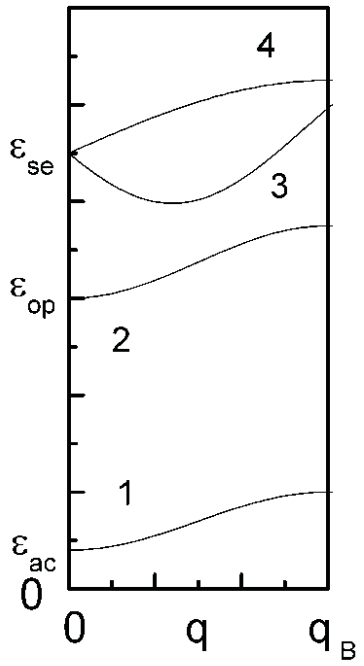

Fig. 2. Scheme of the spectra of the elementary excitations in the model used: 1 – acoustic magnon spectrum, 2 – optical magnon spectrum, 3,4 – lower and upper boundaries of the continuum of single-particle (Stoner) electronic excitations with a spin flip (the figure corresponds to the one-dimensional case with $k_F = 0.4k_B$), ε_{ac} and ε_{op} are the energies at the corresponding zone centers (q=0), ε_{se} is the energy of the Stoner excitations at zero quasimomentum transfer (all three bands are shifted upward by an applied external magnetic field).

$$\div^{+-}_{ë,ë'}(\tilde{a}) = -\frac{1}{v_a}\left\langle\left\langle M^{+}_{ë} \middle| M^{-}_{ë'}\right\rangle\right\rangle_{\tilde{a}},$$

where $\varepsilon = \varepsilon + i\alpha,\ \alpha \to 0,\ \varepsilon = \omega$, ω is frequency of the trial field, v_a is an atomic volume.

Resonant frequencies correspond to the poles of the Green's function $|_{\varepsilon}$, which can be defined from equalization of motion for her.

Calculation of transversal dynamic magnetic susceptibility, conducted by the method of twotemporal late of the Green's function within the framework of the approach developed in [6], resulted in two resonant frequencies of homogeneous precession of constrained *d* - and *f* - the magnetic moments of the system, related to *acoustic* and *optical* to the magnon branches.

Linearizing on the field of H=(0, 0, H^Z) of the got expressions for resonant frequencies of homogeneous precession allowed to define effective *g* - factors, corresponding acoustic and optical to the magnon branches which in linear for 1/S approaching, have a next kind:

$$g^{*}_{ac} = g_f\left[1 - \frac{\langle s^Z\rangle}{\langle S^Z\rangle}\left(1 - \frac{g_d}{g_f}\right)\left(\frac{J_\perp}{J}\right)^2\right],$$

$$g^{*}_{op} = g_d\left[1 - \frac{\langle s^Z\rangle}{\langle S^Z\rangle}\left(1 - \frac{g_f}{g_d}\right)\left(\frac{J_\perp}{J}\right)^2\right].$$

Conclusions

Got expressions for effective g - factors interactive f - and d - magnetic subsystems in narrow-band ferromagnetic contain both izotropic amendments to g - factors uninteractive f - and d - subsystems and amendments depending on the relation of x, y - and z is a component of tensor of local exchange parameters, thus sign of amendments for f - and d - subsystems different.

References

1. Dagotto E., Hotta T., Moreo A. Colossal magnetoresistant materials: the key role of phase separation. Phys. Rep., v. 344, 1 (2001).
2. Erdoes P., Robinson J. The Physics of Actinide Compounds. - New York, London: Plenum Press, 1983.
3. Chachkhiani L.G., Chachkhiani Z.B. Uranium intermetallic compounds. - Tbilisi: Metsniereba, 1990.
4. A. I. Akhiezer, V. G. Bar'yakhtar, and S. V. Peletminski., *Spin Waves*, North-Holland, Amsterdam (1968), Nauka, Moscow (1967).
5. S. V. Vonsovski., *Magnetism*, Vols. 1 and 2, Wiley, New York (1974), Nauka, Moscow (1971).
6. A. B. Beznosov and E. S. Orel. Fiz. Nizk. Temp., v. 30, # 9, 958 (2004).

Вісник ХНУ, серія «Фізика», вип. 26, 2017. с. 51-57

PACS: 51.30.+i Thermodynamic properties, equations of state
UDC: 536.71

Methods of determination of polytrophic effectiveness factor of the centrifugal supercharger

Yu.A. Oleynik, S.A. Saprykin

Ukrainian research institute of natural gases
Ukraine, 61010, Kharkov, Gimnazicheskaya Emb., 20
oleynik.juriy@ndigas.com.ua

Mathematical models of determination of the polytrophic effectiveness factor (EF) of the centrifugal supercharger (CS) of natural gas were analyzed. On this basis four methods of calculation of polytrophic EF of CS were investigated. According to these four investigated methods there was carried out the practical calculation and comparison of changes of values of polytrophic efficiency of CS. The simplest method was allocated, that helps to determine the polytrophic EF of CS with entrance pressure of 0,5-2,3 MPa very quickly.

Keywords: polytrophic process; adiabatic process; polytrophic effectiveness factor.

Проанализированы математические модели определения политропного коэффициента полезного действия (КПД) центробежного нагнетателя (ЦБН) природного газа, на основе чего описаны четыре метода расчёта политропного КПД ЦБН. По описанным четырем методам проведен практический расчет и сравнение изменений значений политропного КПД ЦБН. Выделен самый простой метод, позволяющий быстро определять политропный КПД ЦБН при входных давлениях 0,5-2,3 МПа.

Ключевые слова: политропный процесс; адиабатный процесс; политропный КПД.

Проведено аналіз математичних моделей визначення політропного коефіцієнта корисної дії (ККД) відцентрового нагнітача (ВЦН) природного газу, на основі чого було описано чотири методи розрахунку політропного ККД ВЦН. Згідно з описаними чотирма методами було проведено практичний розрахунок та зрівняння змін значень політропного ККД ВЦН. Виділено найпростіший метод, який дозволяє швидко визначати політропний ККД ВЦН при вхідних тисках 0,5-2,3 МПа.

Ключові слова: політропний процес; адіабатний процес; політропний ККД.

Introduction

For assessment of the technical condition of the centrifugal supercharger (CS) of the natural gas (NG) it is necessary to determine its polytrophic effectiveness factor (EF). The simple method of calculation is necessary to make it under operating conditions CS at compressor station. The existing mathematical models (MM) of determination of polytrophic EC CS [1-6] will be considered in this article. After their analysis the simplest mathematical methods will be allocated, which allow to determine the polytrophic EC CS under operating conditions.

Parameters of natural gas

Let us consider the NG parameters, which are necessary for calculation of polytrophic EC CS. In fig. 1 axes of temperatures, pressure and specific enthalpies of NG at its compression in CS are shown.

On an axis of temperatures of fig. 1 the following temperatures of NG are shown: T_1 – NG temperature on CS entrance, K; T_2 – NG temperature at CS exit at polytrophic process of compression, K; T_{2a} – NG temperature at CS exit at adiabatic process of compression, K.

On an axis of pressure of fig. 1 the following pressure of NG are shown: p_1 – NG pressure on CS entrance, Pa; p_2 – NG pressure at CS exit at polytrophic process of compression, Pa; p_{2a} – NG pressure at CS exit at adiabatic process of compression, Pa.

On an axis of specific enthalpies of fig. 1 specific enthalpies of real NG at adiabatic and polytrophic processes of compression of NG are shown. Also in the drawing specific enthalpies of NG are shown if it has properties of a perfect gas at temperatures $\grave{O}_2$ and $\grave{O}_{2a}$.

For specific enthalpies and specific works in fig. 1 the following designations are entered: h_1 – specific enthalpy of NG on CS entrance, J/kg; h_2 – specific enthalpy of NG at CS exit at polytrophic process of compression of NG, J/kg ; h_{2a} – specific enthalpy of NG at CS exit at adiabatic process of compression of NG, J/kg; $-h_{1i}$, h_{2i} – specific

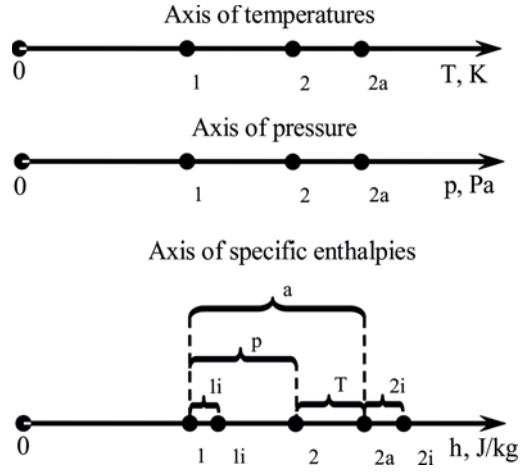

Fig.1. Temperatures, pressure and specific energy of NG on an entrance and an exit of CS.

enthalpies of NG on an entrance of CS and an exit of CS if the compressed NG has properties of a perfect gas, J/kg; e_T – losses of specific energy of NG due to return of heat from NG to the external environment, J/kg; e_{1i}, e_{2i} – difference between a specific enthalpy of NG in perfect condition and NG in a real state at $e_T = 0$, J/kg; A_a – the specific work made by CS over NG at adiabatic process of compression, J/kg; A_p – the specific work made by CS over NG at polytrophic process of compression, J/kg.

In the description of calculations of the NG parameters we won't consider coefficient of compressibility of NG for simplification of definition of η – polytrophic EF CS.

Mathematical models of calculation of polytrophic EF CS

For sizes i_{2a} and i_1 we will write down the equations according to standards [1, 2]:

$$h_{2a} = h_{2i} - e_{2i}; \quad (1)$$

$$h_1 = h_{1i} - e_{1i}; \quad (2)$$

$$h_{2i} = (2{,}6\,R + 149)\,T_2 + 1{,}225\,T_2^2;$$

$$h_{1i} = (2{,}6\,R + 149)\,T_1 + 1{,}225\,T_1^2;$$

$$e_{2i} = R_c\,\delta_2;$$

$$e_{1i} = R_c\,\delta_1;$$

$$\delta_2 = \tau_2\left[\left(\frac{0{,}3468}{\tau_2} + \frac{0{,}3564}{\tau_2^3}\right)\frac{\pi_2}{\tau_2} + \frac{1}{2}\left(\frac{0{,}0273}{\tau_2} - \frac{0{,}117}{\tau_2^3}\right)\left(\frac{\pi_2}{\tau_2}\right)^2\right];$$

$$\delta_1 = \tau_1\left[\left(\frac{0{,}3468}{\tau_1} + \frac{0{,}3564}{\tau_1^3}\right)\frac{\pi_1}{\tau_1} + \frac{1}{2}\left(\frac{0{,}0273}{\tau_1} - \frac{0{,}117}{\tau_1^3}\right)\left(\frac{\pi_1}{\tau_1}\right)^2\right];$$

$$\tau_2 = \frac{T_2}{T_c};\ \tau_1 = \frac{T_1}{T_c};$$

$$\pi_2 = \frac{p_2}{p_c};\ \pi_1 = \frac{p_1}{p_c};$$

where R – gas constant NG, J/(kg·K);

δ_1, δ_2 – corrections of a specific enthalpy of NG which lead values of an enthalpy from a condition of a perfect gas to a condition of a real gas;

τ_1, τ_2 – the specified NG temperature on an entrance of CS and an exit from CS;

π_1, π_2 – reduced pressure of NG on an entrance of CS and an exit from CS;

T_c – critical temperature of NG, K;

p_c – critical pressure of NG, K.

Knowing h_{2a} and h_1 values, it is possible to find specific work of A_a (fig. 1):

$$A_a = h_{2a} - h_1,$$

and then to define specific work of A_p and further to determine polytrophic EF CS by a formula: $\eta = A_p / A_a$ [5, 6].

For specific works as A_p and A_a (fig. 1) we will write down formulas taking into account coefficient of a polytope n and coefficient of an adiabatic k [5]:

$$A_p = \frac{n}{n-1}R(T_2 - T_1); \quad (3)$$

$$A_a = \frac{k}{k-1}R(T_{2a} - T_1). \quad (4)$$

We will transform a formula (3) taking into account dependence of the NG parameters at polytrophic process [5, 6]:

$$A_p = \frac{n}{n-1}R_1\left(\frac{T_2}{T_1} - 1\right);$$

$$A_p = \frac{n}{n-1}R_1\left(\left[\frac{p_2}{p_1}\right]^{\frac{n-1}{n}} - 1\right). \quad (5)$$

Also we will transform a formula (4) taking into account dependence of the NG parameters at adiabatic process [5, 6]:

$$A_a = \frac{k}{k-1} R T_1 \left(\frac{T_{2a}}{T_1} - 1 \right);$$

$$A_a = \frac{k}{k-1} R T_1 \left(\left[\frac{p_{2a}}{p_1} \right]^{\frac{k-1}{k}} - 1 \right). \qquad (6)$$

Formulas (5) and (6) are used more often than formulas (3) and (4) since look more presentably though the result of calculations of A_p and A_a turns out identical.

In a formula of $\eta = A_p / A_a$ [5, 6] we will substitute the equations (3), (4) and we will receive:

$$\eta = \frac{\frac{n}{n-1} R (T_2 - T_1)}{\frac{k}{k-1} R (T_{2a} - T_1)}; \quad \eta = \frac{n}{n-1} \frac{k-1}{k} \frac{T_2 - T_1}{T_{2a} - T_1},$$

and at $T_2 \approx T_{2a}$ assumption, we will receive the simplified formula

$$\eta = \frac{n}{n-1} \frac{k-1}{k}. \qquad (7)$$

The formula (7) is used in the standard [3] where for the CS parameters the following equations are given:

$$\frac{k}{k-1} = 4,6 + 0,0041 (t_{av} - 0) + 3,9 (\Delta_{air} - 0,5) + 5,0 \left(\frac{n-1}{n} - 0,3 \right); \qquad (8)$$

$$t_{av} = \frac{t_1 + t_2}{2};$$

$$\frac{n-1}{n} = \frac{\lg \frac{T_2}{T_1}}{\lg \frac{p_2}{p_1}} = \frac{\ln \frac{T_2}{T_1}}{\ln \frac{p_2}{p_1}}; \quad \frac{n}{n-1} = \frac{\ln \frac{p_2}{p_1}}{\ln \frac{T_2}{T_1}}, \qquad (9)$$

where t_1, t_2 – NG temperature on an entrance and an exit of CS, ºC; t_{av} – average temperature of NG, ºC; Δ_{air} – relative density of NG by air.

The equation (8) is convenient that having defined k / (k-1) value and n / (n-1) value, it is possible to find η on a formula (7) at once.

The following equation for the NG parameters is given in literature [4]:

Table 1

Methods of calculation of values η

Methods	Description of calculation of parameters NG	Calculation η
Method **1** according to MM of the standard [1], rules of calculation [2]	We determine h_{2a}, h_1 values by formulas (1), (2) and we calculate $A_a = h_{2a} - h_1$. We determine $\frac{n}{n-1}$ by a formula (9) and we calculate A_p by a formula (5).	$\eta = \frac{A_p}{A_a}$
Method **2** according to MM of the standard [3]	We determine $\frac{k}{k-1}$ by a formula (8). We determine $\frac{n}{n-1}$ by a formula (9).	On a formula (7)
Method **3** according to MM [4]	We determine $\tilde{n}_{\tilde{o}}$ by a formula (11) and we calculate $\frac{k}{k-1} = \frac{c_p}{R}$ We determine $\frac{n}{n-1}$ by a formula (9).	On a formula (7)
Method **4** according to a formula (7)	We set value k for NG taking into account values of the following parameters: T_1, T_2, p_1, p_2. We determine $\frac{n}{n-1}$ by a formula (9).	On a formula (7)

$$Mc_{p} = 5{,}5 + (5{,}6 + 0{,}017\,t_2)\,\Delta_{air}, \qquad (10)$$

where M – molar mass of NG, kg/kmol; c_p – heat capacity of NG with a constant pressure if NG has properties of a perfect gas, kcal/(kg·ºC).

Dimension of the equation (10) kcal/(kmol·ºC). In literature [4] for $\grave{I}\ \tilde{n}_{\hat{o}}$ two dimensions (kcal/(kmol·ºC) and kcal/(kmol·K)) that can be a typo or accounting not of temperature, and an interval of temperatures when intervals of degrees Kelvin and Celsius are equal:

$$\Delta T = T_2 - T_1 = (t_2 + 273{,}5) - (t_1 + 273{,}5) =$$
$$= t_2 - t_1 = \Delta t,$$

therefore for an interval we can use dimension as kcal/(kmol·ºC), and kcal/(kmol·K).

We will accept assumption that $\tilde{n}_{\hat{o}} \approx \tilde{n}_{\tilde{e}}$ where $\tilde{n}_{\tilde{e}}$ – heat capacity of NG with a constant pressure and adiabatic process of compression. We will separate both members of equation (10) into M and we will substitute in the equation (10) instead of value of an interval of $\Delta\grave{O}$:

$$c_{\tilde{e}} = \frac{1}{M}\left[5{,}5 + (5{,}6 + 0{,}017\Delta\grave{O})\,\Delta_{air}\right],$$

where dimension of $c_{\tilde{e}}$ – kcal/(kg·K).

If in the equation to use ΔT, then great values of $c_{\tilde{e}}$ therefore we will use not ΔT, but ΔT/2 turn out and we will rewrite (10) in a look:

$$c_{\tilde{e}} = \frac{1}{M}\left[5{,}5 + \left(5{,}6 + 0{,}017\frac{\Delta T}{2}\right)\Delta_{air}\right],$$

and for change of dimension of $c_{\tilde{e}}$ of calories in Joules, we will increase the right member of equation on 4187 J (1 kcal = 4187 J):

$$c_{\tilde{e}} = \frac{4187}{M}\left[5{,}5 + \left(5{,}6 + 0{,}017\frac{\Delta T}{2}\right)\Delta_{air}\right], \qquad (11)$$

where dimension of $c_{\tilde{e}}$ – J/(kg·K).

Replacement ΔT on ΔT/2 brought closer value c_p to $c_{\tilde{e}}$ value that we will check further at practical calculations of η.

For $c_{\tilde{e}}$ we will write down expression [6]:

$$c_{\hat{e}} = \frac{k}{k-1}R$$

and we will receive a formula

$$\frac{k}{k-1} = \frac{c_{\tilde{e}}}{R}.$$

In the grant "Centrifugal gas compressors" developed by Solar for the size A_a the following formula is given:

$$A_a = \frac{R_{air}T_1}{\left(\frac{k-1}{k}\right)\Delta_{air}}\left(\left[\frac{p_2}{p_1}\right]^{\frac{k-1}{k}} - 1\right); \qquad (12)$$

$$\frac{R_{air}}{\Delta_{air}} = R,$$

where R_{air} – gas constant of air, J/(kg·K).

The formula for k not to be given in a grant of "Solar". It is possible to assume that the constant value k is used or the program of calculation of $A_{\grave{a}}$ uses different values k in dependence on parameters of gas and modes of behavior of CS.

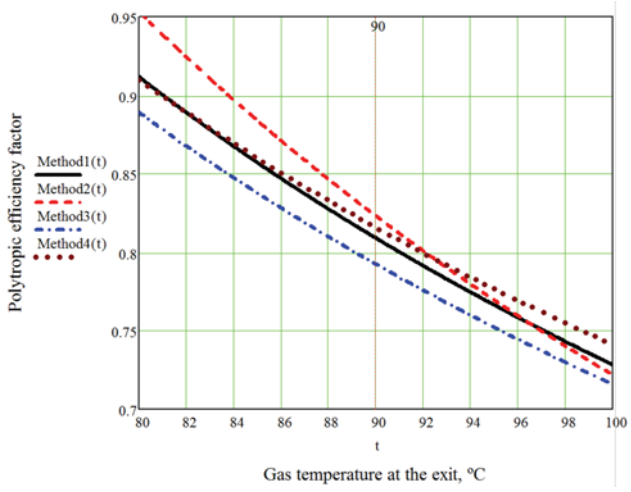

a

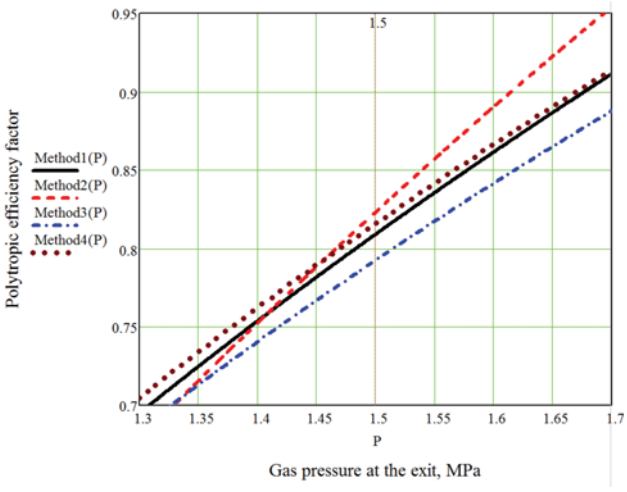

b

Fig. 2 Calculation of η by four methods: a - input data: $p_1 = 0{,}6$ MPa; $p_2 = 1{,}6$ MPa; $t_1 = 4$ ºC; $t_2 = 90$ ºC; $\rho_s = 0{,}73$ kg/m^3; b - the calculated parameters: $\eta_1 = 0{,}8091$; $\eta_2 = 0{,}8232$; $\eta_3 = 0{,}7925$; $\eta_4 = 0{,}8159$; n = 1,3804; $k_2 = 1{,}2934$; $k_3 = 1{,}2794$; $k_4 = 1{,}2900$.

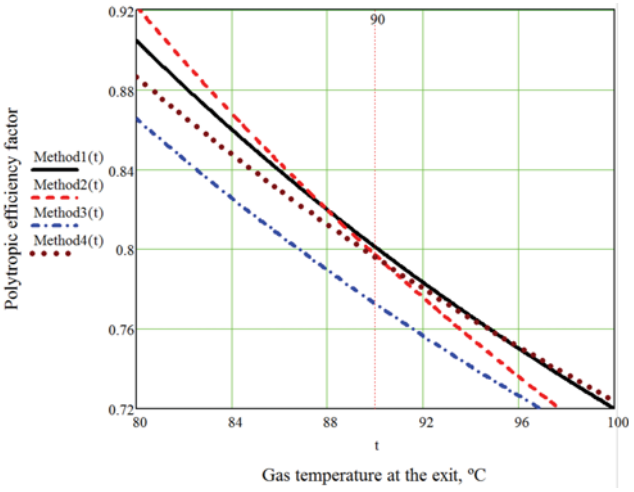

a

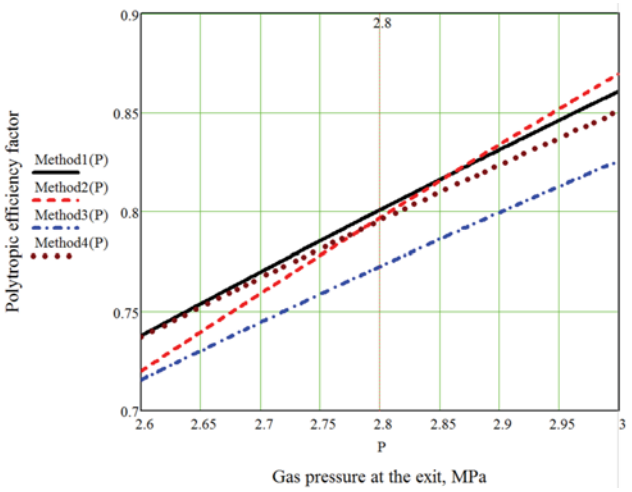

b

Fig. 3 Calculation of η by four methods:a - input data: $p_1 = 1$ MPa; $p_2 = 2{,}8$ MPa; $t_1 = 3$ °C; $t_2 = 90$ °C; $\rho_{\text{в}} = 0{,}73$ kg/m^3; b - the calculated parameters: $\eta_1 = 0{,}8009$; $\eta_2 = 0{,}7969$; $\eta_3 = 0{,}7725$; $\eta_4 = 0{,}7957$; n = 1,3938; $k_2 = 1{,}2906$; $k_3 = 1{,}2792$; $k_4 = 1{,}2900$.

We will rewrite a formula (12), having received the equation similar to the equation (6):

$$A_a = \frac{k}{k-1} T_1 R \left(\left[\frac{p_2}{p_1} \right]^{\frac{k-1}{k}} - 1 \right),$$

$$A_p = \frac{n}{n-1} T_1 R \left(\left[\frac{p_2}{p_1} \right]^{\frac{n-1}{n}} - 1 \right)$$

where assumption is accepted that outlet pressures from the compressor at polytrophic and adiabatic process of compression of gas are equal, that is $p_2 \approx p_{2a}$ (fig. 1).

For A_p we will write down a formula (at $p_2 \approx p_{2a}$):

and for definition of $\eta = A_p / A_a$, we will receive:

$$\eta = \frac{\frac{n}{n-1}}{\frac{k}{k-1}} \frac{\left[\frac{p_2}{p_1} \right]^{\frac{n-1}{n}} - 1}{\left[\frac{p_2}{p_1} \right]^{\frac{k-1}{k}} - 1}. \qquad (13).$$

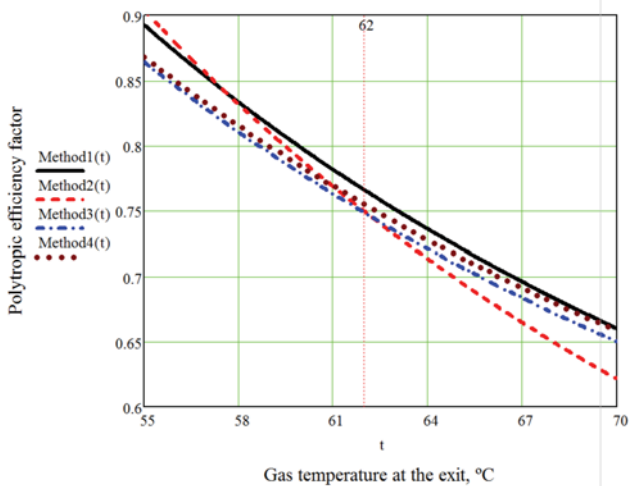

a

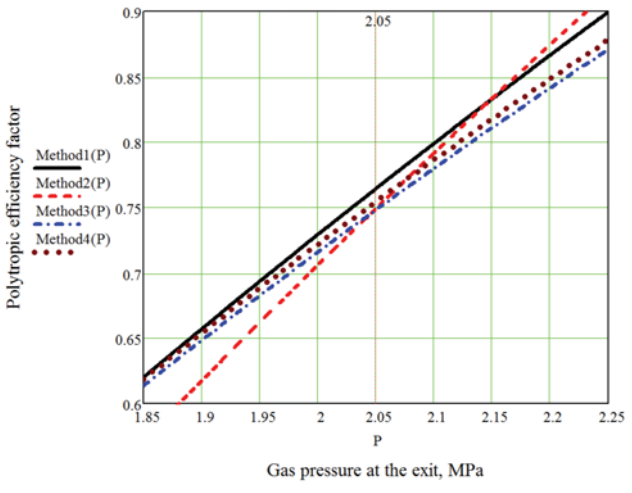

b

Fig. 4 Calculation of η by four methods: a - input data: $p_1 = 2{,}2$ MPa; $p_2 = 3{,}75$ MPa; $t_1 = 33$ °C; $t_2 = 83$ °C; $\rho_{\text{в}} = 0{,}73$ kg/m^3; b - the calculated parameters: $\eta_1 = 0{,}7658$; $\eta_2 = 0{,}7494$; $\eta_3 = 0{,}7484$; $\eta_4 = 0{,}7546$; n = 1,4243; $k_2 = 1{,}2874$; $k_3 = 1{,}2869$; $k_4 = 1{,}2900$.

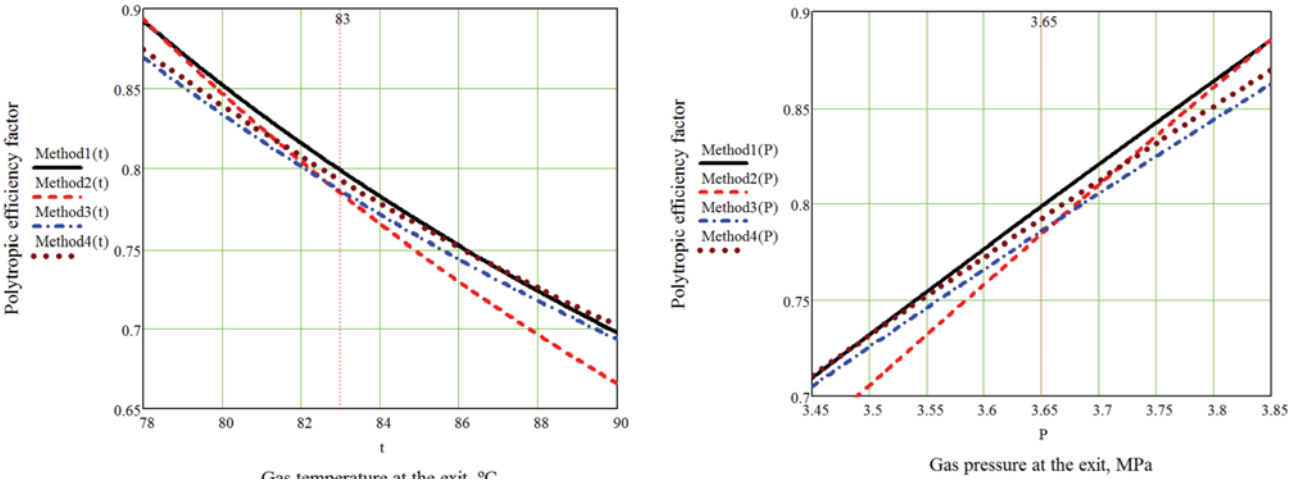

a *b*

Fig. 5 Calculation of η by four methods: a - input data: $p_1 = 2{,}2$ MPa; $p_2 = 3{,}75$ MPa; $t_1 = 33$ °C; $t_2 = 83$ °C; $\rho_s = 0{,}73$ kg/m^3; b - the calculated parameters: $\eta_1 = 0{,}7998$; $\eta_2 = 0{,}7844$; $\eta_3 = 0{,}7955$; $\eta_4 = 0{,}7925$; $n = 1{,}3960$; $k_2 = 1{,}2862$; $k_3 = 1{,}2914$; $k_4 = 1{,}2900$.

We will enter the following designations:

$$\frac{\frac{n}{n-1}}{\frac{k}{k-1}} = S_1 < 1; \quad \frac{\left[\frac{p_2}{p_1}\right]^{\frac{n-1}{n}} - 1}{\left[\frac{p_2}{p_1}\right]^{\frac{k-1}{k}} - 1} = S_2 > 1.$$

also we will write down a formula (13) in a look

$$\eta = S_1 S_2 .$$

As $S_1 < 1$, and $S_2 > 1$, it is possible to receive result when $S_1 S_2 \geq 1$. At practical calculations for a formula (13), values $\eta = 1{,}01 \ldots 1{,}03$ are received that confirms the made assumptions of great value of the work $S_1 S_2$.

Methods of calculation polytrophic EF CS

From the analyzed MM four methods of calculation of η shown in table 1 are allocated. The most difficult calculations are carried out in a method 1, the simplest – in a method 4.

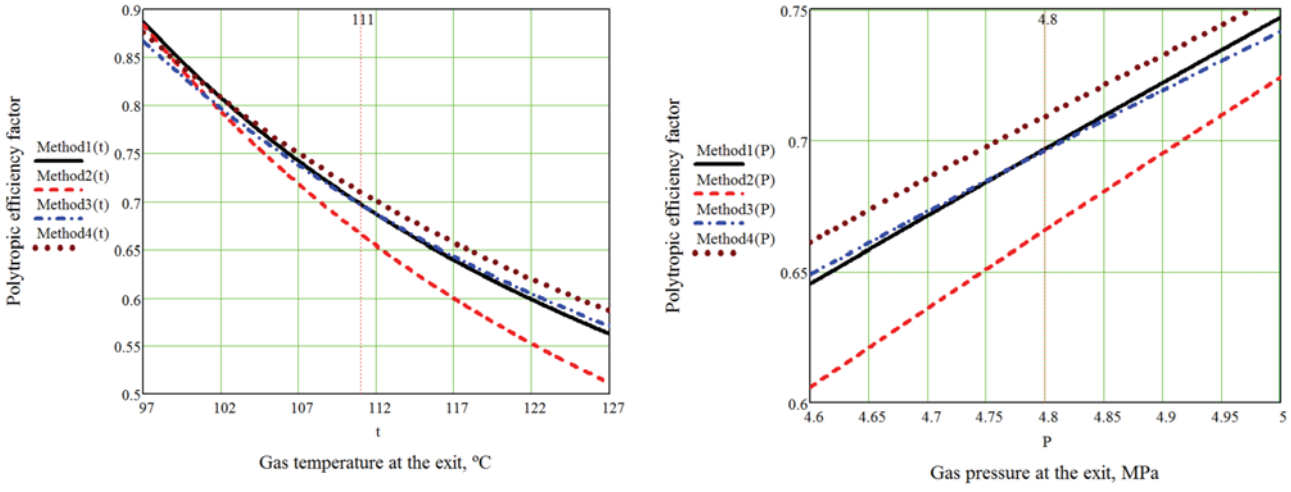

a *b*

Fig. 6 – Calculation of η by four methods:a - input data: $p_1 = 2{,}65$ MPa; $p_2 = 4{,}9$ MPa; $t_1 = 43$ °C; $t_2 = 111$ °C; $\rho_s = 0{,}73$ kg/m^3; b - the calculated parameters: $\eta_1 = 0{,}6967$; $\eta_2 = 0{,}6658$; $\eta_3 = 0{,}6962$; $\eta_4 = 0{,}7093$; $n = 1{,}4640$; $k_2 = 1{,}2675$; $k_3 = 1{,}2831$; $k_4 = 1{,}2900$.

The η values calculated by methods 1-4 (table 1) are given in fig. 2-6.

In fig. 2-6 absolute pressures δ_1, δ_2 are given and the following parameters are used: $\rho_{\text{ст}}$ – NG density under standard conditions (20 ºC, 101325 Pa); η_1 – the η value calculated by a method 1; η_2 – the η value calculated by a method 2; η_3 – the η value calculated by a method 3; η_4 – the η value calculated by a method 4; k_2 – value k when calculating for a method 2; k_3 – value k when calculating for a method 3; $k_4 = 1{,}29$ – the constant value k accepted in a method 4.

The k_1 value (value k when calculating for a method 1) in fig. 2-6 isn't present as η_1 is calculated not by a formula (7) and as the relation A_i / A_a (table 1).

In calculations and schedules of fig. 2-6 the following constant parameters were accepted:

- for a method 3: M = 17,4 kg/kmol;
- for a method 4: k = 1,29.

In fig. 2-6 not only η values at the fixed t_2 value are shown, but also schedules of $\eta(t_2)$ and $\eta(p_2)$ where t_2 and p_2 change in the range of near real value (a dotted line on graphics) given in basic data. Schedules allow to analyze more precisely features of change of η for each method that shows features of MM of calculation of the NG parameters.

Replacement ΔT on $\Delta T/2$ in a formula (11) showed good results in calculations of η (fig. 2-6), but we will note that with entrance pressure 0,5…1,0 MPa the method 3 gives the minimum η values.

Good results for calculation of η were shown by the simplest method 4 (table 1, fig. 2-6) which it is possible to apply under operating conditions CS. At $p_1 = 2{,}65$ MPa the method 4 gives the overestimated values (fig. 2-6) and it is better to use it at $p_1 = 0{,}5$-$2{,}3$ MPa.

By a method 2 at $p_1 = 2{,}65$ MPa the smallest polytrophic EF (fig. 2-6) therefore at $p_1 > 2{,}2$ MPa are better to use a method 3 which is simpler in calculations, than a method 1 was received.

Conclusions

1. According to the analyzed MM four methods of calculation of polytrophic EF CS (table 1) are described.
2. Practical calculations of polytrophic EF CS for four methods are carried out. Schedules at change of temperature and outlet pressure of CS are constructed that allows to compare the nature of change of η for each method.
3. It is shown that it is possible to use the simplest fourth method for calculation of polytrophic EF CS with inlet pressures of CS about 0,5-2,3 MPa.
4. With inlet pressures of CS more than 2,3 MPa it is better to use the third method of calculation (table 1).

References

1. Kompresorni stancii. Kontrol teplotehnichnuh ta ekologichnuch haraktericticik gazoperekachuvalnuh agregativ: SOU 60.3-30019801-011:2004. - [Diisnui з 22.12.2004]. - K.: DK «Ukrtransgaz», 2004. - 117 s.
2. Metodicheskoe ukazaniya po provedennyu teplotehnicheskih i gazodinamicheskih raschetov pri isputaniyah gazoturbinnuh gazoperekachivayuchih agregatov: PR 51-31323949-43-99. - [Deictvitelen s 01.05.1999]. - M.: VNIIGAZ, 1999. - 26 s.
3. Metodica ozenki energoeffektivnosti gazotransportnuh obektov I sistem. STO 2-3.5-113-2007. – [Действителен с 15.11.2007]. – M.: VNIIGAZ, 2007. – 118 s.
4. Dobrohotov V.D. Termodinamika sschatiya prirodnogo gaza i harakteristiki nagnetatelei kompresornuh ctancii dlya magistralnuh gazoprovodov / V.D. Dobrohotov, A.K. Klubnichkin, V.A. Shchurovsky. - M.: VNIIEgazprom, 1974. - 41 s.
5. Saprykin S.A. Opredelenie koeffizienta poleznogo deistviya kompressora / S.A. Saprykin, Yu.A. Oleynik, A.V. Prasko, A.S. Mosin. Zbirnik naukovuh prach // Putannya rozvitku gazovoi promuslovosti Ukrainu. Kharkiv: UkrNDIgaz, 2014. - № 42/2. - S. 98-103.
6. Saprykin S.A. Politropnui koeffizient poleznogo deistviya kompressora / S.A. Saprykin, Yu.A. Oleynik, A.V. Prasko, O. I. Matyushchevska, A.S. Mosin. Zbirnik naukovuh prach // Putannya rozvitku gazovoi promuslovosti Ukrainu. Kharkiv: UkrNDIgaz, 2015. - № 43. - S. 164-172.

Вісник ХНУ, серія «Фізика», вип. 26, 2017. с. 58-63

PACS
UDC 533.15: 530.1

Review of theory of mesocopic systems

V. V. Fedotov

NTUU "Igor Sikorsky Kyiv Polytechnik Institute"

As part of this work, the theory of mesoscopic systems was substantiated. The main effects of mesoscopic systems are provided; it is determined that the macroscopic characteristics of the system are significantly fluctuating within the mesoscopic level. The basic indicators of coherence of the quantum phase are determined and the mechanisms of influence are outlined. Six effects of mesoscopic systems with detailed justification are characterized. The theory of mesoscopic systems is based on the following mesoscopic effects: the Aaronov-Bohm effect; integral quantum output effect; fractional quantum Hall effect; Universal fluctuations of conduction; quantization of conductivity of a quantum point contact; direct currents in mesoscopic rings.

Small scales of time and/or length and low temperatures are characteristic for a mesoscopic regime. Under the conditions where the temperature is reduced, the time/length of the coherence of the phase increases, and the mesoscopic regime extends over larger scales of time/length. At Kelvin temperatures, the time and length scales in semiconductor samples are respectively picoseconds and micrometers.

Prospects for further developments in this area of research are based on a detailed study of mesoscopic effects, based on the growing trend for the production and research of materials containing the smallest structures and having low-dimensional features, that leads to the mesoscopic regime.

Keywords: mesoscopic systems; fluctuation; quantum phase; coherence; nanostructured system; macroscopic characteristics

У рамках даної роботи зроблений огляд теорії мезоскопічних систем. Зазначено основні ефекти мезоскопічних систем, визначено, що макроскопічні характеристики системи значно флуктуюють, у рамках мезоскопічного рівня. Визначено основні показники когерентності квантової фази та окреслено механізми впливу. Охарактеризовано шість ефектів мезоскопічних систем з детальним обґрунтуванням. Теорія мезоскопічних систем ґрунтується на наступних мезоскопічних ефектах: ефект Ааронова-Бома; ефект інтегрального квантового виходу; дробовий квантовий ефект Холла; універсальні флуктуації кондактанса; квантування провідності квантового точкового контакту; постійні струми у мезоскопічних кільцях.

Перспективи подальших розробок у даному напрямку дослідження ґрунтуються на детальному вивченні мезоскопічних ефектів виходячи зі зростаючої тенденції до виготовлення та дослідження матеріалів, що містять найменші структури та мають низькорозмірні риси, що призводить до мезоскопічного режиму.

Ключові слова: мезоскопічні системи; флуктація; квантова фаза; когерентність; наноструктурована система; макроскопічні характеристики.

Аннотация. В рамках данной работы сделан обзор теории мезоскопических систем. Указаны основные эффекты мезоскопических систем, определено, что макроскопические характеристики системы значительно флуктуирует, в рамках мезоскопических уровня. Определены основные показатели когерентности квантовой фазы и обозначены механизмы воздействия. Охарактеризованы шесть эффектов мезоскопических систем с подробным обоснованием. Теория мезоскопических систем основывается на следующих мезоскопических эффектах: эффект Ааронова-Бома; эффект интегрального квантового выхода; дробный квантовый эффект Холла; универсальные флуктуации кондактанса; квантования проводимости квантового точечного контакта; постоянные токи в мезоскопических кольцах.

Перспективы дальнейших разработок в данном направлении исследования основываются на детальном изучении мезоскопических эффектов исходя из растущей тенденции к изготовлению и исследования материалов, содержащих самые структуры и имеют низкоразмерные черты, что приводит к мезоскопических режима.

Ключевые слова: мезоскопические системы; флуктация; квантовая фаза; когерентность; наноструктурированная система; макроскопические характеристики.

Introduction and research problem statement

The constant trend in modern material science is to offer and explore systems that contain the smallest structures. The obtained systems are suitable for a mesoscopic regime, in which the coherence of the quantum phase leads to a change in the electronic states of quantum devices. At the same time, microscopic details of the sample, such as precise configurations of impurities in disordered systems, determine some quantitative behaviour patterns. This may lead to the expressed fluctuations of the quantity measured in different samples, which are macroscopically equivalent.

At the end of the 20th century, the apparent trend towards nanostructured systems appears in physical science, which include semiconductor structures and magnetic

materials, as well as internally nanostructured systems, such as biomaterials and macromolecules. These smallest structures are suited to the so-called mesoscopic regime in which quantum effects become relevant to the behaviour of materials. At the same time, significant progress in the controlled production of submicron solid-state structures, as well as the general availability of low-temperature plants, allowed to systematically investigate artificially created structures with electronic properties having been modified or even prevailing over the effect of quantum interferences. This allows conducting experiments in a mesoscopic regime that directly investigate the quantum properties of phase coherent systems of many bodies.

Research paper's objective. Make an overview of the theory of mesoscopic systems. Describe the basic indicators of the quantum phase coherence and outline the mechanisms of influence.

Analysis of recent research and publications. Good starting points for the study of mesoscopic physics are the recent scientific papers on this subject presented by M.A. Ivanov [1], S.M. Shevchenko [2], M.V. Denisenko and A.M. Satanin [3]. Klinskikh A.F., H. T.T. Nguyen, P.A. Meleshenko [4], in the annex to a series of fundamental "secondary" macroscopic quantum effects, as well as quantum-dimensional effects in mesoscopic systems, present some modern methods of quantum mechanics that have not found any consistent coverage in the academic literature.

Article [5] deals with the investigation of the conductivity of impurities of weakly doped (N <1,017 cm^{-3}) noncompensated (K <10^{-3}) silicon from the electric (E) and magnetic (H) fields at temperatures corresponding to the saturation of the 03 conductivity.

Khalilov V.R. [6] presents the relativistic quantum Aaronov-Bohm effect for a free (in the availability of a three-vector Coulomb potential of Lorentz) and bound fermion states. The author obtained the general scattering amplitude in the combination of three-vector Coulomb potentials of Aaronov-Bohm and Lorentz as a sum of two scattering amplitudes.

However, despite the scale of scientific research on the subject of this paper, the issue of substantiation of the theory of mesoscopic systems remains open and requires detailed elaboration.

Research findings

The mesoscopic regime is an intermediate between the quantum world of microscopic systems (atoms or small molecules) and the classical world of macroscopic systems, such as large fragments of a condensed matter. Mesoscopic systems, as a rule, consist of a large number of atoms, but their behaviour is significantly influenced by the effects of quantum transitions. This is mesoscopic physics on the verge of statistical physics and quantum physics.

The coherence of the quantum phase, which is required for the appearance of interference effects, is maintained only for a finite time τ_φ, which is called the phase separation period. The phase coherence is lost when the system or its components being studied interact with its medium, for example through electron-phonon scattering. In electronic conductors, the time of separation of the final phase corresponds to the length of phase separation L_φ.

Mesoscopic quantum effects appear when the typical time scales or system lengths are less than the time or length of phase separation. In many cases this means that the corresponding size of the system Lmust be less than the phase coherence length [2]

$$L < L_\varphi \qquad (1)$$

For an electron, the time/length of the coherent phase is limited to electron-electron and electron-phonon scattering. These processes are important at high temperatures, but both types of scattering are suppressed at low temperatures, the reason for this is the dependence of the coherence of the phases on the temperature.

It is important to note that only the processes of scattering, in which the excitation (phonon, electron excitation, etc.) of the environment is created or destroyed, result in the loss of phase coherence. Such scattering processes leave a trace inside the environment, which in principle can be observed, and resembles the measurement of the particle trajectory. These processes are usually inelastic and associated with the transfer of energy. However, processes that change the environment without transferring energy can also lead to decoherence.

In contrast, scattering of electrons from static impurities is always elastic. Despite the fact that the phase of electrons could be modified during the scattering process, this occurs in a clearly defined way and does not destroy the effects of coherence of the phases.

Therefore, the mesoscopic regime is characterized by small scales of time and/or length and low temperatures. When the temperature drops, the time/length of phase coherence increases, and the mesoscopic regime extends over larger scales of time/length. At Kelvin temperatures, the scale of time and length in semiconductor samples are respectively picoseconds and micrometers.

Since small finite systems at low temperatures are found in mesoscopic physics, the interlayer interval Δ of the discrete electron spectrum may become larger than the product of the Boltzmann constant and temperature. Then, the electronic and thermodynamic properties of the sample are determined not only by global values, such as the average density of states, but also by the spectrum details. However, the exact spectrum depends on the configuration of impurities, which leads to fluctuations of the observed values between macroscopically indistinguishable samples.

These fluctuations are interesting for study, because qualitative effects are often universal in the sense that they are not dependent on microscopic details.

The theory of mesoscopic systems is based on mesoscopic effects:

– Aaronov-Bohm effect;

– Integral quantum output effect;

– Fractional quantum Hall effect;

– Universal conductance fluctuations;

– Quantization of conductivity of a quantum dot contact;

– Direct currents in mesoscopic rings.

Aaron-Bohm effect

One of the most striking effects of phase coherence is the ability to observe the Aaronov-Bohm oscillations in the conductivity of mesoscopic structures containing small normal metal rings [6]. At low temperatures, when the coherence length of the phase is greater than the length of the ring, the interference of the electron amplitudes is important, which can pass through both one, and through another part of the ring. It is necessary to add to the internal difference of the phases of the two paths the effect of the magnetic field, which leads to the phase shift set as

$$\varphi_B = {}^{2\pi e}/_{h} \oint d\vec{s}\vec{A} = {}^{2\pi e}/_{h}\,\Phi \qquad (2)$$

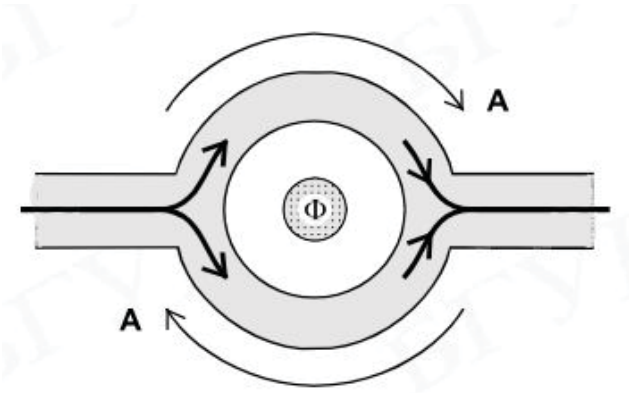

a

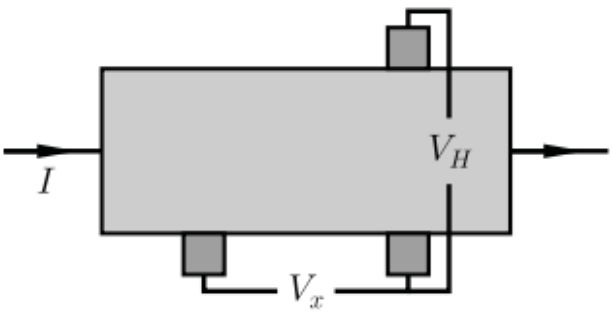

b

Fig. 1 Aaron-Bohm effect: a) distribution of magnetic flux; b) geometry of the Aaronov-Bohm effect. *According to [2,6].*

The integral of a closed loop of a ring from a vector potential $\vec{A}$ gives a phase shift proportional to the magnetic flux Φ through a ring set as the area of the ring multiplied by the (constant) magnetic field strength B perpendicular to the plane of the ring. The conductivity component (the ratio between the current through the sample and the applied voltage) is proportional to $cos\,(\varphi_0 + \varphi_B)$, which leads to observations h/e- of periodic oscillations of conductivity of the device as a function of the magnetic flux penetrating the ring, as shown in Figure 1a.

The longitudinal voltage V_x is measured between two points along one edge of the sample, whereas the Hall voltage is measured between the points on the opposite edges of the samples.

Integral quantum output effect

One of the first and most striking observations of the macroscopic effects of phase coherence in the electronic properties of solid-state devices was the discovery of the integral quantum Hall effect [6] by Klaus von Klitsinger in 1980, awarded the Nobel Prize in 1985.

When measuring the Hall effect in the inverse layer of a silicon MOS (metal-oxide-semiconductor) transistor at low temperatures (T ~ 1 K) and in strong magnetic fields (B> 1 T), the linear dependence of the Hall resistance turns into a number of degrees (plateaus). The value of the resistance on these plateaus is equal to the combination of fundamental physical constants divided by an integer.

When, the plateau is observed on the Hall resistance R_H, longitudinal electrical resistance becomes very small. At low temperatures, the current in the sample can proceed without dissipation (scattering). In the course of research, Klaus von Klitzing used two-dimensional electron gas.

The Hall effect provides that when a conductor is placed in a magnetic field B, it creates a transverse voltage between the opposite sides of the sample, proportional to the longitudinal current I. This dependence can be written through the so-called Hall resistance

$$V_H = R_H I \qquad (3)$$

Classically, using Drude's formula, we get Hall's resistance

$$R_H = {}^{B}/_{en_s} \qquad (4)$$

with two-dimensional electron density n_s. The magnetic field does not affect the longitudinal resistance R_x calculated from the ratio of the voltage drop between the two points on the same side of the sample to the current I within the Drude's theory.

The longitudinal resistance is reduced to zero, with the exception of some values of the magnetic field, where peaks appear.

Fractional quantum Hall effect

The transition to stronger magnetic fields and the decrease of temperatures in two-dimensional electron gases allows observing additional Hall resistance plateaus at fractional filling factors, such as ν = 1/3. This so-called fractional quantum Hall effect was discovered in 1982 [4]. Particularities in case of fractional filling can be traced to the existence of correlated collective quasiparticle excitations [3]. Thus, unlike the integer quantum Hall effect, the Coulomb interaction between electrons is necessary to explain the fractional quantum Hall effect. Quasiparticles have a fractional charge (for example, e / 3 with ν = 1/3). From the shock noise measurements [1], it has recently been confirmed that the charge carriers at ν = 1/3 in the regime of the fractional quantum Hall effect actually have a charge e/3.

Universal fluctuations of conductance

The use of disordered wires in a mesoscopic regime has expressed fluctuations as a function of external parameters such as magnetic field or Fermi energy. These fluctuations were detected by [3] in low temperature (below 1 K) conductivity of the inverse layer in a disordered silicon transistor. Fluctuations are reproduced and reflect the imprint of the sample. The origin of oscillations is the interference of the various paths that electrons can take during passage through the sample, as shown in Figure 2.

In a macroscopically equivalent sample with a microscopically different configuration of impurities, fluctuations are qualitatively similar, but their exact characteristics can be completely different. The most striking feature of the conductivity oscillations is that their typical amplitude is universal in diffusion regime [2].

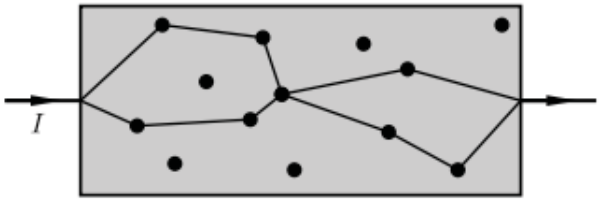

Fig. 2. Possible paths of an electron through disordered wire, with processes of elastic scattering on impurities. The paths of an electron are influenced by the magnetic field or the value of the Fermi wave vector, which leads to oscillations of conductivity in the mesoscopic regime. *According to [6]*

Regardless of the mean conductivity value, the oscillations always form the order of quantum conductivity e^2/h and depend only on the basic symmetries (for example, the symmetry of inversion time) of the system [4]. This can cause the repulsion of the eigenvalues of the matrices of random transmissions. Quantization of conductivity of a quantum dot contact

A point contact is a bond between two leading materials. Such a link can be formed by imposing a restrictive narrowing on the wire or by inducing the electrons to pass through a narrow channel determined electrostatically when they lead from one two- or three-dimensional region of the sample to another. In the case of a very narrow width, narrower than the average free path and the length of the coherence of the phases (), which is called ballistic quantum dot contact. Constant currents in mesoscopic rings

Quantization of conductivity of a quantum dot contact

A point contact is a bond between two conductive materials. Such a link can be formed by imposing a restrictive narrowing on the wire or by inducing the electrons to pass through a narrow channel determined electrostatically when they lead from one two- or three-dimensional area of the sample to another. In case of a very narrow width W, narrower than the average free path and the length of the coherence of the phases ($W \ll l, L_\varphi$), which is called ballistic quantum point contact.

Constant currents in mesoscopic rings. The electrons in the mesoscopic rings can support the current around the ring in a thermodynamic equilibrium, even at zero temperature. This current depends on the magnetic flux and cannot dissipate dissipative. Therefore, it flows forever even in ordinary conductors, and that is why it is called a steady current.

Direct currents in mesoscopic rings. The electrons in the mesoscopic rings can maintain the current around the ring in a thermodynamic equilibrium, even at zero temperature. This current depends on the magnetic flux Φ and cannot scatter dissipatively. Therefore, it flows forever even in ordinary conductors, and that is why it is called a steady current.

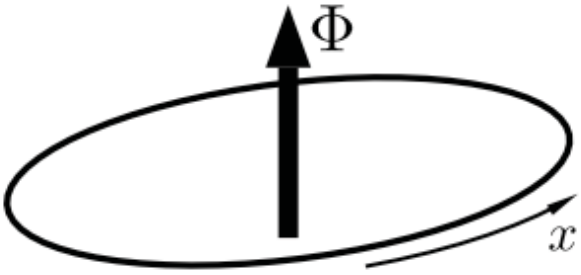

Fig. 3. An ideal one-dimensional ring run through by a magnetic flux Φ. *According to [2,4].*

Figure 3 shows an ideal one-dimensional circle ring $L \ll L_\varphi$. It is well known that a magnetic field cannot affect the behavior of one-dimensional systems. This, however, does not occur when the one-dimensional system is closed on the ring. In this topology, the flux Φ connecting the ring leads to a phase shift $2\pi\Phi / \Phi_0$

accumulated by an electron moving around the ring, $\Phi_0 = h/e$ is a quantum of the flux. Using a calibration transformation, this phase shift can be given by [2] in the boundary state, eliminating the magnetic vector potential from the Schrödinger equation for electrons and leading to generalized periodic boundary conditions

$$\psi(x=0) = exp(i2\pi\Phi/\Phi_0)\psi(x=L) \quad (5)$$

for single-particle wave functions $\psi(x)$. It follows that all the electronic properties of the rings must be periodic in a magnetic flux, the period of which is a quantum of the flux Φ_0, similar to the Aaronov-Bohm effect.

The wave function of non-interacting electrons in a pure ring are flat waves

$$\psi(x) \propto exp(ikx) \quad (6)$$

The boundary state of equation (5) limits the possible wave vectors k to values

$$k_n = 2\pi/L\left(n - \Phi/\Phi_0\right)$$

where $n = \{0, \pm1, \pm2, \pm3, \ldots\}$. Flux dependence of the corresponding one-particle energies

$$E_n = \hbar^2 k_n^2/2m = 1/2m\left[h/L\left(n - \frac{\Phi}{\Phi_0}\right)\right]^2 \quad (8)$$

which is shown in Figure 4. The direct current at zero temperature is set as the sum of currents $e\hbar k_n/mL$ from the lowest levels in the ring. The direct current can be written as

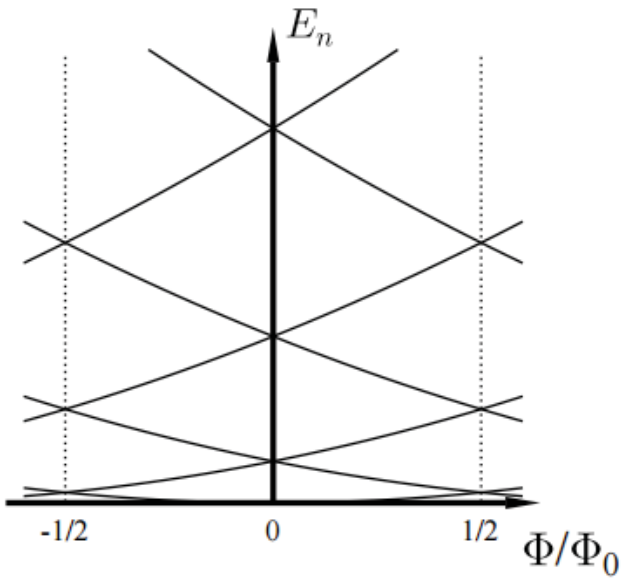

Fig. 4. The dependence of the flux on the lowest energies of one particle in the ring, for -3 ≤ n ≤ 3.*According to [2,4].*

$$I_p = -dE/d\Phi \quad (9)$$

with the total electron energy E. Since, at a given value of Φ, the sign of the derivative one-particle energies relative to the magnetic flux fluctuates with a quantum number n, the total steady current decreases by eliminating adjacent levels. The resulting current with a large number of particles dominating over the last electron (at the Fermi level) and order

$$I_p^{ld} \sim ev_F/L \quad (10)$$

with the Fermi speed v_F.

In disordered rings of finite width with elastic free path length $l \ll L$, the theoretical value is more difficult to obtain even for non-interacting electrons. In a diffusion regime a steady current of the following order is expected

$$I_p^{diff} \sim ev_F/L\,\frac{l}{L} \quad (11)$$

decreasing in the ratio l/L.

The experimental value of the direct current in diffusion rings [2, 3] is much larger (at least for an order) than this theoretical prediction. It is believed that the discrepancy is due to the electronic interaction, which was neglected when deriving the equation (11). Despite the fact that electronic interaction seems to play an important role, it is also important to assert that interactions cannot affect the steady current in pure rotary-invariant 1d rings [2, 6], and the non-binding result (10) is consistent with an experimental one for a pure semiconductor ring in a ballistic regime [3].

This led to a large theoretical activity associated with the combined effect of interactions and disorders for increasing the steady currents in the mesoscopic rings. Despite the fact that different theoretical approaches indicate an increase in steady current in disordered samples due to repulsion of Coulomb interactions, there is still no quantitative understanding of experiments.

Conclusions from this study and prospects for further developments in this area

As part of this research paper, the theory of mesoscopic systems was reviewed. In a mesoscopic regime there are many interesting, sometimes unexpected effects due to phase coherence of electronic wave functions. Some of these effects are very promising for use in nanoelectronic devices or quantum standards in metrology.

The most outstanding example, the quantum Hall effect, is already used as the standard of resistance. On the other hand, mesoscopic systems provide an opportunity to

study the basic features of quantum mechanics. They also allow studying directly the features of interacting correlated quantum systems of many bodies. Examples are the fractional quantum Hall effect and transport spectroscopy of interacting electrons at quantum dots.

Prospects for further developments in this area of research are based on a detailed study of mesoscopic effects coming from the growing trend for the production and research of materials containing the smallest structures and having low-dimensional features, which leads to the mesoscopic regime.

References

1. Ivanov M. A. Dynamichni zakonomirnosti rezonansnykh kvantovykh system: avtoref. dys. avtoreferat dys. na zdobuttia nauk. stupenia kand. fiz.-mat. nauk: spets. 01.04.02 / M. A. Ivanov. – D., 2015. – 16 s.
2. Shevchenko S. M. Strumovi stany v mezoskopichnykh normalnykh ta nadprovidnykh systemakh: avtoreferat dys. na zdobuttia nauk. stupenia kand. fiz.-mat. nauk: spets. 01.04.02 / S. M. Shevchenko. – Kh., 2003. – 16 s.
3. Denysenko M. V. Mezoskopycheskye fluktuatsyy veroiatnostei perekhoda mezhdu urovniamy kubyta v pole byharmonycheskoho syhnala / M. V. Denysenko, A. M. Satanyn // Tezysы dokladov Foruma molodыkh uchenыkh NNHU. Nyzhnyi Novhorod, 16-18 sentiabria 2013 h. – S. 131.
4. Klynskykh A. F. Rasseianye эlektrona na dvumernom kulonovskom potentsyale v uslovyiakh эffekta Aaronova-Boma / A. F. Klynskykh, Khanh T. T. Nhuen, P. A. Meleshenko // Vestn. Voronezh. hos. un-ta. Seryia: Fyzyka. Matematyka. – 2010. – № 2. – S. 241-246.
5. Hurvych Yu. A., Melnykov A. P., Shestakov L. N. Mezoskopycheskye эffektы v provodymosty po prymesiam slabolehyrovannoho nekompensyrovannoho kremnyia v neomycheskoi oblasty / Yu. A. Hurvych, A. P. Melnykov, L. N. Shestakov // Vestnyk Pomorskoho unyversyteta, seryia «Estestvennыe nauky». – 2005. – № 1. – S.92-97.
6. Khalilov V. R. Relativistic Aharonov-Bohm effect in the presence of planar Coulomb potentials / V. R. Khalilov // Phys. Rev. A. – 2005. – Vol. 71. – P. 012105(1) –012105(6).

Вісник ХНУ, серія «Фізика», вип. 26, 2017. с. 64-72

УДК 537:378.4. 011.3-057.175 (477,54-25)
ББК 22.33. д Пильчиков
П 32

Микола Дмитрович Пильчиков – видатний фізик, один з піонерів бездротової телеграфії та основоположник радіокерування

(До 160 річниці з дня народження)

В.П. Пойда[1], В.І. Білецький[1], В.В. Нерубенко[1], К.І. Байрамова[1], М.І. Боброва[1], К.О. Мінакова[2], О.В. Семенов,[2] О.П. Сук[2], Е.С. Юнаш[2], О.М. Меньшова[2]

[1)] Харківський національний університет імені В.Н. Каразіна
Україна, 61022, м. Харків, пл. Свободи, 4
[2)] Національний технічний університет «Харківський політехнічний інститут»
Україна, 61002, м. Харків, вул. Кирпичова, 2

Наведені біографічні дані видатного фізика Миколи Дмитровича Пильчикова та розглянуто його основні наукові досягнення у галузі фізики, геофізики, метеорології, бездротової телеграфії та радіокерування. Описані нещодавно знайдені та відновлені деякі фізичні прилади, якими користувався М.Д. Пильчиков при проведенні дослідів.
Ключові слова: рефрактометр, бездротова телеграфія, радіокерування, реле, передавальна антена іскрової радіостанції.

Приведены биографические данные выдающегося физика Николая Дмитриевича Пильчикова и рассмотрены его основные научные достижения в области физики, геофизики, метеорологии, беспроводной телеграфии и радиоуправления. Описаны недавно найденные и восстановленные некоторые физические приборы, которыми пользовался Н.Д. Пильчиков при проведении опытов.
Ключевые слова: рефрактометр, беспроводная телеграфия, радиоуправление, реле, передающая антенна искровой радиостанции.

Biographical data of the outstanding physicist Nikolai Dmitrievich Pilchikov are given and his main scientific achievements in the field of physics, geophysics, meteorology, wireless telegraphy and radio control are considered. Some physical devices used by N.D. Pilchikov during the experiments, recently found and recovered are described.
Keywords: refractometer, wireless telegraphy, radio control, relay, transmitting antenna of a spark radio station.

У наше сьогодення повертаються імена незаслужено забутих вчених, які за часів свого життя вони були широковідомими в наукових колах, бо зробили вагомий внесок у розвиток світової науки. До них належить і Микола Дмитрович Пильчиков – геніальний фізик із надзвичайним талантом першопрохідника, в доробку якого десятки відкриттів та винаходів світового значення (Рис. 1). Основоположник радіокерування та фотогальванографії, один з перших дослідників властивостей рентгенівських променів, радіоактивності, дослідник геомагнетизму, метеорології, оптики, розробник оригінальних пристроїв для бездротової телеграфії. М.Д. Пильчиков відзначався різносторонністю наукових інтересів та виключною працездатністю, мав високі організаційні здатності і моральні устої, досконало оволодів сімома мовами. Він постійно прагнув пов'язати теоретичні дослідження з практикою. За чисельні наукові заслуги його поважали і вважали рівним собі багато славетних фізиків. М. Д. Пильчиков був обраний членом різних наукових установ Росії, Франції, Німеччини, Австрії. Біографічні дані про М.Д. Пильчикова та основні відомості про його життєвий шлях і науково-педагогічну діяльність опубліковані в [1-4]. Опис документів, що склали архів вченого, наведений в [5].

Микола Дмитрович Пильчиков народився 21 травня 1857 року в м. Полтаві. Його батько, Дмитро Павлович Пильчиков, учасник національно-демократичного руху, член Кирило-Мефодіївського братства, член Полтавської громади, активний пропагандист україножильства. Він був особисто знайомий з Тарасом Шевченком, підтримував стосунки з Пантелеймоном Кулішем, з галицькими громадськими і культурними діячами та з Михайлом Драгомановим. Дмитра Пильчикова вважали своїм духовним наставником Олександр Кониський, Панас Мирний

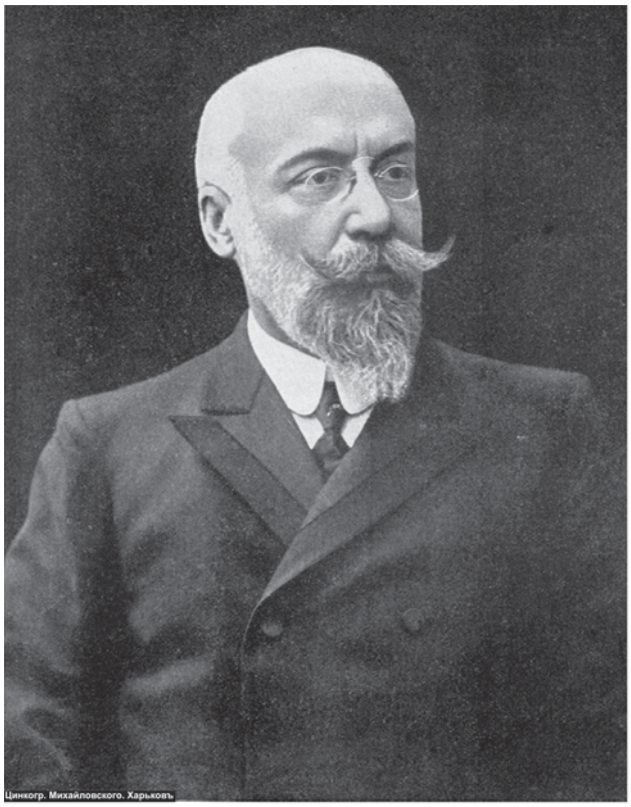

Рис. 1. Фотопортрет М.Д. Пильчикова [1].

(Панас Якович Рудченко), Іван Карпенко-Карий (Іван Карпович Тобілевич). Мати Миколи Дмитровича Пильчикова – Людмила Капітонівна Юр'єва походила із збіднілої дворянської родини. Вона померла, коли М.Д. Пильчикову не минуло й року.

До чотирнадцяти років Микола Пильчиков перебував вдома. Батько з надзвичайною любов'ю і самовідданістю виховував і навчав свого єдиного сина. Подальшу освіту Микола Пильчиков почав здобувати з 1871 року в 1 Полтавській чоловічій класичній гімназії, де виділявся талановитістю до наук, особливо до фізики і математики.

Ще гімназистом Микола Пильчиков познайомився з Панасом Мирним і вони, незважаючи на вікову різницю, стали друзями. Їх поєднували високі помисли про служіння простому народу. Микола Пильчиков та Панас Мирний брали участь у просвітницькому русі в Полтаві, входили до таємного товариства «Унія».

У серпні 1876 року М.Д. Пильчиков вступив на фізико-хімічне відділення фізико-математичного факультету Харківського імператорського університету і разом з батьком став проживати у Харкові. Спочатку вони мешкали у найманих квартирах, а потім у власному будинку на Гімназичній набережній. Студент Пильчиков старанно вчився, із захопленням працював у фізичному кабінеті університету. Його вчителями були: професор хімії М.М. Бекетов, професор механіки В.Г. Імшенецький, професори фізики А.П. Шимков і Ю.Г. Морозов, доцент фізики О.К. Погорілко, професор геометрії К.О. Андрєєв.

У 1878 році, ще до появи в Європі відомостей про механічний фонограф Т. Едісона, М.Д. Пильчиков розробив схему електричного фоноавтографа. Свою першу наукову доповідь – реферат на тему: «Дослідження Крукса, що стосуються четвертого стану матерії», текст якого не зберігся, студент 4 курсу Пильчиков М.Д. виголосив на засіданні фізико-хімічної секції Товариства дослідних наук при Харківському університеті 14 листопада 1879 року. Захоплення навчанням, у якому мав відмінні успіхи, лабораторними роботами, конструюванням та вдосконаленням фізичних приладів, безкорислива допомога викладачам та працівникам фізичного кабінету в устаткуванні лабораторії для фізичного практикуму, ретельне відвідування засідань фізико-хімічної секції Товариства дослідних наук помітно виділяли Пильчикова М.Д. серед інших студентів. Успішно закінчивши у 1880 році університетський курс зі званням кандидата Харківського університету, він фактично став єдиним гідним претендентом на одержання стипендії для підготовки до професорського звання. Залишити М.Д. Пильчикова в університеті та надати йому можливість підготувати магістерську дисертацію рекомендував професор Шимков А.П. На кафедрі фізики і фізичної географії М. Д. Пильчиков почав працювати як стипендіат з листопада 1880 року.

У 1882 – 1883 роках М.Д. Пильчиков склав екзамени на ступінь магістра і активно зайнявся науковою роботою. Вже через рік після закінчення університету він зробив кілька повідомлень про результати своїх досліджень на засіданнях фізико-хімічної секції Товариства дослідних наук. Усього за 14 років роботи в Харківському університеті М.Д. Пильчиков на засіданнях Товариства дослідних наук виголосив 14 доповідей, які відображали основні напрямки його наукової діяльності, що стосувалися вивчення фізико-хімічних процесів, які здійснюються при електролізі, суті капілярних явищ, закону заломлення світла, методів рефрактометрії, механізмів утворення звичайної та кульової блискавок, причин утворення граду, а також спектральної поляризації світла, розсіяного земною атмосферою. Низка доповідей вченого була присвячена пропагуванню нових методів дослідження та ознайомленню слухачів із принципом дії, створених ним нових фізичних приладів: рефрактометра, диференціального аерометра, термостата, автоматичного регулятора гальванічного струму, фотоелектричного регулятора, інклінатора для вимірювання вертикальної складової земного магнетизму, сейсмографа. М.Д. Пильчиков разом з І.П Осиповим вдосконалили Статут Товариства

дослідних наук та впорядкували випуск його праць.

У січні 1884 року М.Д. Пильчиков був призначений на посаду позаштатного лаборанта, а у грудні 1885 року на посаду приват-доцента Харківського університету. З цього часу він читав в університеті лекції з історії фізики, з експериментальної фізики і різних розділів математичної фізики, з теорії потенціалу, математичної і фізичної оптики, механічної теорії теплоти, теорії пружності, теорії електрики, а також з метеорології, атмосферної електрики та земного магнетизму. Він також проводив різноманітні наукові дослідження, постійно здійснював комплектування фізичного кабінету приладами, виготовленими в майстернях відомих європейський фірм.

Широке визнання у російських та європейських геофізиків і географів здобули результати досліджень Курської магнітної аномалії, які були проведені М.Д. Пильчиковим у 1883 – 1884 роках та у подальші роки. Він першим висловив гіпотезу про те, що Курська і Белгородська магнітні аномалії пов'язані із наявністю в цих місцевостях великих запасів залізної руди, розміри і місця залягання яких можуть бути визначені шляхом проведення детальних магнітних досліджень. За досягнення у дослідженні магнітних аномалій М.Д. Пильчиков був нагороджений срібною медаллю Російського географічного товариства.

У 1888 році за результатами досліджень Курської магнітної аномалії М.Д. Пильчиков у Санкт-Петербурзькому університеті захистив магістерську дисертацію «Материалы к вопросам о местных аномалиях земного магнетизма» і отримав науковий ступінь магістра фізики і фізичної географії.

У 1888 – 1889 роках він перебував у Франції, де пройшов ґрунтовне наукове стажування, працюючи в лабораторіях під керівництвом видатних французьких вчених: Марі-Альфреда Корню, майбутнього Нобелівського лауреата Габрієля Іонаса Ліппмана, Елетера-Елі-Ніколи Маскара.

У майстерні фізичних приладів, яка належала паризькому оптику і механіку Жюлю Дюбоску, М.Д. Пильчиков замовив виготовлення двох своїх приладів, які були подані на Всесвітню міжнародну виставку, що відбулася у 1889 році в Парижі. Один з цих приладів – рефрактотометр Пильчикова – в подальшому став постійно випускатись майстернею Дюбоска і набув широкого поширення та отримав схвальні відгуки від різних фахівців, зокрема від працівників фізичних та медичних лабораторій.

М.Д. Пильчиков брав участь у Всесвітній міжнародній виставці, що відбулася 1889 році у Парижі. Там він, зокрема, познайомився з Густавом Ейфелем – творцем Ейфелевої вежі. Пізніше, у 1904 році і у 1907 році, з дозволу Г. Ейфеля М.Д. Пильчиков провів дослідження з поляризації світла та іонізації атмосфери, які виконав безпосередньо на Ейфелевій вежі.

М.Д. Пильчиков брав участь у роботі 2-го Міжнародного конгресу електриків, який відбувся 24-31 серпня 1889 року в Парижі. Російську делегацію на цьому конгресі очолював професор О.Г Столєтов, з яким у М.Д. Пильчикова склались теплі, дружні стосунки. У подальшому цих вчених поєднувала творча співпраця, спрямована на реформування фізичної освіти в Російській імперії та на створення фізичних лабораторій і фізичних інститутів, спеціально побудованих та добре оснащених різними сучасними приладами, найбільш придатними для проведення наукових досліджень з різних галузей фізики.

На одному із засідань 2-го Міжнародного конгресу електриків М.Д. Пильчиков вперше побачив досліди з електромагнітними хвилями Генріха Герца, які показав професор М.Д. Єгоров. Ці досліди є фізичною основою принципу бездротової телеграфії і радіокерування, перші пристрої для яких у подальшому були розроблені О.С. Поповим, Г. Марконі та М.Д. Пильчиковим.

У 1889 та в 1890 роках М.Д. Пильчиков брав участь у роботі Міжнародних конгресів метеорологів, які відбулися в Парижі.

16 грудня 1889 року М.Д. Пильчикова було призначено виконувачем обов'язків екстраординарного професора Харківського університету. Це стало для нього стимулом для активізації організаційної, наукової, викладацької та просвітительської діяльності.

У 1890 році М.Д. Пильчиков виступив одним із засновників журналу «Метереологический вестник», в якому публікувались результати метеорологічних та геофізичних досліджень, а також популяризувалось значення метеорології для практики. У цьому ж журналі М.Д. Пильчиков публікував результати своїх досліджень. У 1893 році ним, зокрема, була опублікована стаття «Об исследовании высших слоев атмосферы». У цій статті вчений вперше у світі запропонував конструкцію і описав принцип дії прообразу сучасного скафандра, якого він назвав «портаеронавтом».

У 1891 році за ініціативи М.Д. Пильчикова в Харківському університеті були створені магнітно-метеорологічне відділення фізичного кабінету та метеорологічна станція і налагоджено проведення систематичних метеорологічних досліджень.

У цей же час М.Д. Пильчиков розпочав дослідження у галузі атмосферної оптики. В подальшому він експериментально обґрунтував причини голубого кольору неба, встановив залежність різниці інтенсивності поляризації в голубих та червоних променях від мутності атмосфери, а також детально дослідив поляризацію місячного світла, розсіяного атмосферою.

У 1894 році М.Д. Пильчиков звільнився з

Харківського університету. У 1894 – 1902 роках він працював на посаді виконувача обов'язків екстраординарного професора Новоросійського імператорського університету (м. Одеса).

В Одесі М.Д. Пильчиков провів низку експериментальних досліджень з вивчення фізико-хімічних процесів при електролізі, результати яких стали фізичною основою відкритого ним методу фотогальванографії. Теоретичне обґрунтування спостережуваних явищ, яке було викладене у низці статей та монографії «Материалы к вопросу о приложении термодинамического потенциала к изучению электродинамической механики» М.Д. Пильчиков здійснив на основі праць Дж. Гіббса. Він також зайнявся вивченням рентгенівських променів одразу ж після їх відкриття В.К. Рентгеном у листопаді 1895 року. Свої перші рентгенограми жаби, рака, риби, миші, жука та корала Микола Дмитрович одержав 19 січня 1996 року. Він запропонував конструкцію потужної рентгенівської трубки, так званої фокус-трубки М.Д. Пильчикова, яка давала можливість суттєво скоротити тривалість експозиції (з години до 3 секунд) при проведенні рентгенологічних досліджень.

М.Д. Пильчиков був одним з перших у світі дослідників радіоактивності. Він товаришував із П'єром Кюрі та Марією Склодовською-Кюрі, успішно досліджував радіоактивні властивості відкритого ними радію.

У вересні 1897 року в Одесі відбувся 4-й з'їзд начальників телеграфів та залізничних електриків, на якому виступив О.С. Попов із доповіддю «Про телеграфування без дротів» [6]. Доповідь, що відбулася в Будинку Російського Технічного товариства, супроводжувалася демонструванням дії іскрового радіопередавача системи Попова, оснащеного антеною (вібратором Попова) і радіоприймача системи Попова. Асистентом О.С. Попова при показі дослідів із бездротової телеграфії був М.Д. Пильчиков.

Вже наступного року, а саме 25 березня 1898 року на публічній лекції, яка за повідомленням одеської газети «Южное обозрение» відбулася у залі Одеської біржі [3,4,7], М.Д. Пильчиков продемонстрував перед науковцями та представниками громадськості результати своїх власних досліджень із бездротової телеграфії та радіокерування. Вчений, використовуючи радіохвилі, які генерував іскровий передавач, на певній відстані від нього запалив світло у моделі маяка, привів у дію модель залізничного семафора, зробив постріл із маленької гармати. У невеликому басейні, розміщеному безпосередньо в приміщені Біржової зали, він дистанційно підірвав мініатюрну міну. При цьому для більшої наочності та ефектності цим вибухом була потоплена модель яхти. Це був перший у світі приклад використання радіокерування. Пізніше, «з легкої руки» французького фізика Едуарда Бранлі [8], ця галузь науки стала називатись «телемеханікою». Схожими дослідженнями в США, незалежно від Пильчикова, займався Нікола Тесла. 1 липня 1898 року Тесла подав заявку на патент, у якому запропонував розробку системи радіокерування кораблем [8]. М.Д. Пильчиков не став патентувати свої розробки і продавати їх представникам іноземних держав навіть за суму, яка складала за даними, наведеними в [4], 1 мільйон франків, оскільки сподівався поставити їх на службу військовому відомству Росії. Очільникам військового і морського міністерств Російської імперії він неодноразово пропонував для розгляду сконструйований ним спеціальний пристрій селективного прийому радіосигналів – «протектор» (у сучасному розумінні – електричний фільтр), що виділяє радіосигнали тільки від певного адресата, відфільтровуючи їх від сигналів-завад радіоприйому і захищає прилади бездротової телеграфії, а також сконструйовані вченим різноманітні радіокеровані пристрої (міни, бездротові електричні керма, торпеди, автоматичні семафори і маяки) від дії на них електромагнітних хвиль стороннього походження. «Протектор» Пильчикова, додатково оснащений розробленим ним пристроєм для запису інформації з двома перами, створював можливість здійснити захищену радіопередачу інформації, що не потребувала шифрування тексту радіотелеграфної депеші з використанням спеціальних шифрів [3,4].

У 1902 році М.Д. Пильчиков звільнився з Новоросійського університету і почав працював на посаді ординарного професора Харківського технологічного інституту Імператора Олександра III, в якому він створив і оснастив різноманітними приладами фізичну лабораторію – одну з найкращих серед лабораторій тодішніх вищих навчальних закладів Російської імперії.

З 31 серпня до 4 вересня 1903 року в районі Херсонеського мису були проведені випробування пристроїв для бездротової телеграфії, сконструйованих М.Д. Пильчиковим. Сигнали в радіоефір посилала передаюча радіостанція з Херсонеського маяка, а приймали їх прилади винахідника, що були встановлені на транспортному судні «Днестр». На приймальній радіостанції «Днестра» ці коливання виділяла фільтро-резонансна система («протектор» Пильчикова). Досліди пройшли успішно. Було, зокрема, встановлено [3,4,9], що на відстані, значно більшій за існуючі нормативи, прилади Пильчикова забезпечували нормальну роботу приймальної станції для бездротової телеграфії конструкції Дюкрете-Попова (рис. 2), яка на той час використовувалась на російському флоті [6,10-12].

З літературних джерел відомо [3,4], що прилади, які були розроблені М.Д. Пильчиковим для

Рис. 2. Загальний вигляд приймальної іскрової радіостанції для бездротової телеграфії конструкції Попова-Дюкрете [12]. Літерою Р позначене електромагнітне реле Дюкрете.

вдосконалення апаратури бездротової телеграфії, а також їх схеми та описи до нашого часу не збереглися.

Однак у результаті пошукових досліджень, нещодавно проведених у фізичному кабінеті НТУ «Харківський політехнічний університет», нами були виявлені, відреставровані та випробувані деякі прилади для бездротової телеграфії, якими користувався вчений.

На Рис. 3 наведений загальний вигляд дисків вібратора (антени) передавача для бездротового телеграфування, який вірогідно використовував М.Д. Пильчиков при проведенні своїх дослідів.

Рис. 3. Загальний вигляд латунних дисків вібратора радіопередавача для бездротового телеграфування.

Конструкція цього вібратора системи Бьєркнеса з латунними дисками та іскровим проміжком, як зазначено в [6,11,12], була запропонована О.С. Поповим навесні 1897 року. Електроди цього вібратора, що закінчуються латунними кульками розрядника, поміщували у скляну посудину з технічним маслом. Перший примірник цього приладу був виготовлений на Електромеханічному заводі Кронштадтського порту за кресленнями О.С. Попова [6,11,12]. Він був випробуваний при проведенні перших дослідів з бездротового телеграфування з використанням військових кораблів спочатку в Фінській затоці Балтійського моря у 1898 році, про що свідчить фотографія того часу (Рис. 4), наведена в [11], а потім у 1899 році і на Чорному морі [6,11,12]. Один з таких вібраторів (Рис. 5 а), як зазначено в [12], зберігся до цього часу. Він експонується в Центральному музеї зв'язку імені О.С. Попова у Санкт-Петербурзі.

Рис. 4. Фотографія корабельного передавача О.С. Попова, що використовувався при проведенні дослідів із радіозв'язку між кораблями Балтійської ескадри у 1897 році [11].

На Рис. 5 б представлений загальний вигляд вібратора з латунними дисками, якими, вірогідно, користувався М.Д. Пильчиков, що був реконструйований нами. Можна висунути припущення, що диски для вібратора могли бути передані М.Д. Пильчикову разом з

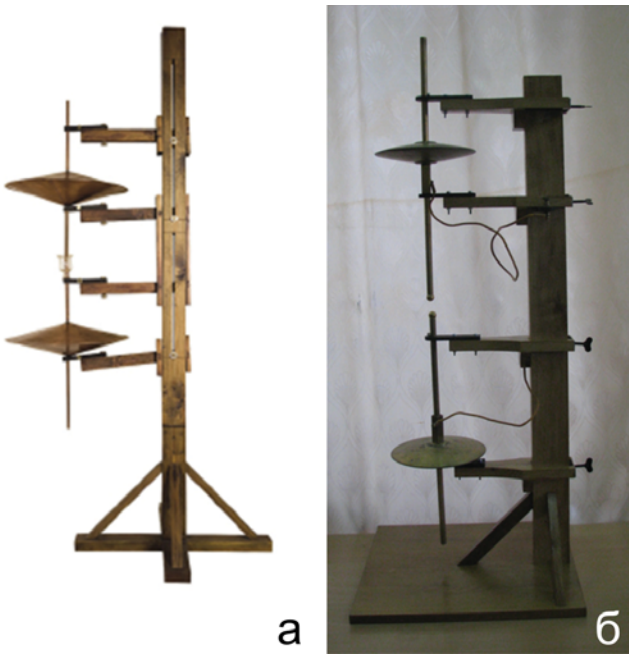

Рис. 5. Загальний вигляд вібраторів передавача для бездротового телеграфування з латунними дисками: а – що експонується в Центральному музеї зв'язку імені О.С. Попова [12]; б – що був реконструйований нами.

іншим обладнанням, виготовленим у Кронштадті влітку 1902 року, при підготовці до проведення дослідів, що відбулися, як було зазначено вище, за його участю в 1903 році в Севастополі. Ці диски могли бути виготовлені на замовлення М.Д. Пильчикова і раніше, а саме в 1897 або у 1898 році. Можливо їх виготовив славетний механік Новоросійського університету Й.А. Тимченко, з яким вчений тісно співпрацював під час роботи в Одесі. Можна завбачити, що у такому разі саме ці диски, вірогідно, були використані М.Д. Пильчиковим для показу дослідів з радіоуправління, що відбулися 25 березня 1898 року в Біржовій залі [3,4,7], а також 29 жовтня 1898 року на засіданні одеського відділення Російського Технічного товариства [3,4,13] На цьому засіданні безпосередньо під час доповіді професора Пильчикова шляхом використання радіохвиль був увімкнений електричний дзвінок і підірваний невеликий вибуховий пристрій.

Як вказано в [4,5], в архіві М.Д. Пильчикова зберігся лист від О.С. Попова, який був написаний ним 22 жовтня 1904 року, такого змісту: «Глибокошановний Миколо Дмитровичу! Незабаром після Вашої телеграми з Парижа я відправив поштою до Харкова на Ваше ім'я за адресою Фізичної лабораторії технологічного інституту реле, одержане від Дюкрете. Досі я не мав звісток, дійшло воно за призначенням, чи ні? Не одержуючи відомостей про ваше повернення, я не надсилав до цього часу рахунок, який тепер при нагоді долучаю. Щиро вдячний і готовий до послуг О. Попов». Надпис на звороті: «P.S. Повторяю ще раз, що коли б реле Вам не було тепер потрібне, то прошу повернути його, воно не стане для мене обтяжливим і може бути пущена в діло. О. П.»

Надіслане у 1904 році О.С. Поповим М.Д. Пильчикову реле Ежена Дюкрете (Рис. 6), яке той разом з Марешаллем і Ріголло спеціально сконструював для приймальної станції бездротової телеграфії системи Попова-Дюкрете [6,10,12], нещодавно було випадково знайдене в підсобному приміщенні великої лекційної аудиторії фізичного корпусу НТУ «Харківський політехнічний інститут» під час її підготовки до капітального ремонту. Реле, як видно з написів на його корпусі, пройшло інвентаризацію у 1942 році під час окупації м. Харкова і, вірогідно, з метою збереження було поміщене

Рис. 6. Загальний вигляд реле Ежена Дюкрете.

працівниками фізичного кабінету в гідроізольований пакунок і надійно заховане в потаємній ніші. Нами була проведена реставрація, регулювання і випробування дії цього приладу. Встановлено, що реле Дюкрете діє за принципом електровимірювального приладу магнітоелектричної системи. Досліди показали, що воно є дуже чутливим. Завдяки використанню такого реле у приймальній станції системи Попова-Дюкрете зразка 1904 року (див. Рис. 1), як зазначено в [6], вдалось суттєво підвищити дальність стійкого прийому депеш бездротової телеграфії. Станціями бездротової телеграфії системи Попова-Дюкрете були оснащені кораблі Чорноморської і Балтійської ескадри та частина кораблів Тихоокеанських ескадр, які брали участь у Російсько-Японській війні 1904 – 1905 років. Така ж іскрова радіостанція у 1904 році була розміщена на постійній основі на Ейфелевій вежі, що, у певній мірі, врятувало її від демонтажу.

М.Д. Пильчиков був ініціатором заснування у Харківському технологічному інституті друкованого органу – «Известий Харьковского технологического института». Він був редактором перших чотирьох томів цього видання. У 2 томі «Известий Харьковского технологического института» [6] М.Д. Пильчиков повідомив про те, що він «продовжував розробку різних питань з бездротової телеграфії, придумав та виготовив нове реле». Тому реле Дюкрете, яке було надіслане О.С. Поповим, вірогідно було потрібне М.Д. Пильчикову для проведення порівняльних дослідів, спрямованих на встановлення характеристик реле, розробленого ним самим, або ж для перевірки можливості одночасного використання обох цих приладів у апаратурі бездротової телеграфії, яку він розроблював.

Реле Пильчикова, конструкція якого до сьогодні ще не була відома фахівцям, у результаті проведення спеціальних пошуків нещодавно було виявлене нами в колекції приладів фізичного кабінету НТУ «Харківський політехнічний інститут». Його загальний вигляд до та після реставрації показаний на Рис. 7. Слід завбачити, що це чутливе реле, розроблене М.Д. Пильчиковим, вірогідно могло використовуватись не тільки для того, щоб автоматично відновлювати вихідні резистивні характеристики когерера завдяки удару по його трубці молоточком електричного дзвоника, ввімкненого цим реле, та здійснювати ввімкнення телеграфного апарата Дюкрете для запису на паперову стрічку телеграфних депеш, але й і як пристрій, що міг бути складовою частиною «протектора» Пильчикова. Змінюючи довжину насадок якоря реле (на Рис. 4 б вони позначені цифрами 1 і 2), який є своєрідним фізичним маятником, можна було змінювати його момент інерції і, значить, цілеспрямовано задавати або змінювати період (частоту) його коливань.

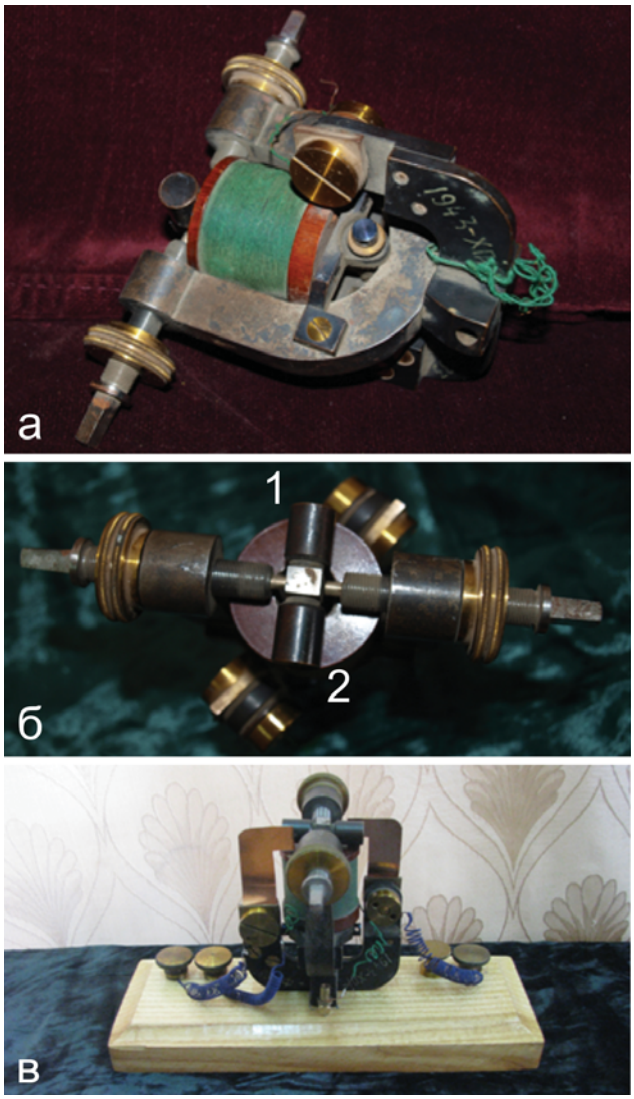

Рис. 7. Загальний вигляд реле М.Д. Пильчикова: а, б – до реставрації, в – після реставрації. Цифрами 1 і 2 позначені насадки якоря реле.

У зв'язку з початком Російсько-Японської війни 1904 – 1905 років подальші випробування і впровадження радіопристроїв, розроблених М.Д. Пильчиковим, безпосередньо на флоті, вірогідно, не проводились. Однак у 2 томі «Известий Харьковского технологического института» [14] М.Д. Пильчиков зазначив про те, що він «придумав і в модельному виді виготовив протимінний захист для броненосців та крейсерів. За роботи з бездротової телеграфії і протимінного захисту суден професору Пильчикову була винесена подяка Командувача флотом у Тихому океані від 1 вересня 1904 року за № 18».

З відомостей, які наведені в [3,4] та містяться в архівних документах [5], відомо, що за розпорядженням Морського відомства М.Д. Пильчиков разом зі своїми співробітниками, зокрема з Д.А. Кутневичем, О.М. Ільєвим та В.В. Гайдак-Кондуренком, провів у 1904-1906 роках дослідження, спрямовані на встановлення оптимальних умов стабільної, безвідмовної роботи

німецької іскрової радіостанції «Телефункен» системи Арко і Слабі, яка використовувалась на Тихоокеанському російському флоті та, як зазначено в [6], складалась із недопрацьованих, погано змонтованих і ненадійних приладів.

Ці досліди були проведені і у зв'язку з необхідністю розроблення мобільної версії іскрової радіостанції. Для цього комплект приладів, а саме: приймальна станція фірми «Телефункен», велика індукційна спіраль (котушка Румкорфа) передавальної станції, акумулятори до неї та динамомашина для їх заряджання, яка працювала від бензинового двигуна, були змонтовані на автомобілі фірми «Котеро», спеціально придбаному М.Д. Пильчиковим у 1905 році за кошти Морського відомства. Це була перша в Російській імперії діюча пересувна радіостанція, змонтована на автомобілі. При проведенні дослідів автомобіль переміщувався по території парку Харківського технологічного інституту. Стаціонарна станція бездротового телеграфу виробництва фірми «Телефункен», а також прилад для автоматичної реєстрації гроз були змонтовані у спеціально збудованому на території Харківського технологічного інституту павільйоні при метеорологічній обсерваторії. І до сьогодні над дахом фізичного корпусу НТУ «Харківський політехнічний інститут» здіймається металева конструкція у вигляді корабельної щогли із двома скляними ізоляторами, яку, вірогідно, використовував М.Д. Пильчиков для розміщення передавальної та приймальної антен. Є дані про те, що після завершення Російсько-Японської війни, а саме влітку 1907 року, він провів разом зі своїми співробітниками на берегах озер у Бермінводах низку дослідів з радіокерування та оптики.

При проведенні досліджень сонячного затемнення у 1905 році у місті Філіппвіллі (Алжир) М.Д. Пильчиков користувався спеціально сконструйованим ним «фотографічним телескопом», який на його замовлення виготовив відомий французький оптик Секретан.

М.Д. Пильчиков брав активну участь у роботі фізичної секції VII, VIII, IX, X і XI-го з'їздів російських дослідників природи та лікарів, а також у роботі І Менделеєвського з'їзду із загальної і прикладної хімії. Він головував на засіданнях, виступав із доповідями, спілкувався з відомими російськими вченими, які брали участь у роботі цих з'їздів.

М.Д. Пильчиков був майстерним лектором. Він активно популяризував новітні досягнення фізичної науки в Харкові та в інших містах, читаючи публічні лекції, що супроводжувались показом дослідів. Ці лекції вченого збирали тисячні аудиторії слухачів.

У 1893 – 1894 роках М.Д. Пильчиков був головою Харківського міського товариства велосипедистів-любителів. У 1893 році за його ініціативою і під його безпосереднім керівництвом на північній ділянці Університетського саду, що виходить до нинішньої площі Свободи біля приміщення колишнього Ветеринарного інституту, для любителів велосипедного спорту був побудований циклодром (велотрек).

М.Д. Пильчиков був вченим-енциклопедистом, людиною широкої ерудиції й високої культури, що давало йому можливість заявити про себе не тільки як про дослідника в різних галузях фізики та метеорології, але й як про вченого гуманіста, громадського діяча, європейська освіченість та загальний культурний кругозір якого поєднувались із українським патріотизмом.

Вчений входив до кола діячів просвітницького руху на Харківщині, до яких належали: Х. Алчевська, М. Бекетов, В. Данилевський, С. Раєвський, П. Єфименко, О. Потебня, Я. Щоголів, М. Лободовський, В. Мальований. Разом з М. Міхновським, Г. Хоткевичем, О. Зайкевичем, Х. Д. та Х. О. Алчевськими М.Д. Пильчиков активно працював на ниві пропаганди української національної ідеї.

Любов до мистецтва та літератури сформувалась у М.Д. Пильчикова з дитячих років під впливом батька і збереглась у нього назавжди. Він займався перекладами літературних творів українською мовою, писав ліричні вірші, які друкувались за підписом «М.П.». Крім літературної творчості, М.Д. Пильчиков професійно займався живописом і майстерно грав на скрипці. Він відвідував концерти, театральні вистави та художні виставки.

Трагічно і таємниче завершилося життя вченого. За офіційною версією, викладеною у [1,4], професор Пильчиков М.Д. покінчив життя самогубством 6 травня 1908 року о 7 годині ранку, перебуваючи на лікуванні у приватній клініці для нервово хворих, яка належала приват-доценту Харківського університету І.Я. Платонову. До сьогоднішнього дня ще не одержані вичерпні відповіді на низку питань такого змісту. Хто ж все-таки натиснув на спусковий гачок револьвера «Бульдог», постріл якого обірвав життя вченого? Він сам чи агент однієї з іноземних держав, які могли «полювати» за винаходами М.Д. Пильчикова? Чи могла людина з простреленим серцем не втратити свідомість від больового шоку та втрати крові, а осмислено покласти револьвер на нічний столик, лягти в ліжко і скласти руки на грудях? Чи брав професор Пильчиков у лікарню матеріали, в яких були описані схеми та принципи дії його приладів? В архіві, який був розібраний одразу ж після смерті вченого, їх так і не вдалося знайти.

Відспівування тіла покійного професора Пильчикова М.Д. відбулося у Рождественсько-Богородичній (Каплунівській) церкві. Поховання тіла відбулось на Іоанно-Усікновенському міському кладовищі 8 травня 1908 року. Студенти на руках несли

Рис. 8. Могила М.Д. Пильчикова на 13 цвинтарі м. Харкова.

труну з тілом професора Пильчикова М.Д. від церкви до кладовища. Зараз могила М.Д. Пильчикова (Рис. 8) знаходиться на цвинтарі № 13 м. Харкова, на «площадці знаменитих харків'ян».

Нещодавно одна з вулиць м. Харкова була названа на честь М.Д. Пильчикова. У Центральній науковій бібліотеці Харківського національного університет імені В.Н. Каразіна зберігаються книги з особистої бібліотеки М.Д. Пильчикова, яку він заповів Харківському університету. У фізичних кабінетах Харківського національного університету імені В.Н. Каразіна та НТУ «Харківський політехнічний інститут» зберігаються та до цього часу використовуються при показі лекційних демонстрацій прилади, які у свій час придбав (у тому числі і за власні кошти) і використовував професор М.Д. Пильчиков.

Література

1. Е.А. Роговский. Профессор Н.Д. Пильчиков и его труды. Харьков: Издание Общества Физико-Химических Наук при Харьковском Университете, (1913), 29 с.
2. Н.Л. Полякова, Е.А. Попова - Кьяндская. Николай Дмитриевич Пильчиков. *УФН*, **Т.53**, В.1. 131 (1954).
3. В.І Бавер, В.О. Каменєва. Микола Дмитрович Пильчиков. К.: Техніка, (1964), 68 с.
4. В.П. Плачинда. Микола Дмитрович Пильчиков. К.: Наукова думка, (1983), 198 с.
5. Микола Дмитрович Пильчиков, 1857 – 1908: Опис документальних матеріалів особистого фонду 783. К.: Наукова думка, (1970), 164 с.
6. Изобретение радио А.С. Поповым. Сборник документов и материалов / Под редакцией члена-корреспондента Академии наук СССР А.И. Берга. Москва-Ленинград: Издательство Академии наук СССР, (1945), 309 с.
7. Газета *«Южное обозрение»*. (1898), 23 марта.
8. Евгений Матонин. Никола Тесла. М.: Издательство АО «Молодая гвардия», (2014), 380 с.
9. Отчет о состоянии Харьковского Технологического Института Императора Александра III за 1903 год. *Известия Харьковского Технологического Института Императора Александра III*, **Т. 1**, Харьков. 39 (1905).
10. Жорж Дари. Электричество во всех его применениях. Санкт-Петербург: Типография Суворина, (1903), 438 с.
11. В.И. Шамшур. А.С. Попов и советская радиотехника. М.: Военное издательство военного министерства Союза ССР, (1952), 122 с.
12. История радиосвязи в экспозиции Центрального музея связи имени А.С. Попова: Каталог (фотоальбом) / Н.А. Борисова, В.К. Марченков, В.В. Орлов и др. СПб: Центральный музей связи имени А.С. Попова, (2008), 188 с.
13. Газета «Южное обозрение». (1898), 31 октября.
14. Отчет о состоянии Харьковского Технологического Института Императора Александра III за 1904 год. *Известия Харьковского Технологического Института Императора Александра III*, **Т. 2**, Харьков. 41 (1906).

ІНФОРМАЦІЯ ДЛЯ АВТОРІВ СТАТЕЙ

журналу «Вісник ХНУ». Серія «Фізика»

У журналі «Вісник ХНУ». Серія «Фізика» друкуються статті та стислі за змістом повідомлення, в яких наведені оригінальні результати теоретичних та експериментальних досліджень, а також аналітичні огляди літературних джерел з різноманітних актуальних проблем фізики за тематикою видання.

Мова статей – українська, англійська та російська.

ТЕМАТИКА ЖУРНАЛУ

1. Теоретична фізика.
2. Фізика твердого тіла.
3. Фізика низьких температур.
4. Фізика магнітних явищ.
5. Оптика та спектроскопія.
6. Загальні питання фізики і серед них: методологія та історія фізики, математичні методи фізичних досліджень, методика викладання фізики у вищій школі, техніка та методика фізичного експерименту тощо.

ВИМОГИ ДО ОФОРМЛЕННЯ РУКОПИСІВ СТАТТЕЙ

Загальний обсяг тексту рукопису статті повинен займати не більше, ніж 15 сторінок.

Рукопис статті складається з титульної сторінки, на якій вказанно: назва статті; ініціали та прізвища авторів; поштова адреса установи, в якій була виконана робота; класифікаційний індекс за системами PACS та УДК; анотації на окремому аркуші з прізвищем та ініціалами авторів і назвою статті, викладені українською, російською та англійською мовами; основний текст статті; список літератури; підписи під рисунками; таблиці; рисунки: графіки, фотознімки.

Анотація повинна бути за об'ємом не меньш ніж 500 сімволів. Стаття повинна бути структорована. Висновки потрібно пронумеровати та в них потрібні бути висновки а не переписана анотація.

Електронний варіант рукопису статті повинен відповідати таким вимогам: текст рукопису статті повинен бути набраний у форматі MicrosoftWord версії 2013, вирівнювання тексту повинне бути здійснене за лівим краєм, гарнітураTimesNewRoman, без прописних букв у назвах, букви звичайні рядкові, з полями ліворуч, праворуч, зверху і знизу по 2,5 см, формули повинні бути набрані в MathType (не нижче версії 6,5), у формулах кирилиця не допускається, символи з нижніми і верхніми індексами слід набирати в MicrosoftWord, ширина формули не більше 70 мм, графіки та фотографії необхідно подавати в графічному форматі, розрізнення не менше 300 dpi, поширення файлів повинно бути *.jpg, шириною в одну чи дві колонки, для однієї колонки розміри: завширшки 8 мм, для двох колонок – 16 мм. Масштаб на мікрофотографіях необхідно представляти у вигляді масштабної лінійки.

ВИМОГИ ДО ОФОРМЛЕННЯ ГРАФІКІВ

Товщина ліній не більше 0,5 мм, але не менше 0,18 мм. Величина літер на підписах до рисунків не більш 14 pt , але не менше 10 pt, гарнітура Arial.

ПРИКЛАД ОФОРМЛЕННЯ СПИСКУ ЛІТЕРАТУРИ

1. Л.Д. Ландау, Е.М. Лифшиц. Теория упругости, Наука, М. (1978), 730 с.
2. И.И. Іванов. ФТТ, 25, 7, 762 (1998).
3. A.D. Ashby. Phys.Rev., A19, 213 (1985).
4. D.V. Vert. In Progress in Metals, ed. by R. Speer, USA, New York (1976), v.4, p.17.

ДО РЕДАКЦІЇ НАДАЄТЬСЯ

1. Два роздруковані примірники рукопису статті, які підписані її авторами.
2. Електронна версія рукопису та дані щодо контактів для спілкування з її авторами. Для цього потрібно надіслати електронною поштою, тільки на адресу **physics.journal@karazin.ua**.
3. Направлення від установи, де була виконана робота, і акти експертизи у двох примірниках; адресу, прізвище, повне ім'я та батькові авторів; номери телефонів, E-mail, а також зазначити автора рукопису, відповідального за спілкування з редакцією журналу.

Матеріали рукопису статті потрібно направляти за адресою: Редакція журналу «Вісник Харківського національного університету імені В.Н. Каразіна. Серія: фізика», Лебедєву С.В., фізичний факультет, майдан Свободи, 4, Харківський національний університет імені В.Н. Каразіна. тел. (057)707-53-83.

Наукове видання

Вісник Харківського національного університету імени В.Н.Каразіна

Серія “Фізика”

випуск 26

Збірник наукових праць

Українською, російською та англійською мовами.

Комп’ютерне верстання С.В. Лебедєв

Підписано до друку 22.09.2017. Формат 60x84 1/8.

Папір офсетний. Друк ризограф. Ум. друк. арк. 11,9. Обл.-вид. арк 18,7.

Наклад 100 пр. Зам. №

Надруковано: ХНУ імені В.Н. Каразіна
61022, Харків, майдан Свободи, 4.
Тел.705-24-32

Свідоцтво суб'єкта видавничої справи ДК №3367 від 13.01.09